High-spin states and coupling of bands

E. Nadzhakov

Institute of Nuclear Research and Nuclear Energy, Bulgarian Academy of Sciences, Sofia
Fiz. Elem. Chastits At. Yadra **10**, 1294–1404 ((November–December 1979)

The effects of coupling of bands, especially as manifested in high-spin states of even–even nuclei, are reviewed. The development of methods such as the self-consistency method, the random phase approximation, the cranking model and the projection method is described. An attempt is made at a unified microscopic description of the effects of rotation–vibration coupling. The application of the theory to high angular momenta is discussed. The excitation of high-spin states by heavy ions is considered. Investigations into nuclear structure by in-beam energy and lifetime measurements are discussed. Questions relating to the mechanism of the compound nucleus reaction and the population of the yrast band are posed. Experiments that contributed to the discovery of phenomena such as back-bending and yrast region traps are discussed.

PACS numbers: 21.60.Ev, 21.60.Jx, 21.10.Hw, 21.10.Re

INTRODUCTION

In modern physics, investigations into nuclear structure occupy a special position between the physics of elementary particles, which is regarded as the vanguard of physics, and the physics of many-particle systems. It combines the complexity of the as yet unsolved problem of the fundamental interaction of elementary particles (which distinguishes it from other many-particle systems) with the complexity of a many-particle system with all its theoretical problems and diversity of experimental phenomena.

The nuclear many-particle system is distinguished by various features from other many-particle systems. At the theoretical level, they are due to: 1) the small number of nucleons, which leads to specific finite-system effects, in contrast to solid-state and plasma physics; 2) the absence of a heavier subsystem, which results in a great variety of shapes and associated excitations, in contrast to atomic and molecular physics; 3) the possibility of excitation of mesonic degrees of freedom, which leads to a nuclear physics of a new type having little in common with the ordinary many-body problem.

From the experimental point of view, the nuclear system also has specific features due to the variety of possible means of influencing it (the diversity of the "probes"), exciting different degrees of freedom, and opening up different aspects of the nucleus. Besides electromagnetic radiation, one can use as probes neutrinos, electrons, a variety of mesons, neutrons, protons, hyperons, and various heavy ions. As a result, modern investigations are based primarily on nuclear reactions, which, in contrast to radioactive decay, excite the nucleus over a wider spectrum and, moreover, more specifically.

It is well known that a frontal attack on the solution of the nuclear many-body problem with a computer has no prospect of success and is meaningless. Nuclear physics, like the physics of other many-particle systems, therefore proceeds by seeking elementary excitation modes. In the nucleus, these are a single-particle and single-quasiparticle motions, and also the collective motions: vibration, rotation, pairing vibration, and so forth. The collective modes are relatively complex and varied excitations in which many nucleons participate simultaneously; nevertheless, they can be described theoretically by means of a small number of degrees of freedom. Experimentally, they can be selectively excited if the probe and conditions are properly chosen. Especially favorable for the excitation of collective modes are heavy ions, which explains their potential in nuclear physics as probes leading to phenomena of great variety.

Nevertheless, the elementary modes are manifested in a pure form only in limited ranges of nuclei, probes, and conditions of excitation. Experiments reveal particularly interesting phenomena in the transition regions in which several coupled modes are simultaneously operative. We have, for example, the regions of nuclei that are transitional between spherical and deformed shape,[1] or the regions of excitation of high spins.[2] In both cases, the coupled modes are vibration, rotation, pairing vibration, and single-particle motions.

The most topical cases of coupled modes are observed at high spins. Here we encounter phase transitions in nuclei with rotation[3,4] due to the interaction of rotational bands of various vibrational, pairing-vibrational, or quasiparticle structure,[5,6] i.e., back-bending and the phenomena related to it. Also topical are the effects of the structure of the yrast band and the region of states near it (Fig. 1) at high and ultrahigh spins,[7,8] and, in particular, yrast region traps. We restrict ourselves here to considering heavy nuclei.

The review consists of two parts, a theoretical and an experimental part. A method developed in conjunction with colleagues at the Laboratory of Theoretical Physics and the Laboratory of Nuclear Reactions at the Joint Institute at Dubna is presented. Simultaneously, the review aims to give a fairly complete survey of the present state of these questions. Because of the vast amount of literature, this will be cited in two ways. References to papers presented well in other reviews will be made through these reviews, while references that are more important for the present exposition or new papers will be quoted individually. The survey of the literature was terminated in August 1978.

 0090-4759/79/060516-46$02.80

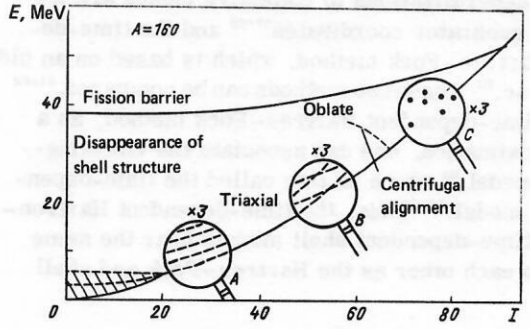

FIG. 1. Expected changes in the structure of nuclei in the region of the yrast band for high and ultrahigh spins.[7]

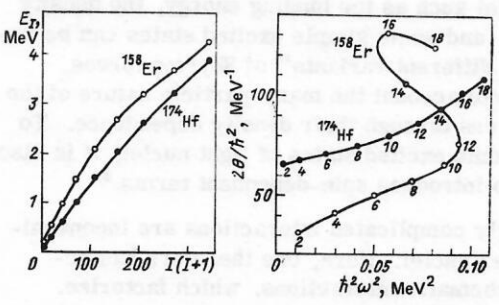

FIG. 2. Nucleus exhibiting back-bending ($^{158}_{68}$Er) and nucleus without this effect ($^{174}_{72}$Hf) represented in two ways: E_I plotted against $I(I+1)$ and $2J(2\vartheta/\hbar^2)$ plotted against $\omega^2(\hbar^2\omega^2)$ (Ref. 4).

1. INTRODUCTORY COMMENTS ON THE THEORY OF COLLECTIVE MOTIONS IN NUCLEI

The first indication of a collective nature of the low-lying states of even–even nuclei was the fact that the $E2$ (electric quadrupole) transitions were found to be strongly enhanced compared with the expectation for single-particle transitions.[9] The generalized model of Refs. 10 and 11 gave a rotational interpretation of this phenomenon, in which the $E2$ moments of nuclei found to be an order of magnitude greater than the single-particle moments indicated a static deformation.[12] Rotational spectra were discovered at the same time as Coulomb excitation.[13,14] They were also identified in α-decay spectra.[15] Higher levels were excited by multiple Coulomb excitation[16] and in reactions with α particles (α, xn) (Ref. 17), protons $(p, 2n)$ (Ref. 18), and ions heavier than α particles (HI, xn) (Ref. 19).

A completely new situation arose with the discovery of *back-bending*, an effect[20] that is sometimes called a *phase transition* in nuclei with rotation. The literature on this effect is very extensive; reviews of experiment and theory can be found in Refs. 3–6 and 21–23. The essence of this phenomenon is that the transition energies $E_I - E_{I-2}$ between neighboring levels of the bands I and $I-2$ do not increase linearly with the spin I but deviate very strongly from such a dependence and in a definite region of high spins decrease with I. Recently, a second back-bending has been discovered at even higher spins.[24] This effect is interpreted in terms of the moment of inertia of neighboring levels J and the angular frequency ω. Then in Fig. 2 for spins in the back-bending region a drastic increase in $2J$ is obtained simultaneously with a decrease in ω^2 (Ref. 4).

Of particular interest is the observation of not only an yrast band but also bands close to it in $^{154}_{64}$Gd (Refs. 25 and 26), $^{154}_{66}$Dy (Ref. 27), and $^{156}_{66}$Dy (Refs. 28–30). Theory was presented with new problems after the discovery of bands of different parity in, for example, $^{156}_{68}$Er (Ref. 31), $^{162}_{68}$Er (Ref. 32), $^{164}_{68}$Er (Refs. 33 and 34), and traps at high (see, for example, Refs. 35–38) and ultrahigh spins.[39]

However, in phenomenological approaches like that developed in the generalized model—some of them will be considered below—difficulties of both fundamental and practical nature frequently arise. The fundamental difficulties are associated with the fact that the different modes are usually described in the language of different models which are not related to a "microscopic" approach, i.e., the models are not derived from the solution of the many-particle problem. Therefore, it is very difficult to understand what, for example, is rotation of the nucleus from the point of view of the many-particle problem. The practical problems arise because the different languages used to describe the different modes do not make it easy to construct even a phenomenological model—to say nothing of a microscopic model—of coupled modes and to describe the phenomena mentioned above.

We see that microscopic approaches are needed. But here we must mention some features of nuclear physics, which lead to a situation in which microscopic approaches are hardly developed. By this, we mean approaches associated with the solution, albeit approximate, of the many-particle problem on the basis of the fundamental nucleon–nucleon interaction, the solution being taken as far as the stage of comparison with experiment. Features of nuclei that hinder this are:

1) the fact that, despite considerable progress in the elucidation of the nucleon–nucleon interaction, this problem is not yet solved;

2) there are fundamental doubts whether a transition should be made at the present stage from the fundamental interaction to an effective interaction in the nucleus on the basis of the solution of the Bethe–Goldstone equation.

Thus, there arise approximations of the first type associated with the interaction. In view of the great uncertainties for complex nuclei, preference is given to a more modest microscopic approach, which Solov'ev has called *semimicroscopic*.[40] It is based on direct parametrization of the actual effective interaction, and this parametrization, which is closer to phenomenology, is determined by comparison with experiment. There have been introduced various forms of effective interaction—Gaussian, Yukawa, Woods–Saxon, etc., —and these have greater or lesser historical significance. There have also been introduced local, density-dependent interactions; we may mention Landau and Migdal,[41] Skyrme,[42] and Moszkowski.[43] In connection with the development of the self-consistent Hartree–Fock[44] and Brueckner–Hartree–Fock[45] methods of calculation of nuclei it was found that some properties of the ground

state of nuclei such as the binding energy, the density distribution, and some simple excited states can be reproduced by different variants[46] of Skyrme forces, which take into account the many-particle nature of the effective forces through their density dependence. To reproduce some excited states of light nuclei, it is also necessary to introduce spin-dependent terms.[47]

These fairly complicated interactions are inconvenient in heavier nuclei. Here, one therefore has recourse to schematic interactions, which factorize. They can be obtained by expanding the effective interaction in multipole interactions.[48] The long-range part is approximated by low multipolarities, i.e., the quadrupole[49] or one or two of the following. The short-range part is approximated by a monopole two-body interaction[49] or an interaction of even higher multipolarity, for example, quadrupole pairing.[50,51] If such residual effective interactions are added to the single-particle Hamiltonian of the spherical or deformed shell model with Nilsson potential or to the modified Hamiltonian of the shell model in a spherical or deformed Woods–Saxon basis, the well-known superfluid multipole model of the nucleus is obtained.[40,49] If a spherical basis and monopole pairing plus a quadrupole interaction is used, the upshot is the Kumar–Baranger model,[52] in which, however, the deformation is taken, not from an independent calculation or empirically, but on the basis of the transition to an optimal deformed basis, the Hartree–Fock–Bogolyubov method being used. Thus, this approach also aims to describe the transition region,[52,53] although with semiquantitative results.

Despite the approximations to the effective interactions, it is only light nuclei that can be attacked by direct diagonalization or the use of group theory. This gives rise to approximations of the second kind, which are associated with the method of solution of the many-particle problem. They are decisive for the success of any nuclear theory, in particular theories of collective motions, and they depend on the resourcefulness of the theoretician, who must make an optimal selection of one or several coupled elementary excitation modes.

At the beginning of the development of microscopic theories, it was assumed that it would be a help to replace the coordinates by suitable variables that describe also the collective modes,[54] it being necessary to guess the new coordinates. It turns out to be better merely to restrict the choice of the modes on the basis of certain general considerations and to create a microscopic approach which subsequently makes more precise the structure of the modes, rendering it automatically optimal. For the more complicated nuclei, this is as yet the only fruitful path. For the single-particle and single-quasiparticle modes we have the Hartree–Fock and Hartree–Fock–Bogolyubov methods,[55,56] and also their generalizations,[40,48] and these play the main part in all many-particle problems. In the language of second quantization, this is the method of optimal choice of the particle–hole or quasiparticle basis. As is well known,[48] it can be regarded as a microscopic derivation and derivation and development of the shell model.

Natural generalizations to collective modes are the method of generator coordinates[57-59] and the time-dependent Hartree–Fock method, which is based on an old idea of Dirac.[60] These two methods can be compared.[61,62] With the time-dependent Hartree–Fock method, as a first approximation, one can associate the vibrating-potential model,[63] which is also called the time-dependent shell model.[48] Thus, the time-dependent Hartree–Fock and time-dependent shell models bear the same relation to each other as the Hartree–Fock and shell models.

For a collective motion of small amplitude, the time-dependent Hartree–Fock method leads[48] to the random phase approximation, taken from the theory of plasma oscillations[64] and developed in nuclear theory.[65-67] This is the most effective method for describing vibrations of spherical and deformed nuclei (Refs. 40, 48, and 68–70). It introduces operators of creation B_μ^+ and annihilation B_μ of phonons, treating them as quasibosons, $[B_\lambda, B_\mu^+] = \delta_{\lambda\mu}$, and assuming for them, in the quasiparticle variant,[71] simple structure in the form of a superposition of products of operators of creation α_i^+ and annihilation α_i of two quasiparticles:

$$B_\mu^+ = \sum_{ij} (y_{ij}^{(\mu)} \alpha_i^+ \alpha_j^+ + z_{ij}^{(\mu)} \alpha_i \alpha_j). \quad (1)$$

The amplitudes $y_{ij}^{(\mu)}$ and $z_{ij}^{(\mu)}$ of this structure and, thus, the transition probabilities are determined from the equations of motion[48]

$$[\hat{H}, B_\mu^+] = [\hat{h}, B_\mu^+] = \omega_\mu B_\mu^+; \quad \hat{h} = \sum_\mu \omega_\mu B_\mu^+ B_\mu \quad (2)$$

in conjunction with the parameters ω_μ of the quasiboson "model" Hamiltonian $\hat{h}$, which give the energies of the different vibrational excitations. Equations (2) can be obtained directly from the time-dependent Schrödinger equations if one assumes a harmonic time dependence

$$B_\mu^+(t) \equiv \exp(i\hat{H}t) B_\mu^+ \exp(-i\hat{H}t) = \exp(i\omega_\mu t) B_\mu^+. \quad (3)$$

Rotational collective motion has properties that led to new types of approach. We have, first, a collective motion of large amplitude, and second, fairly complicated three-dimensional kinematics. These circumstances were responsible for the fact that over a period of more than 20 years a huge number of investigations have been made with but limited success and without solution of the problem as a whole. Among all the approaches, only two have led to practical results. They are developments of the cranking model and the projection methods.

Inglis's cranking model[72] was introduced as a time-dependent shell model or a generalized model for rotations and preceded a corresponding model for vibrations.[63] Subsequently, the model was given a variational microscopic derivation, which made it self-consistent,[73,74] and pairing was also included.[75,76] We shall here give an equivalent microscopic interpretation based on the introduction of a collective variable.[77] The cranking model amounted to the introduction, instead of (3), of the rotating variable

$$\hat{\theta}(t) \equiv \exp(i\hat{H}t)\hat{\theta}\exp(-i\hat{H}t) = \exp(i\omega\hat{I}_x t)\hat{\theta}, \quad (4)$$

in which it is assumed that $\hat{\theta}$ satisfies the analog of the quasiboson relation $[\hat{I}_x, \hat{\theta}] = 1$ and has a quasiparticle

structure of the type (1). From the time-dependent equation (4), the equation of the model is obtained; it is the analog of (2):

$$[\hat{H}, \hat{\theta}] = \omega \hat{I}_x. \tag{5}$$

The projection methods of Refs. 57, 58, 78, and 79 are special cases of the method of generator coordinates. From the deformed Hartree–Fock–Bogolyubov vacuum $|\ \rangle = \sum_K a_K |K\rangle$ there are projected components with good angular momentum

$$|IM\rangle = \sum_K P^I_{MK} a_K |K\rangle, \tag{6}$$

this being implemented by a superposition of states with different positions in space obtained after application of the operator

$$P^I_{MK} = \frac{2I+1}{8\pi^2} \int d\Omega D^{I*}_{MK}(\Omega)\, \hat{R}(\Omega). \tag{7}$$

The formula uses $\hat{R}(\Omega)$, the operator of finite three-dimensional rotations, and $D(\Omega)$ functions. Components with good quantum number of nucleons of each type p and n are projected similarly.[80]

The microscopic theory of nuclear rotation was developed[81,82] by the deeper Klein–Kerman approach to collective motion (see Ref. 83, and also Ref. 84). It is based on a generalized self-consistent theory of Hartree–Fock type for single-particle amplitudes coupling an even nucleus and a neighboring odd nucleus. Related approaches were proposed later by Rohozinski,[85] and also by Belyaev and Zelevinskiĭ.[86] The latest method was developed recently in Refs. 87 and 88 and taken to the stage of calculations. Nevertheless, the problem of a general approach to coupled modes has not been solved.

The main method for studying coupled modes in even systems is the method of boson expansions, which represents pairs of fermion operators in terms of bosons. It derives from a special approach in the theory of ferromagnetism.[89] In nuclear physics, two main approaches are known: those of Belyaev and Zelevinskiĭ[90] and Matumori *et al.*[91] The former is simpler and has been developed further.[92-95] The second is distinguished by projecting onto a physical space with finite basis, with the consequence that it does not violate the Pauli principle. This approach was developed in Ref. 96. We should also mention the work of Marshalek and Weneser[97] in connection with the cranking model, for the creation of a model of the transition region, and for the description of rotation.[98] For the projection and cranking methods and the development of a model of the transition regions the papers of Refs. 99–101 are interesting, and, in connection with the Hartree–Fock–Bogolyubov method, Ref. 102.

With regard to the microscopic theory of high-spin states and the crossing of bands, the greatest success has been achieved by the methods that combine the self-consistent methods and the cranking model,[103] and they will be considered in detail below. We mention the criticisms[104-107] of the cranking model in the backbending region. Of conceptual interest is the proposal to use coherent states, which were introduced into the modern stage of quantum theory of Glauber[108] (see also Ref. 109), to describe collective motion of large amplitude.[110] To describe such motion, it was again proposed to develop the method of generator coordinates[111] and the time-dependent Hartree–Fock method.[111-113] It was also suggested that the self-consistent cranking methods should be combined with the random phase approximation in order to correct the quasiclassical limitation of the cranking model and take into account quantum correlations in high-spin states.[114]

Thus, although there exists a great variety of approaches to collective motions, the problem of coupled modes has not been completely solved. In particular, it is still important to develop a microscopic theory of nuclear structure at high and ultrahigh spins.

2. PHENOMENOLOGY OF THE ENERGIES OF LOW-SPIN STATES

Deviations from the simple rule $E_I = (2J)^{-1} I(I+1)$ for a rigid rotator were already noted[16-19] in the low-spin region for excitation of levels up to $I^\pi = 8^+ - 12^+$. For the ground-state band of even–even nuclei, it was then proposed to use the expansion[115]

$$E_I = AI(I+1) + BI^2(I+1)^2 + CI^3(I+1)^3 + \ldots, \tag{8}$$

However, this was found to have a poor convergence.[19] Therefore, a different expansion—the Harris expansion[116]—with the introduction of a rotation velocity ω was introduced:

$$\left.\begin{aligned} E_I &= \alpha\omega^2 + \beta\omega^4 + \gamma\omega^6 + \ldots; \\ \sqrt{I(I+1)} &= 2\alpha\omega + \tfrac{4}{3}\beta\omega^3 + \tfrac{6}{5}\gamma\omega^5 + \ldots \end{aligned}\right\}. \tag{9}$$

This expansion was introduced on the basis of Inglis's cranking model,[72] which, despite being quasiclassical, provided a first understanding of rotation in terms of single-particle motions. The convergence of (9) is much better than that of (8), so that only two parameters are sufficient to describe the smooth anadiabatic deviations up to spins 8–12. An updated fitting of the parameters in (9) to the experiments, including higher spins, is also known.[117]

For nuclei in the transition region between spherical and deformed nuclei, in which the adiabatic treatment is invalid and the bands are said to be *quasirotational*, the variable-moment-of-inertia model[118] was proposed; in it, it is assumed that the moment of inertia J depends on the spin I in accordance with the two-parameter formula

$$E_I = I(I+1)/2J + V(J);\ V(J) = C(J - J_0)^2/2;\quad \partial E_I/\partial J = 0. \tag{10}$$

It was shown[118,119] that this model is equivalent to the Harris expansion (9) with two parameters and leads to a linear dependence of J on ω^2. Even better results for transition nuclei that are very nearly spherical, but poorer results for moderately high spins, are given by the different two-parameter formula of Ejiri[120]:

$$E_I = \omega I + I(I+1)/2J. \tag{11}$$

There was also proposed[121] a direct extension of (10) so as to treat simultaneously g, β, and γ bands by the introduction of variable vibrational frequencies. There has also been proposed an approach for the simultan-

eous description of the ground-state band and band based on a gamma-vibrational state[122,123] by combining the model of an asymmetric rotator[124] and the model with a variable moment of inertia. All these models consider basically the level energies of the bands.

In Ref. 125, there was proposed the phenomenological formula

$$E_I = \frac{J_0}{c}\left\{\left[1+\frac{c}{J_0^2}I(I+1)\right]^{1/2}-1\right\}, \quad (12)$$

in which two parameters are again introduced: the moment of inertia J_0 at zero spin $I=0$ and the coefficient c of the anadiabatic deviations. Comparison of the energies of the levels showed that the formulas (9) with two terms and (12) reproduce experiment up to 12^+ or 14^+ equally well and approximately within the experimental errors. The moment of inertia has a value typical of deformed rare-earth elements of order 30 MeV^{-1}, and the anadiabaticity coefficient c introduced here is of order 5 MeV^{-2}. The first coefficient $A=(2J_0)^{-1}$ in (8) is of order 15 keV. The usual second anadiabaticity coefficient B in (8) is related to c (when higher terms are ignored) by $B=-c/(8J_0^3)$, and thus this coefficient is of order −20 eV.

Formula (12) has two main features. The first is that it can be justified by the model of a soft rotator,[126] which was proposed independently of the widely known variable-moment-of-inertia model.[118] The soft-rotator model (a two-dimensional analog is given in Ref. 126) gives the energies

$$E_{nI}=\frac{2}{\sqrt{c}}\left[\frac{1}{2}\left(\frac{J_0}{\sqrt{c}}\right)+n\right]+\frac{J_0}{c}\left\{\left[1+\frac{c}{J_0}I(I+1)\right]^{1/2}-1\right\}. \quad (13)$$

Thus, in the soft-rotator model the energies (13) are obtained from the contribution of the β vibrations (the first term, which depends only on n) and the rotations with allowance for anadiabaticity (the second term, which depends only on I). The second term is identical with (12). Formula (12) can be derived from the soft-rotator model in the same way as the two-parameter Harris formula (9) from the variable-moment-of-inertia model (10). However, formula (13) predicts something more. The first term gives equidistant levels of a harmonic vibrator with energy separation $\omega_0=2/\sqrt{c}$, with $c=4/\omega_0^2$. These formulas relate the anadiabaticity coefficient c in the ground-state band to the energy ω_0 of the β-vibrational level. The connection can be tested, and this is done in Table I, in which we give the theoretical anadiabaticity coefficients c calculated from the experimental vibrational frequencies and compare them with the experimental values of c determined from fitting in the ground-state band. It can be seen that the coupling to the β band explains qualitatively the variation of c, although the value of c calculated from this coupling is always smaller than the experimental value. This could be due to the neglect of coupling to other bands.

TABLE I. Anadiabaticity coefficient c.

Nucleus	ω_0, MeV	c, MeV^{-2}	
		Theory	Experiment
$^{160}_{66}Dy$	1.275	2.461	4.77
$^{160}_{68}Er$	0.894	5.005	7.08
$^{164}_{68}Er$	1.246	2.576	4.28
$^{170}_{70}Yb$	1.069	3.500	3.83
$^{172}_{72}Hf$	0.871	5.273	6.12

We now show that the soft-rotator model is a variant of models of the variable-moment-of-inertia type. Indeed, formula (12) can be obtained from (10) by the variational procedure of such models if the choice for $V(J)$ in them is replaced by

$$V(J)=J/(2c)+J_0^2/(2cJ)-J_0/c. \quad (14)$$

A second feature of (12) is due to the fact that it is directly related to an expansion[127] that is the inverse of (8):

$$I(I+1)\equiv f(E_I)=bE_I+cE_I^2+\ldots;\ b=2J_0. \quad (15)$$

Terminating this expansion after the second term and solving for E_I, we obtain (12). This shows that the inverse expansion (15) is, as regards convergence, no worse than the generally used Harris expansion (9). On the other hand, (15) does not introduce concepts such as the angular velocity ω, which are not well defined in quantum theory.

Formula (12) is known in the literature as the Holmberg–Lipas formula even though it was proposed earlier by Mikhaĭlov *et al.*[125] and the fact that Holmberg and Lipas[128] themselves noted that the formula had been proposed before them in Ref. 129.

3. PHENOMENOLOGY OF THE ENERGIES OF HIGH-SPIN STATES: BACK-BENDING

The back-bending region ($I\approx 14$–16 for the rare-earth elements) cannot be described by the smooth two-parameter formulas discussed above. Indeed, let us translate Fig. 2 (Refs. 21 and 3) into a different form by replacing ω^2 by the argument E (Fig. 3). From the first two terms of formula (15), we obtain

$$2J=b+2cE, \quad b=2J_0, \quad (16)$$

i.e., the moment of inertia is a linearly increasing function of $E=E_I$. Thus, formula (16) can describe only the initial linear region of the increase of $2J$ in Fig. 3. But in the same figure we see that there is an abrupt increase in $2J$ in the back-bending region, i.e., near E_0.

Many phenomenological models were proposed to describe the energies of high-spin levels by means of several adjustable parameters.[130-134] The majority of

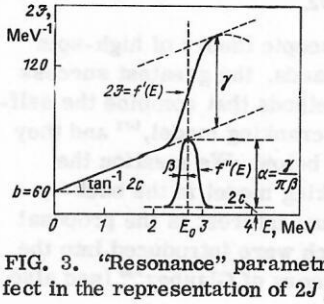

FIG. 3. "Resonance" parametrization of the back-bending effect in the representation of $2J$ plotted against $E=E_I$ (Ref. 148).

these models extended the variable-moment-of-inertia model by including terms of higher orders[135-137] (in Ref. 137, the various phenomenologies were systematized from the point of view of a generalized variable-moment-of-inertia model) or by the inclusion of an asymmetric deformation.[138-140] The use of a phenomenological boson Hamiltonian[141-143] is interesting.

Among the phenomenological approaches, a special position is taken by the model of the crossing of hybridization of bands,[144,145] which was also combined with the variable-moment-of-inertia model.[146] The idea is already implicit in the rotation–vibration model of Ref. 147. Here, the drastic change in the moment of inertia is attributed to crossing of the ground-state band and a "superband" with a higher moment of inertia. In such a scheme, one can also interpret the down-bending,[3] i.e., the reduction of the moment of inertia at even higher spins after the back-bending region. This scheme obtained experimental confirmation (see Sec. 26).

None of these approaches solve the problem of the physical nature of the back-bending or, in other words, the structure of the intersecting superband. Possible mechanisms and their theoretical and experimental selection will be considered below. Nevertheless, one can show that even the phenomenology in the representation given in Fig. 3 (Refs. 148 and 149) permits the drawing of certain conclusions concerning these mechanisms. Figure 3 corresponds to the following parametrization of $f(E)$ from formula (15)[1)]:

$$\left.\begin{aligned} 2J = f'(E) &= b + 2cE_s'[1-\exp(-E/E_s')] \\ &+ \frac{\gamma}{\Pi}\left[\operatorname{arctg}\frac{E-E_0}{\beta} + \operatorname{arctg}\frac{E_0}{\beta}\right]\exp(-E/E_s''), \quad \beta \neq 0; \\ &= b + 2cE_s'[1-\exp(-E/E_s')] + \gamma\theta(E-E_0)\exp(-E/E_s''); \\ &\qquad\qquad \beta = 0 \end{aligned}\right\} \quad (17)$$

(Ref. 149), or, more precisely, to the limiting case $E_s' = E_s'' \to \infty$ (damping is not taken into account). It can be seen immediately that the first two terms give the smooth component of the increase of $2J$ with E, and the third term gives a strongly varying component, which thus is responsible for the back-bending. As will be shown below, the two components correspond to two different mechanisms of anadiabatic variation of J.

The physical meaning of the parameters b and c of the smooth component of (17) can be deduced by comparing it with (16), which corresponds to (12). The physical meaning of the parameters E_0, β, and γ of the back-bending component of (17) can be seen by comparison with a simple model of two bands with constant moments of inertia J_g and J_s—the ground-state band with energies $I(I+1)/(2J_g)$ and a superband with energies $\Delta E + I(I+1)/(2J_s)$, $J_s > J_g$, these crossing at the point E_0. Suppose they interact by means of the matrix element V. We can then obtain approximately the following expressions for the parameters of the back-bending component; $E_0 = \Delta E J_s/(J_s - J_g)$, which is the intersection energy, $\gamma = 2(J_s - J_g)$, which is the difference between the doubled moments of inertia of the two bands, and $\beta = [2^{2/3}-1]^{1/2} 2\sqrt{J_s J_g}/J_s - J_g|V|$, where $[2^{2/3}-1]^{1/2} \approx 1.53284$. Strong back-bending (see Fig. 3) will be observed where the difference $J_s - J_g$ between the moments of inertia of the crossing bands is large and their interaction $|V|$ is small. In the case $E_s = E_s' = E_s''$, fitting of (17) to the experimental energies of the yrast levels of many nuclei exhibiting back-bending yielded a systematic set of parameters of the model of crossing bands with allowance for the smooth component and damping (E_s) with respect to Z and N (Ref. 149).

We mention that the use of the energies of not only the yrast levels but also several crossing bands, as in the original model,[144,145] makes it possible to extract more parameters from the experiments,[150] but only in the few cases when other bands were observed.[25-30] We shall return to this problem below.

4. TRANSITION PROBABILITIES

The adiabatic approach to the transition probabilities of the generalized model is based on factorization of the wave function into $D^I_{KM}(\Omega)$, which takes into account rotation in terms of the collective coordinates (the three Eulerian angles Ω of the orientation of the deformed potential well in space), and into $|\alpha(K)\rangle$, which depends on the remaining "internal" coordinates. Using both the rotational and mirror symmetry, we can express the adiabatic wave function in the form[151]

$$|\alpha(K)\,IM\rangle = \frac{1}{\sqrt{2(1+\delta_{K0})}}\sqrt{\frac{2I+1}{8\pi^2}}\,[|\alpha(K)\rangle D^I_{KM} + (-)^{I+K}\,|\overline{\alpha(K)}\rangle D^I_{-KM}], \quad (18)$$

where the state $|\overline{\alpha(K)}\rangle$ is the state $|\alpha(K)\rangle$ rotated through π about an axis perpendicular to the symmetry axis of the nucleus. Then for the reduced transition probabilities

$$B(FL;\ \alpha_i(K_i)\,I_i \to \alpha_f(K_f)\,I_f) = (2I_i+1)^{-1}\,|\langle I_f\alpha_f(K_f)\|\hat{F}_L\|\alpha_i(K_i)\,I_i\rangle|^2, \quad (19)$$

where $\hat{F}_{LM} = \hat{Q}_{LM}$ or $\hat{M}_{LM}$ is the operator of an E or M transition of multipolarity L, and $\langle f\|\hat{F}_L\|i\rangle$ is the reduced matrix element, we obtain the adiabatic formula[151]

$$\begin{aligned} \langle f\|\hat{F}_L\|i\rangle &= \langle I_f\alpha_f(K_f)\|\hat{F}_L\|\alpha_i(K_i)\,I_i\rangle \\ &= [(1+\delta_{K_f0})(1+\delta_{K_i0})]^{-1/2}(-)^{I_f-K_f}[(2I_f+1)(2I_i+1)]^{1/2} \\ &\times\left[\begin{pmatrix} I_f & L & I_i \\ -K_f & K & K_i\end{pmatrix}\langle\alpha_f(K_f)|\hat{F}_{L,\,K=K_f-K_i}|\alpha_i(K_i)\rangle\right. \\ &\left.+(-)^{I_i+K_i}\begin{pmatrix} I_f & L & I_i \\ -K_f & \overline{K} & -K_i\end{pmatrix}\langle\alpha_f(K_f)|\hat{F}_{L,\,\overline{K}=K_f+K_i}|\overline{\alpha_i(K_i)}\rangle\right] \end{aligned} \quad (20)$$

which is the analog of the rigid-rotator formula for the energies. On its basis, one can obtain the so-called *Alaga rules*,[152] or *branching rules*, i.e., the ratios of the probabilities (19) do not depend on the internal matrix elements $\langle\alpha_f(K_f)|\hat{F}_{LK}|\alpha_i(K_i)\rangle$ in the cases when the second term in (20) vanishes. By analogy with the anadiabatic deviations of the energies [see, for example, (8)], there are also anadiabatic deviations from (20), which we shall call *deviations from the Alaga*

[1)] *Translator's Note.* The Russian notation for the trigonometric, inverse trigonometric, hyperbolic trigonometric functions, etc., is retained here and throughout the article in the displayed equations.

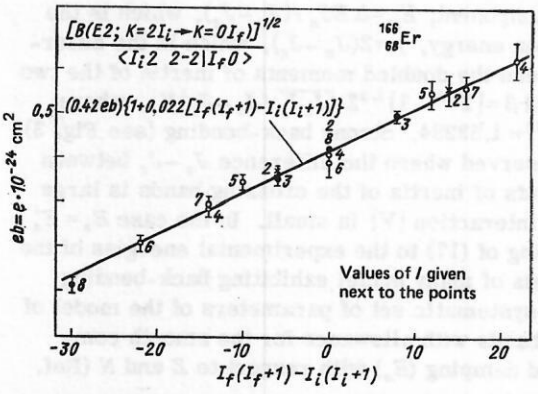

FIG. 4. Anadiabatic effects of band coupling in the probabilities of $E2$ transitions between the γ band ($K=2$) and the ground-state band g ($K=0$) of $^{166}_{68}$Er (Ref. 2).

rules. They are obtained in their simplest and most complete form on the basis of the rotator model or the model of a particle plus a rotator,[153] which takes into account the coupling of the rotational bands through the Coriolis forces, as was done by Mikhaĭlov.[154] This model was subsequently developed with many applications to odd nuclei in a number of papers quoted in Ref. 154a.

A well-known special case of the anadiabatic deviations of the reduced matrix element and, thus, $B(E2)$, within the ground-state (g) band is[4,155]

$$\langle I_f g \| \hat{Q}_2 \| g I_i \rangle = \langle I_f g \| \hat{Q}_2 \| g I_i \rangle_{ad} \left\{ 1 + \frac{1}{2} \alpha [I_f(I_f+1) + I_i(I_i+1)] - 2\sqrt{\frac{2}{3}} \delta \left[I(I+1) - \frac{3}{4} \right] \delta_{if} \right\}, \quad (21)$$

where $\langle I_f g \| \hat{Q}_2 \| \mu I_i \rangle_{ad}$ is given by (20). Also, for transitions between the ground-state band and the β- and γ-vibrational bands we have

$$\langle I_f g \| \hat{Q}_2 \| \mu I_i \rangle = \langle I_f g \| \hat{Q}_2 \| \mu I_i \rangle_{ad} \times \{ 1 + (1/2)\zeta [I_f(I_f+1) - I_i(I_i+1)] \}, \quad \mu = \beta,\ \gamma, \quad (22)$$

where $\zeta = \zeta_0 = 2z_0$ for $\mu = \beta$ and $\zeta = \zeta_2 = z_2$ for $\mu = \gamma$; z_0 and z_2 are the coefficients adopted in the literature (Refs. 156 and 157 and also Refs. 151 and 23) (Fig. 4). The well-known coefficient $\gamma = \gamma_I$ of nonaxial deformation is related to δ by[155]

$$\operatorname{tg} \gamma_I = I(I+1)\,\delta/\sqrt{2}. \quad (23)$$

We give the connection between the parameters $\rho = \delta r^2/r^2$, α, and δ and the relative changes $\delta v/v$ in the volume from the ground 0^+ state to the 2^+ state. The model of a triaxial ellipsoid gives

$$\frac{6}{(\lambda^{-1}+\mu^{-1}+1)(1+\lambda+\mu)} \frac{\delta v}{v} = \rho - 12 \frac{((2\lambda)^{-1}+(2\mu)^{-1}-1)(1-(\lambda+\mu)/2)}{(\lambda^{-1}+\mu^{-1}+1)(1+\lambda+\mu)} \times \left[\alpha - \frac{\delta}{\sqrt{6}} + \frac{\sqrt{6}}{4} \frac{\mu^{-1}-\lambda^{-1}}{(2\lambda)^{-1}+(2\mu)^{-1}-1} \delta \right], \quad (24)$$

where λ and μ are the ratios of the squares of the x and y axes of the ellipsoid to the z axis, and they are given by

$$\frac{1-(\lambda+\mu)/2}{(\lambda\mu)^{1/3}} = \frac{5}{2} \frac{Q_e}{ZA^{2/3}r_0^2}; \quad \frac{\lambda-\mu}{(\lambda\mu)^{1/3}} = \frac{5}{\sqrt{3}} \operatorname{tg} \gamma \frac{Q_e}{ZA^{2/3}r_0^2}. \quad (25)$$

For an ellipsoid of revolution $\gamma = 0$ and $\lambda = \mu$, and (24) reduces to the model given in Ref. 155, which itself generalized the model of Ref. 158. In (25), Q_e is the experimental value of the internal $E2$ moment, and $r_0 = 1.2$ F. Using formula (24), one can find the experimental and theoretical values of $\delta v/v$ from data on ρ, α, and δ.

In the literature, use is sometimes made of the renormalized values $\bar{\alpha}, \bar{\delta}, \bar{z}_0, \bar{z}_2$ (Ref. 23), which are related to our α, δ, z_0, z_2 by

$$\left. \begin{aligned} \alpha &= \bar{\alpha}/(1+\sqrt{3/2}\,\bar{\delta}), \quad z_0 = \bar{z}_0; \\ \delta &= \bar{\delta}/(1+\sqrt{3/2}\,\bar{\delta}), \quad z_2 = \bar{z}_2/(1+2\bar{z}_2). \end{aligned} \right\} \quad (26)$$

We also give the connection of the parameters $\bar{\alpha}$ and $\bar{\delta}$, on the one hand, and $\bar{z}_0$ and $\bar{z}_2$, on the other, in the phenomenological model of coupling of the g, β, and γ bands[159]:

$$\left. \begin{aligned} \bar{\alpha} &= \alpha_0 + \alpha_2, \quad \alpha_0 = 2\bar{z}_0 \frac{B(E2;\ g0 \to \beta 2)}{B(E2;\ g0 \to g2)}; \\ \bar{\delta} &= \sqrt{6}\,\alpha_2, \quad \alpha_2 = \frac{1}{6}\bar{z}_2 \frac{B(E2;\ g0 \to \gamma 2)}{B(E2;\ g0 \to g2)}. \end{aligned} \right\} \quad (27)$$

Attempts have been made to apply the rotator model to even–even nuclei to calculate the anadiabatic effects manifested in the energies and the transition probabilities on the basis of direct coupling with Coriolis forces.[157] However, consistent results were not usually obtained,[151,160] and this made it necessary to introduce additional terms. They can be understood in the sense of Ref. 161, which says that such effects cannot be explained by the coupling of a small number of bands[151] and that one needs a microscopic approach to the coupling of rotations to a large number of quasiparticle modes. Nevertheless, this work did yield empirical information about the coupling of bands, which is given in Ref. 23. This information, in conjunction with additional evaluation of the experimental data made here, will be discussed below in connection with microscopic calculations.

5. THE GROUP APPROACH

Of particular importance in the development of our understanding of nuclear rotation was the group approach initiated by Elliott.[162] He used an $SU(3)$ classification of the states of particles and showed how there arises a separation of the internal and collective motions in a spherical potential through residual interactions. Subsequently, the basis was modified.[163] This approach was used for actual calculations of light nuclei with, for example, an open $2s$–$1d$ shell.[164] In heavier nuclei, groups were generally used for phenomenological parametrization,[165,166] and other groups were also introduced to describe rotations of deformed nuclei. We have here the noncompact groups $SL(3,R)$ (Ref. 167), $T(5) \otimes SO(3)$ (Ref. 168), $CM(3)$ (Ref. 169), and $Sp(6,R)$ (Ref. 170), which make it possible to consider infinite bands. For the transition region, there were considered the groups $Sp(10,R)$ (Ref. 171), and also $Sp(12,R)$ and $N(6) \otimes Sp(12,R)$ (Ref. 172) [$N(6)$ is the Heisenberg group in the notation given in Ref. 173].

For the transition region, semimicroscopic approaches were also developed on the basis of the groups $R(5)$ (Ref. 174) and $SU(6)$ (Ref. 175). However, in Ref. 174 the two-dimensional case is described, and in Ref. 175 the transition to the deformed limit is not particularly clear. In the creation of a microscopic model of

the transition region, an interesting attempt was made to overcome the convergence difficulties of the boson expansions on the transition to deformed nuclei by following an idea taken from the theory of magnetism.[176] This idea was to work with finite boson expansions[177] and give a theory of the transition region.[178] However, in this approach too the microscopic transition to the deformed limit is not clear. We note in this connection the interesting idea of Ref. 179, which introduces a boson for a vibrator with a nonzero initial deformation. In this connection, we also refer to the model described in Ref. 143.

In light nuclei the hopes of exploiting group theory to introduce suitable coordinates for describing collective modes were more or less justified. We have here the methods of K harmonics or hyperspherical harmonics,[180-182] generalized hyperspherical functions,[183] and a method similar to this last one, which uses a group classification of states.[184]

Let us conclude here with an opinion: The less than rapid development in this field is due to the fact that it is only the combination of group approaches with information about the dynamics of the system that can hope for success.

6. TRANSITION OPERATORS IN THE THEORY OF COUPLED BANDS

It is not only from nuclear physics that we are aware of the fundamental part played by various elementary transition operators that generate simple, including collective, excitation modes in physical many-particle systems. Usually, such operators are chosen to have, first, simple algebraic properties (for example, fermion or boson anticommutation or, respectively, commutation relations), second, a relatively simple quasiparticle structure (for example, linear or bilinear combinations of particle creation and annihilation operators), and, third, to be such that the Hamiltonian of the system be expressible in terms of these operators in a relatively simple manner in a certain approximation—the action of these operators on a state which is not excited, including a multiple state, should generate eigenstates of the Hamiltonian, i.e., states representing superpositions of elementary modes (for example, the Hamiltonian should be expressible approximately as a superposition of products of fermion or boson creation operators and the corresponding annihilation operators).

A good example is provided by the phonon operators in the theory of vibrations.[40,48] Indeed, let us consider a space of different rotational bands. We include in the scheme bands based on many-phonon states $|\alpha\rangle$. To this end, we introduce a notation for the index of the α band in terms of the numbers of phonons of different species (n_{μ_1} and n_{μ_2}), i.e., $\alpha=\{n_\mu^\alpha\}=(n_{\mu_1}^\alpha, n_{\mu_2}^\alpha, \dots)$. The creation operator of a phonon of species μ in the space of the vibrational band is[48]

$$B_\mu^+=\sum_{n_\mu, n_{\mu_1}, \dots} n_\mu^{1/2}|n_\mu, n_{\mu_1}, \dots\rangle\langle \dots n_{\mu_1}, n_\mu-1|. \tag{28}$$

The phonons 1) are bosons, since $[B_\lambda, B_\mu^+]=\delta_{\lambda\mu}$; 2) they can be expressed approximately as bilinear combinations of particle creation and annihilation operators [RPA method; see (1)]; conversely, they can be defined exactly as bilinear combinations, but then they have quasiboson commutation relations; 3) the Hamiltonian in the harmonic approximation can be expressed as a bilinear combination of the phonon creation and annihilation operators [RPA method; see (2)].

It is not always possible to combine these three requirements in a simple manner. An example is rotation, in which such operators between states of the same rotational band were introduced in Ref. 185 for $K=0$ bands and in Ref. 127 for all rotational bands. The case of coupling of vibrations with rotations was considered in Ref. 127. In Ref. 186, these papers are reviewed and some symmetry properties of transition operators are derived. Here, we introduce a further generalization of these operators for many-phonon bands $|\alpha IM\rangle$, where α are the quantum numbers of the bands defined above, and I and M are, respectively, the quantum numbers of the angular momentum and its projection (for example, onto the z axis), i.e., the quantum numbers of the given state of the band; by K we denote the lowest I value of the band (its K number). These states may be simply real eigenstates of the many-particle Hamiltonian unknown to us. They may also be states obtained by approximate methods, for example, the Hartree–Fock–Bogolyubov method for the ground state of an even–even nucleus, an RPA-type procedure for one- and two-quasiparticle and vibrational states, etc., and the projection method for obtaining good quantum numbers I and M. To obtain a symmetrized wave function, one uses the rules of the generalized model, $|\alpha IM\rangle_s=[2(1+\delta_{K_\alpha 0})]^{-1/2}[|\alpha IM\rangle + (-)^{I+K_\alpha}|\overline{\alpha} IM\rangle]$ where the second state in the brackets is obtained from the first by a rotation of the internal coordinates in the projection integral (6) and (7) by the angle π around the y axis. We now give the definition of the transition operator:

$$B_{IM}^{\varkappa_2\varkappa_1}=\sum_{\substack{I_1M_1\\ I_2M_2\\ \alpha}} N(\alpha_2, \varkappa_2)N(\alpha_1, \varkappa_1)[(2I_2+1)(2I_1+1)]^{1/2} \times\begin{pmatrix} I & I_1 & I_2\\ K & K_{\alpha_1}-K_{\alpha_2}\end{pmatrix}\begin{pmatrix} I & I_1 & I_2\\ M & M_1-M_2\end{pmatrix} \times(-)^{M_2-K_{\alpha_2}}|\alpha_2=\alpha+\varkappa_2 I_2 M_2\rangle\langle M_1 I_1\alpha_1=\alpha+\varkappa_1|. \tag{29}$$

Here K_α is the K number of the band $|\alpha IM\rangle$; $K=K_{\alpha_2}-K_{\alpha_1}=K_{\varkappa_2-\varkappa_1}=\sum_\mu(n_\mu^{\varkappa_2}-n_\mu^{\varkappa_1})K_\mu$ is the K number of the phonon μ. We introduce the notation

$$N(\alpha,\varkappa)=\prod_\mu[n_\mu^\alpha(n_\mu^\alpha-1)\dots(n_\mu^\alpha-n_\mu^\varkappa+1)]^{1/2}=\prod_\mu\left[\frac{n_\mu^\alpha!}{(n_\mu^\alpha-n_\mu^\varkappa)!}\right]^{1/2}. \tag{30}$$

Formula (29) is a simultaneous generalization of the formula for phonons (28) and for rotons.[185] The linear combination in M_1M_2 is chosen to make the operator (29) an irreducible tensor and thus to have known commutation relations with the angular momentum $\hat{\mathbf{I}}$ (Refs. 187 and 188). The linear combination in I_1I_2 is chosen to make the matrix elements of (29) between states of two bands differing by $\varkappa_2-\varkappa_1=\{n_\mu^{\varkappa_2}-n_\mu^{\varkappa_1}\}$ phonons equal, apart from two factors $N(\alpha,\varkappa)$, to the matrix elements of the D_{KM}^I functions.[187,188] The sum over α means

elimination of projection onto one rotational band. It can be seen that $(B^{\varkappa_2\varkappa_1}_{IM})^+ = (-)^{K_{\varkappa_1}-\varkappa_2+M} B^{\varkappa_1\varkappa_2}_{I-M}$. One can prove corresponding multiplication rules of the type of the rules for D functions.

The multiplication rules make it possible to express all the operators $B^{\varkappa_2\varkappa_1}_{IM}$ as polynomials in $B^+_{\mu' I' M'}$ and $B_{\mu'' I'' M''}$ (in the normal order with the annihilation operators on the right), where $B^+_{\mu IM}$ is the creation operator of a single μ phonon, a special case of $B^+_{\varkappa IM} = B^{\varkappa 0}_{IM}$ for $\varkappa = (n^\varkappa_\mu = 1, n^\varkappa_{\mu 1 \neq \mu} = 0, \dots)$. The rotons[185,186] are expressed as follows: $R^+_{IM} = \sum_\varkappa B^{\varkappa\varkappa}_{IM}$, and they are Hermitian: $R^+_{IM} = (-)^M R_{I-M}$. Further, any single-phonon operator can be expanded in a linear combination of $B^+_{\mu|K\mu|M'} R^+_{I''M''}$, as can be seen from the multiplication rules; here, $B^+_{\mu|K\mu|M}$, is a genuinely single-phonon operator that transmits the smallest possible spin K_μ. Finally, as can be seen from (29), all the operators $B^+_{\varkappa IM}$ commute with one another and with R^+_{IM}. The same is true of all the $B_{\varkappa IM}$. However,

$$[\underbrace{B_{\mu_1 I_1}}_{IM}, B^+_{\mu_2 I_2}] \equiv (-)^{I_1-I_2+M}\sqrt{2I+1}\sum_{M_1M_2}\begin{pmatrix} I_1 & I_2 & I \\ M_1 & M_2 & -M\end{pmatrix} \times (-)^{K_{\mu_1}+M_1}[B_{\mu_1 I_1 M_1}, B^+_{\mu_2 I_2 M_2}]$$
$$= \delta_{\mu_1\mu_2}(-)^{I_1-I_2}\sqrt{2I+1}\begin{pmatrix} I_1 & I_2 & I \\ -K_{\mu_1} & K_{\mu_2} & 0\end{pmatrix} R^+_{IM} \qquad (31)$$

and therefore there are here no simple boson relations. Instead, it turns out that the commutator of the single-phonon annihilation or creation operators of one type reduces to an operator that acts only within one band.

Let us establish the behavior of (29) under the spatial inversion P and time reversal T. We denote by $\Pi_\varkappa = \Pi_\mu(\Pi_\mu)^{n^\varkappa_\mu}$ the spatial parity of the band $|\varkappa IM\rangle$, where Π_μ is the parity of the phonon $B^+_{\mu IM}$. We shall call $\Pi_{\varkappa_2-\varkappa_1} = \Pi_{\varkappa_2}\Pi_{\varkappa_1}$ the spatial parity of the operator $B^{\varkappa_2\varkappa_1}_{IM}$. Then

$$\left.\begin{aligned} PB^{\varkappa_2\varkappa_1}_{IM}P^{-1} &= \Pi_{\varkappa_2-\varkappa_1}B^{\varkappa_2\varkappa_1}_{IM};\\ TB^{\varkappa_2\varkappa_1}_{IM}T^{-1} &= \Pi_{\varkappa_2-\varkappa_1}(-)^{I+M}B^{\varkappa_2\varkappa_1}_{I,-M}.\end{aligned}\right\} \qquad (32)$$

Thus, the components $B^{\varkappa_2\varkappa_1}_{IM}$ have P parity $\Pi_{\varkappa_2-\varkappa_1}$, and the tensor $B^{\varkappa_2\varkappa_1}_{IM}$ (I integral) has T parity $\Pi_{\varkappa_2-\varkappa_1}(-)^I$. In the same case of integral I, we shall use the Hermitial combinations

$$\left.\begin{matrix} O^{\varkappa_2\varkappa_1(+)}_{IM} \\ iO^{\varkappa_2\varkappa_1(-)}_{IM}\end{matrix}\right\} = B^{\varkappa_2\varkappa_1}_{I,M} \pm (-)^M (B^{\varkappa_2\varkappa_1}_{I,-M})^+, \qquad (33)$$

in which $O^{(\pm)}$ has T parity $\pm\Pi_{\varkappa_2-\varkappa_1}(-)^I$ in accordance with (32). In what follows, we shall also use phonon-number operators for phonons of type μ:

$$\hat{n}_\mu = \sum_M B^+_{\mu|K_\mu|M}B_{\mu|K_\mu|M} = B^{\mu\mu}_{00} \qquad (34)$$

with eigenvalue for the state $|\alpha IM\rangle$ equal to n^α_μ and K-number operator,[186] which can also be expressed in terms of (34),

$$\hat{K} = \sum_M (-)^M R^+_{1M}\hat{I}_{-M} = \sum_\mu K_\mu \hat{n}_\mu \qquad (35)$$

with eigenvalue K_α.

We can now see that the algebra of the elementary operators $B^+_{\mu|K\mu|M}$, $B_{\mu K_\mu M}$, R^+_{1M} (and R^+_{2M} for incomplete bands), and $\hat{I}_M$ is closed. One can also prove completeness of such a system of operators in the sense that any transition operator $|\alpha_f I_f M_f\rangle\langle M_i I_i \alpha_i|$ in the state space of all the bands can be constructed in terms of them, and this can be done in the normal order indicated above.

7. EXPANSION OF A PHYSICAL OBSERVABLE WITH WITH RESPECT TO TRANSITION OPERATORS

The algebraic formalism derived above makes it possible to implement a "phenomenology" based, not on empirical considerations, but on an expansion of a physical multipole observable $\hat{F}_{LM}$. Of course, in our choice of the transition operators, which combine the properties of phonons for describing vibrations[48] and D functions for describing rotations,[151] the characteristics of the generalized model are included as a zeroth approximation. Such an expansion was proposed and systematically generalized in Refs. 127, 186, 189, and 190.

We introduce the tensor

$$T_{LM} = \underbrace{\hat{\mathbf{I}}\hat{\mathbf{I}}\cdots\hat{\mathbf{I}}}_{LM}$$

(L times $\hat{\mathbf{I}}$), where $\underbrace{\quad}_{LM}$ denotes the coupling of the factors through Clebsch–Gordan coefficients, in this case, the successive coupling of neighboring factors up to the maximal angular momentum. In particular $T_{LL} = (\hat{I}_{+1})^L$, and any component T_{LM} can be obtained from T_{LL} by commutation with the operator $\hat{I}_{-1}$, which reduces the weight by 0(3).

Then, using the completeness of the system of elementary transition operators (Sec. 6) and the angular-momentum algebra,[187,188] we obtain a general expansion of any irreducible tensor with respect to these operators:

$$\left.\begin{aligned} \hat{F}_{LM} &= \sum_{\varkappa_1,\varkappa_2;\lambda_1,\lambda_2;L_2} f(\varkappa_1,\varkappa_2;\lambda_1,\lambda_2;L_2)(\hat{\mathbf{I}}^2)^{\lambda_2}\underbrace{B^{\varkappa_2\varkappa_1}_{L_2}T_{L_1}}_{LM}(\hat{\mathbf{I}}^2)^{\lambda_1};\\ &\text{where}\\ &L_2 = |K|+1,\ |K|+2,\ \dots\ L;\quad \lambda_2 = 0,\ 1;\\ &L_2 = |K|;\quad \lambda_2 = 0,\ 1,\ \dots\ \min(2|K|,\ 2L);\quad L_1 = |L-L_2|.\end{aligned}\right\} \qquad (36)$$

Thus, in (36) the coupling is up to the maximal angular momentum $L = L_2 + L_1$ if $|K| < L$, and to the minimal $L = L_2 - L_1$ if $|K| \geq L$. We note the symmetry of the expression $B_{L_2}T_{L_1}$ in (36): although the operators B_{L_2} and T_{L_1} do not commute, we can interchange their positions. In (36), we can also use elementary transition operators by

$$B^{\varkappa_2\varkappa_1}_{LM} \sim \underbrace{\prod_\mu (B^+_{\mu|K_\mu|})^{n^{\varkappa_2}_\mu}\prod_\mu (B_{\mu|K_\mu|})^{n^{\varkappa_1}_\mu}}_{L''=|K_{\varkappa_2-\varkappa_1}|}\underbrace{(R^+_2)^m[R^+_1]}_{L'=2m[+1]} \qquad (37)$$
$$L=L'+L'',\ M$$

and find the coefficient of proportionality by applying the multiplication rules of Sec. 6. Here, the coupling to L' is coupling to the maximal possible value $2m$ or $2m+1$, if L' is even or odd; the coupling to L'' is up to the minimal possible value determined by $K = K_{\varkappa_2-\varkappa_1}$, the number in (29); the coupling to L is up to the maximal value.

By means of the expansion (36), the basic problem of separating kinematic and dynamic effects can be solved. Indeed, all matrix elements of combinations of the ele-

mentary transition operators on the right-hand side can be calculated algebraically by means of the rules of Sec. VI, and they will contain the entire kinematics of the dependence on the states, i.e., the dependence on the spins and numbers of the phonons. The entire dynamics resides in their coefficients.

We have two ways of taking into account coupling of the bands. The first is to use an expansion of the Hamiltonian, assuming that the basis $|\alpha IM\rangle$ is not exact and taking into account the influence of the mixing terms on the energies and states. This is similar to the usual method of taking into account band mixing.[151,154] The second is to use an expansion of the multipole moments responsible for the transitions, assuming that the basis is exact, the corrections to the transition probabilities then being obtained from the higher terms of this expansion. We shall investigate both methods in Secs. 8 and 9.

8. MODEL HAMILTONIAN OF CROSSING BANDS

The idea of obtaining a "model" Hamiltonian $\hat{h}$ of coupled bands by truncating the expansion (36) in the special case of zero multipolarity $\hat{F}_{00}=\hat{h}$ was proposed in Ref. 186 and implemented in Refs. 191 and 192. This makes it possible to find the energies of the levels of the crossing bands and obtain the renormalization of the transition probabilities phenomenologically, in the same way as is done when allowance is made for band mixing by Coriolis forces[151,154] by fitting the parameters of $\hat{h}$ to the experiments. However, such an approach can also be combined with microscopic methods of calculating the parameters of the model Hamiltonian and, in particular, the strengths of the coupling (see Sec. 11).

We restrict ourselves to a space of four bands: ground-state band (g), single-phonon bands (β or 0) and (γ or 2), and a "superband" (s or 1) with $K^\pi=1^+$ to realize crossing of bands in the analogous model of back-bending.[144,145] We apply to $\hat{h}$ the expansion (36) for $L=0$, taking into account the Hermiticity and the T parity. We restrict ourselves to terms up to the fourth degree. We use the combinations (33), but for convenience of the calculation we shall, here and in the following section, renormalize B, taking it simply equal to the right-hand side of (37). We modify the result somewhat by introducing the projection operators $P(\hat{n}_\mu)$, $\mu=0,1,2$, where $P(n_\mu)=0$ for $n_\mu=0$ and $P(n_\mu)=1$ for $n_\mu=1,2,\ldots$, and the soft-rotator operator $f^{-1}(\hat{\mathbf{I}}^2)$ given, for example, by (10), (11), or (12). We shall assume that the moment of inertia of the many-phonon bands of one type μ is the same as for the single-phonon band J_μ, i.e., the variations of it due, for example, to the influence of pairing blocking[40] are already saturated by a single phonon. Then

$$\hat{h}=(2J)^{-1}\hat{\mathbf{I}}^2+\sum_{\mu=0,1,2}\{[(2J_\mu)^{-1}-(2J)^{-1}]P(\hat{n}_\mu)\hat{\mathbf{I}}^2+\omega_\mu\hat{n}_\mu\}$$
$$+\chi_0 O_{00}^{\beta g(+)}\hat{\mathbf{I}}^2+\chi_1\sqrt{\frac{3}{2}}\underbrace{O_1^{ig(+)}T_1}_{00}+\chi_2\sqrt{5}\underbrace{O_2^{\gamma g(+)}T_2}_{00}$$
$$+\chi_{10}\sqrt{\frac{3}{2}}\underbrace{O_1^{i\beta(+)}T_1}_{00}+\chi_{12}\sqrt{\frac{5}{2}}\underbrace{O_1^{i\gamma(+)}T_1}_{00}+\chi_{20}\sqrt{5}\underbrace{O_2^{\gamma\beta(+)}T_2}_{00}. \quad (38)$$

The first line is simply the model Hamiltonian of a soft rotator plus harmonic vibrators with allowance for the different moments of inertia of the ground state and the excited states; the second line is the coupling of the ground-state band to the single-phonon bands; and the third is the coupling of the single-phonon bands to each other.

We shall demonstrate the possibility of diagonalizing $\hat{h}$ in (38) in the space of many-phonon bands, restricting ourselves for simplicity to the creation operators of single-phonon states $B^+_{\mu K\mu M}$ with only $K_\mu\geq 0$. To construct the many-phonon states, it is more convenient to use the following creation operators of the β, s, and γ phonons:

$$b_0^+=B^+_{\beta 00}\hat{\mathbf{I}}^2\quad b_1^+=\underbrace{B^+_{s1}T_1}_{00}\quad b_2^+=\underbrace{B^+_{\gamma 2}T_2}_{00}, \quad (39)$$

since 1) they do not change the spin I of the state, being scalars, and 2) $\hat{h}$ in (38) can be expressed very simply in terms of them. After this, it can be seen that $\hat{h}$ does not take us out of the space of the basis many-phonon states

$$|\alpha, IM\rangle=|n_0n_1n_2,\quad IM\rangle=N_\alpha(b_0^+)^{n_0}(b_1^+)^{n_1}(b_2^+)^{n_2}|0,\ IM\rangle, \quad (40)$$

where N_α is a normalization factor; $K=K_\alpha=K_{n_1n_2}=0\cdot n_0+1\cdot n_1+2\cdot n_2$. After fairly lengthy work to establish the algebra of the b^+_μ and b_μ on the basis of the rules of Sec. VI, we can calculate N_α and by means of it find the matrix $\hat{h}$ in the basis (40), where to simplify the notation we omit IM; $D(I,K)=I(I+1)-K(K+1)$:

$$\hat{h}|n_0n_1n_2\rangle=\Big[(2J)^{-1}D(I,0)$$
$$+\sum_{\mu=0,1,2}\{[(2J_\mu)^{-1}-(2J)^{-1}]P(n_\mu)D(I,0)+\omega_\mu n_\mu\}\Big]|n_0n_1n_2\rangle$$
$$+\chi_0 D(I,0)[n_0^{1/2}|n_0-1n_1n_2\rangle+(n_0+1)^{1/2}|n_0+1n_1n_2\rangle]$$
$$+\tfrac{1}{2}\chi_1[(n_1D(I,K-1))^{1/2}|n_0n_1-1n_2\rangle$$
$$+((n_1+1)D(I,K))^{1/2}|n_0n_1+1n_2\rangle]$$
$$+\tfrac{1}{2}\chi_2[(n_2D(I,K-1)D(I,K-2))^{1/2}|n_0n_1n_2-1\rangle$$
$$+((n_2+1)D(I,K+1)D(I,K))^{1/2}|n_0n_1n_2+1\rangle]$$
$$+\tfrac{1}{2}\chi_{10}[((n_0+1)n_1D(I,K-1))^{1/2}|n_0+1n_1-1n_2\rangle$$
$$+(n_0(n_1+1)D(I,K))^{1/2}|n_0-1n_1+1n_2\rangle]$$
$$-\tfrac{1}{2}\chi_{12}[((n_1+1)n_2D(I,K-1))^{1/2}|n_0n_1+1n_2-1\rangle$$
$$+(n_1(n_2+1)D(I,K))^{1/2}|n_0n_1-1n_2+1\rangle]$$
$$+\tfrac{1}{2}\chi_{20}[((n_0+1)n_2D(I,K-1)D(I,K-2))^{1/2}|n_0+1n_1n_2-1\rangle$$
$$+(n_0(n_2+1)D(I,K+1)D(I,K))^{1/2}|n_0-1n_1n_2+1\rangle]. \quad (41)$$

In special cases, this matrix can be decomposed and one can see the physical meaning of the solution that reproduces the band crossing and thus the back-bending.[192]

In the general case, this fairly simple matrix can be diagonalized by a numerical calculation in the complete space of the many-phonon bands. The parameters can be fitted to the experimental energies of the crossing bands. Preliminary results for the nucleus $^{156}_{66}$Dy show that, in contrast to the simple use of the rotation–vibration model,[150] a satisfactory description is here obtained for the energies in the region of the yrast band, i.e., for the levels of the yrast line and those near it.

9. MULTIPOLE MOMENTS

We now apply the expansion (36) to calculation of the reduced matrix elements of the multipole transition operator $\hat{F}_{LM}$ and, thus, of the reduced transition probabilities (19). This is the second approach, the reverse of the usual band-mixing approach.[154] Thus, we can: 1) reproduce, in particular, the results of the generalized model,[151] and 2) give the most general form of the deviations from them, generalizing Ref. 154. The general form of the anadiabatic deviations in one band was derived in Ref. 186; in a space of the ground-state bands and single-phonon bands, in Ref. 189; and in the space of many-phonon bands, in Ref. 190. The deviations from the Alaga rules[152] for the $E2$ moment in one band are compared with the deviations obtained in the standard manner on the basis of the rotator model[154] in Ref. 193 and in the space of the g, β, and γ bands in Ref. 191; in Ref. 194, this result is generalized by the inclusion of a fourth s band ($K^{\pi}=1^{+}$).

Applying the algebra of the transition operators of Sec. 6 and the angular-momentum algebra,[187,188] we find the reduced matrix elements $\hat{F}_{LM}$ (Ref. 190):

$$\begin{aligned}&\langle I_f\alpha_f\|\hat{F}_L\|\alpha_iI_i\rangle\\ &=\sum_{\substack{\varkappa_2\leqslant\alpha_f,\ \varkappa_1\leqslant\alpha_i;\ \lambda_1,\ \lambda_2;\ L_2;\\ \alpha_f-\varkappa_2=\alpha_i-\varkappa_1}} f(\varkappa_1,\ \varkappa_2;\ \lambda_1,\ \lambda_2;\ L_2)\,N(\alpha_f,\ \varkappa_2)\,N(\alpha_i,\ \varkappa_1)\\ &\times(-)^{I_f-K_{\alpha_f}}[(2I_f+1)(2I_i+1)]^{1/2}\begin{pmatrix} I_f & L_2 & I_i\\ -K_{\alpha_f} & K_{\varkappa_2-\varkappa_1} & K_{\alpha_i}\end{pmatrix}\\ &\times 2^{-L_1/2}L_1!\left[\frac{(2I_i+L_1+1)!}{(2L_1)!\,(2I_i-L_1)!}\right]^{1/2}\\ &\times[I_f(I_f+1)]^{\lambda_2}[I_i(I_i+1)]^{\lambda_1}(-)^{I_f+I_i+L}[2L+1]^{1/2},\end{aligned}\tag{42}$$

where

$$\begin{aligned}&L_2=|K_{\varkappa_2-\varkappa_1}|+1,\ |K_{\varkappa_2-\varkappa_1}|+2,\ \ldots\ L;\ \lambda_2=0,\ 1;\\ &L_2=|K_{\varkappa_2-\varkappa_1}|;\ \lambda_2=0,\ 1\ \ldots\ \min(2|K_{\varkappa_2-\varkappa_1}|,\ 2L);\ L_1=|L-L_2|.\end{aligned}$$

We apply[191,194] (36) and (42) to the case when the operator $\hat{F}_{LM}$ is Hermitian and T-even and $L=2,4,\ldots$; as an example, we can consider the $E2, E4,\ldots$ moments. We restrict ourselves to the space of the g, β, s, and γ bands in even–even nuclei and transitions between them. We terminate the expansion (36) at the terms of second degree. The degree of the R^{+} operators is not counted, and the degree of the terms with commutators is assumed to be what it is after the commutation has been performed. These rules are related to the order of magnitude of the corresponding term. We assume that the quantities $B^{\varkappa_2\varkappa_1}_{K\,|M}$ are renormalized, as is explained in the text to formula (38). As a result $([\ldots]$ denotes the commutator and $\{\ldots\}$ the anticommutator, and the terms with the asterisk are important only for the ML moment):

$$\begin{aligned}\hat{F}_{LM}=&a_0R^{+}_{LM}+\frac{a_2}{2}\{R^{+}_{LM},\ \hat{1}^2\}+\frac{a_3}{2}\underbrace{\{R^{+}_{L-1},\ T_1\}^{(*)}}_{LM}\\ &+\frac{a_4}{2}\underbrace{\{R^{+}_{L-2},\ T_2\}}_{LM}+b_0O^{\beta g(+)}_{00}R^{+}_{LM}+\frac{b_1}{2i}O^{\beta g(-)}_{00}[R^{+}_{LM},\ \hat{1}^2]\\ &+\frac{b_3}{2}O^{\beta g(+)}_{00}\underbrace{\{R^{+}_{L-1},\ T_1\}^{(*)}}_{LM}+c_0\underbrace{O^{sg(+)}_{1}R^{+}_{L-1}}_{LM}\\ &+\frac{c_1}{2i}[\underbrace{O^{sg(-)}_{1}R^{+}_{L-1}}_{LM},\ \hat{1}^2]+\frac{c_3}{2}\underbrace{\{\underbrace{O^{sg(+)}_{1}R^{+}_{L-2}}_{L-1},\ T_1\}}_{LM}\\ &+d_0\underbrace{O^{\gamma g(+)}_{2}R^{+}_{L-2}}_{LM}+\frac{d_1}{2i}[\underbrace{O^{\gamma g(-)}_{2}R^{+}_{L-2}}_{LM},\ \hat{1}^2]\\ &+\frac{d_3}{2}\underbrace{\{\underbrace{O^{\gamma g(+)}_{2}R^{+}_{L-3}}_{L-1},\ T_1\}}_{LM}+bB^{\beta\beta}_{00}R^{+}_{LM}+cB^{ss}_{00}R^{+}_{LM}\\ &+dB^{\gamma\gamma}_{00}\ R^{+}_{LM}+f_0\underbrace{O^{s\beta(+)}_{1}R^{+}_{L-1}}_{LM}+g_0\underbrace{O^{s\gamma(+)}_{1}R^{+}_{L-1}}_{LM}+h_0\underbrace{O^{\gamma\beta(+)}_{2}R^{+}_{L-2}}_{LM}.\end{aligned}\tag{43}$$

The reduced matrix elements (42) are illustrated in Table II for the case $L=2$ ($E2$ moment) of the operator $\hat{F}_{2M}=\hat{Q}_{2M}$ in formula (43). It can be seen from Table II that the known coefficients determining the deviations from the Alaga rules for the g–g, g–β, and g–γ transitions, augmented by the δ we have introduced, are related to the coefficients of the expansion (43) as follows:

$$\left.\begin{aligned}&\alpha=a_2/a_0;\ \zeta_0=2z_0=-b_1/b_0;\\ &\delta=a_4/a_0;\ \zeta_2=z_2=-d_1/d_0.\end{aligned}\right\}\tag{44}$$

Using (42) and Table II, we can solve the problem of separating the kinematic effects from the dynamical. The kinematics, or the dependence on the initial and final states through the spins I_i and I_f and the phonon numbers α_i and α_f, is calculated explicitly. The entire dynamics resides in the coefficients, which do not de-

TABLE II. Reduced matrix elements of the $E2$ moment between states of the g, β, s, and γ bands.

Transition				Reduced matrix element $\langle I_f\alpha_f\|\hat{F}_{L=2}\|\alpha_iI_i\rangle$
α_f	α_i	zeroth order	first order	second order
g	g	a_0^*		$+\frac{1}{2}a_2[I_f(I_f+1)+I_i(I_i+1)]$
				$-2\sqrt{\frac{2}{3}}a_4\left[I(I+1)-\frac{3}{4}\right]\delta_{if}$
β	β	a_0^*		$+b^*+\frac{1}{2}a_2[I_f(I_f+1)+I_i(I_i+1)]$
				$-2\sqrt{\frac{2}{3}}a_4\left[I(I+1)-\frac{3}{4}\right]\delta_{if}$
s	s	a_0^*		$-\sqrt{\frac{1}{3}}c^*+\frac{1}{2}a_2[I_f(I_f+1)+I_i(I_i+1)]$
				$-2\sqrt{\frac{2}{3}}a_4\left[I(I+1)-\frac{3}{4}\right]\frac{I(I+1)}{I(I+1)-3\times1^2}\delta_{if}$
γ	γ	a_0^*		$+\sqrt{\frac{1}{5}}d^*+\frac{1}{2}a_2[I_f(I_f+1)+I_i(I_i+1)]$
				$-2\sqrt{\frac{2}{3}}a_4[I(I+1)-\frac{3}{4}]$
				$\times\frac{I(I+1)}{I(I+1)-3\times2^2}\delta_{if}$
g	β		b_0^*	$-\frac{1}{2}b_1[I_f(I_f+1)-I_i(I_i+1)]$
g	s	$-\sqrt{\frac{1}{2}}c_0^*$		$+\frac{1}{2}\sqrt{\frac{1}{2}}c_1[I_f(I_f+1)-I_i(I_i+1)]$
				$-\sqrt{\frac{1}{2}}c_3[I_i\delta_{I_f,\,I_i+1}-(I_i+1)\delta_{I_f,\,I_i-1}$
				$+\frac{(2I-1)(2I+3)}{3}\delta_{if}]$
g	γ		d_0^*	$-\frac{1}{2}d_1[I_f(I_f+1)-I_i(I_i+1)]$
s	β			$\sqrt{\frac{1}{2}}f_0^*$
s	γ			$\sqrt{\frac{3}{10}}g_0^*$
β	γ			h_0^*

Note. In units of $(-)^{I_f-K_f}[(2I_f+1)(2I_i+1)]^{1/2}\begin{pmatrix} I_f & L=2 & I_i\\ -K_f & K_f-K_i & K_i\end{pmatrix}$

*The adiabatic terms of the generalized model of Ref. 151 are indicated. In the terms with $\delta_i, I=I_f=I_i$ (Refs. 191 and 194).

pend on the states, f. Further, it can be seen that the reduced matrix elements have been derived in a model-independent manner, in contrast to the well-known derivations.[154] Formula (42) reproduces the adiabatic reduced matrix elements of the generalized model[151] or the Alaga rules (20) (Ref. 152) if the state is symmetrized and in (42) only the $\lambda_1=\lambda_2=0$, $L_2=L$ terms are taken. Finally, (42) generalizes the well-known results[154] on the deviations from the Alaga rules in two respects: 1) the dependence on the spins I_i and I_f of the states is obtained without the restrictions of Ref. 154, and 2) the dependence on the phonon nunbers α_i and α_f is obtained.

10. GENERALIZED EQUATION-OF-MOTION METHOD

The equation-of-motion method[48] for vibrations [see (2)] can be generalized in the case of coupled modes.[195] We consider a basis of the space of many-particle states of the nucleus; it can, for example, be $|\alpha IM\rangle$ (see Sec. 6 . Here, we shall simply denote it as $|\alpha\rangle, |\beta\rangle$. We shall distinguish it from the usually employed deformed basis consisting of the Hartree–Fock–Bogolyubov vacuum $|\ \rangle$ and the quasiparticle excited states $|i\rangle, |k\rangle$. We denote all the transition operators considered in Sec. 6 by $\hat{r}_\mu$, from which it can be seen that their matrix elements, i.e., $r^{(\mu)}_{\alpha\beta}$, are known by definition in the basis $|\alpha\rangle$:

$$\hat{r}_\mu=\sum_{\alpha\beta} r^{(\mu)}_{\alpha\beta}|\alpha)(\beta|, \tag{45}$$

but not in the basis $|i\rangle$. Finding them in the basis $|i\rangle$ amounts to finding the quasiparticle structure in accordance with the example of finding the coefficients y and z in (1). Conversely, our physical observables $\hat{F}_{LM}$ are known in the basis $|i\rangle$. These are, for example, the two-particle $\hat{H}$ or the single-particle EL and ML moments $\hat{Q}_{LM}$ and $\hat{M}_{LM}$. In the basis $|\alpha\rangle$, only the general form of their expansion (36) has been proposed, and they are as yet unknown, since the coefficients f are unknown. Instead of following the usual procedure and seeking the connection between the bases $|\alpha\rangle$ and $|i\rangle$, it may be simpler to find the structure of $\hat{r}_\mu$ in $|i\rangle$, and ultimately directly the structure of $\hat{F}$ in $|\alpha\rangle$, which solves the problem.

We begin with the problem of the structure of $\hat{r}_\mu$ in the basis $|i\rangle$. We assume that the parameters $p=\{p_j\}$ on which $\hat{h}=\hat{h}(p)$ depends are chosen in such a way that for a space of definite low-lying states $|\alpha\rangle$, $\alpha\in D$, the Hamiltonian $\hat{h}$ has the same eigenstates and energies as $\hat{H}$. Then, if $|\ )$ is any linear combination of $|\alpha\rangle$, $\alpha\in D$,

$$(\hat{H}-\hat{h})|)=0. \tag{46}$$

Suppose that we have chosen r_μ satisfying the operator equation

$$[\hat{H}-\hat{h},\ \hat{r}_\mu]=0, \tag{47}$$

which is our generalized equation of motion. Equation (47) is the necessary and sufficient condition that $\hat{r}_\mu$ have no matrix elements coupling the space D_n of the eigenstates of $\hat{H}-\hat{h}$ with eigenvalue E_n to any other $D_m, E_m\neq E_n$. In particular, (47) is the sufficient condition for $\hat{r}_\mu$ to have no matrix elements coupling $D=D_0, E_0=0$ to $D=\sum_{n\neq 0}D_n, E_n\neq 0$.

If we have found one state $|\ )$ satisfying (46) and solutions of the dynamical equations (47) satisfying the additional kinematic conditions (45), we can recover the complete basis $|\alpha\rangle$ of the space D. This follows from the completeness of $\hat{r}_\mu$ (see Sec. 6 . In practice, $|\ )$ is identified in the first approximation with the Hartree–Fock–Bogolyubov vacuum $|\ \rangle$ for $\hat{H}-\hat{h}$ (and sometimes in the zeroth approximation simply for $\hat{H}$). The inclusion of $\hat{h}$ amounts to solving the Hartree–Fock–Bogolyubov problem for $\hat{H}$ with the restrictions imposed by the different terms of $\hat{h}$ in (38), the physical meaning of which will be elucidated below.

We now turn to the choice of the microscopic Hamiltonian $\hat{H}$. Although the method enables us to choose $\hat{H}$ in general form, the expressions simplify strongly if we restrict ourselves to factorizable interactions. Therefore,

$$H=\hat{H}_0+H_P+H_Q, \tag{48}$$

where $\hat{H}_0$ is the diagonal part of the Hartree–Fock–Bogolyubov Hamiltonian:

$$\hat{H}_0-\sum_{\sigma=p,\ n}\lambda_\sigma\hat{N}_\sigma=\sum_j E_j\alpha_j^+\alpha_j; \tag{49}$$

$\hat{H}_P$ is in general a multipole pairing[51]

$$H_P=-\frac{1}{4}\sum_{\substack{\mu=-\lambda\\ \lambda;\ \sigma=p,\ n}}^{\lambda} g^\sigma_{\lambda\mu}:\hat{P}^{\sigma+}_{\lambda\mu}\hat{P}^{\sigma}_{\lambda\mu}: \tag{50}$$

$\hat{H}_Q$ includes not only a multipole ($\tau=+$) but also a spin-multipole ($\tau=-$) interaction[40]:

$$\hat{H}_Q=-\frac{1}{2}\sum_{\substack{\mu=-\lambda\\ \lambda;\ \tau=\pm;\ \sigma,\ \sigma'=p,\ n}}^{\lambda} \varkappa^{\tau\sigma\sigma'}_{\lambda\mu}:\hat{Q}^{\tau\sigma+}_{\lambda\mu}\hat{Q}^{\tau\sigma'}_{\lambda\mu}: . \tag{51}$$

The notation :...: in (50) and (51) presupposes a normal product with respect to the Bogolyubov quasiparticles, i.e., the residual interaction obtained by subtracting the Hartree–Fock–Bogolyubov part, since this last must be reproduced by means of formula (49). In the nonexchange approximation, this amounts to subtracting from each operator $\hat{P}$ and $\hat{Q}$ its expectation value with respect to the Hartree–Fock–Bogolyubov vacuum $|\ \rangle$.

In the detailed formulas of Sec. 11 and in the practical calculations of Secs. 12 and 13, we shall restrict ourselves to monopole pairing: $\hat{P}^\sigma, g^\sigma_{00}=G_\sigma$ and quadrupole interaction: $\hat{Q}^\sigma_{2\mu}, \varkappa^{+\sigma\sigma'}_{2\mu}=\varkappa^{\sigma\sigma'}_{\mu}$ (Ref. 40), and we shall return to a more general form in Sec. XIV.

11. GENERALIZED DENSITY MATRIX

The well-known concept of the generalized density matrix $\varkappa_{ij}=\langle|\hat{\varkappa}_{ij}|\rangle$ (Ref. 40) with the operator matrix

$$\hat{\varkappa}_{ij}=\begin{pmatrix}\hat{\rho}_{ij} & -\hat{\sigma}^+_{ij}\\ \hat{\sigma}^+_{ij} & \delta_{ij}-\hat{\rho}^+_{ij}\end{pmatrix} \tag{52}$$

and $\hat{\rho}_{ij}=a_j^+a_i$, $\hat{\sigma}_{ij}=a_ia_j$, is very convenient for working with not only single-particle $\hat{Q}$ operators (51) but also the operators $\hat{P}$ (50), which do not conserve the particle number. If $|\ \rangle$ is the quasiparticle vacuum, the matrices ρ_{ij} and σ_{ij} are connected on account of the relation $\varkappa^2=\varkappa$ (Ref. 40).

This method can be combined with the method of coherent states.[108,110] A suitable state for one rotational

band was first introduced in Ref. 186. It was then generalized to complex angular momenta[189] and to three[191] and four[194] interacting bands. To be specific, we shall consider four coupled bands in deformed even–even nuclei, namely, ground-state (g), β vibrational (β), superband (s), and γ vibrational (γ).[191,194] We begin by making more precise the elementary transition operators and their combinations that we shall use. In addition to the angular momentum components $\hat{I}_M$, we also introduce the following "selected" elementary operators:

$$\left.\begin{aligned} &\hat{r}_r^{(+)}=\frac{\mathrm{i}}{\sqrt{6}}(R^+_{2,1}+R^+_{2,-1});\quad \hat{r}_r^{(-)}=\frac{1}{\mathrm{i}}\hat{r}_r^{(+)};\\ &\hat{r}_\mu^{(\pm)}=\frac{(\pm)^K}{1+\delta_{K,0}}(Q^{\mu g}_{K,K}(\pm^{(-)^K})+(-)^K Q^{\mu g}_{K,-K}(\pm^{(-)^K}));\\ &\mu=\beta,s,\gamma;\quad K=|K_\mu|=0,1,2. \end{aligned}\right\} \tag{53}$$

There are seven of them: $\hat{r}_r^{(+)}$, $\hat{r}_\mu^{(\pm)}$, $\mu=\beta$; s and γ, which are Hermitian and T-even; and $\hat{r}_r^{(-)}$, which is anti-Hermitian and T-odd. We introduce the coherent state

$$|x\rangle=\exp\Big[\mathrm{i}\sum_{\substack{\varepsilon=+,-\\ \varkappa=r,\beta,s,\gamma}} x^\varepsilon_\varkappa \hat{r}^{(\varepsilon)}_\varkappa\Big]|\rangle \tag{54}$$

and the extended density matrix with expectation value with respect to $|x\rangle$ instead of $|\ \rangle$:

$$\begin{aligned} &\varkappa_{ij}(x)=\langle x|\hat{\varkappa}_{ij}|x\rangle\\ &=\sum_{\nu_r^\pm,\nu_\beta^\pm,\nu_s^\pm,\nu_\gamma^\pm}\varkappa_{ij}^{(\nu_r^\pm\nu_\beta^\pm\nu_s^\pm\nu_\gamma^\pm)}(x_r^-)^{\nu_r^+}\dots(x_\sigma^-)^{\nu_\sigma^+}. \end{aligned} \tag{55}$$

On the right-hand side of (55), we have $\varkappa_{ij}^{(\nu_r^\pm\nu_\beta^\pm\nu_s^\pm\nu_\gamma^\pm)}$, which are proportional to the $\nu_r^\pm$, $\nu_\beta^\pm$, $\nu_s^\pm$, $\nu_\gamma^\pm$-th derivative with respect to the parameters $x_r^\pm$, $x_\beta^\pm$, $x_s^\pm$, x_γ. The physical meaning of the parameters x can be elucidated by means of

$$\left.\begin{aligned} &\langle x|\hat{I}^2|x\rangle=\langle|\hat{I}^2|\rangle+(x_r^+)^2,\quad (x_r^-=0);\\ &\langle x|\hat{n}_\mu|x\rangle=\langle|\hat{n}_\mu|\rangle+\frac{2}{1+\delta_{K,0}}[(x_\mu^+)^2+(x_\mu^-)^2],\quad \mu=\beta,s,\gamma. \end{aligned}\right\} \tag{56}$$

Thus, the state (54) not only conserves the angular momentum but also the phonon numbers.

We are now in a position to formulate a unified microscopic theory of coupled rotation–vibration modes. For $\hat{F}_{LM}$, the EL moment ($L=2,4,\dots$), we can use the technique set forth in Sec. VI, and for the angular momentum, the technique considered in Refs. 187 and 188. After lengthy transformations, we can determine all the coefficients of the expansion (43) and thus (see Table II) as linear combinations of the traces $\mathrm{Tr}(F_{LM}\rho^{(\nu_r^\pm\dots\nu_\gamma^\pm)})$. They are derived explicitly in Refs. 155, 189, 191, and 194. The unified approach is illustrated schematically in Fig. 5 for three bands together with the order of the effect (the degree of the parameters x).

Explicit microscopic expressions for the traces (see Fig. 5) can be found by combining the methods presented in Secs. 10 and 11. This leads to the dynamical equation

$$\langle x|[\hat{\varkappa}_{ij},\hat{H}-\hat{h}]|x\rangle=0. \tag{57}$$

In Ref. 155 the traces were found for one band, in Ref. 191 for three coupled bands, and in Ref. 194 with a generalization to a fourth superband. In conjunction with the kinematic conditions (56), the solutions (57) lead to a complete microscopic determination of the coefficients of the expansion of the model Hamiltonian (38) and

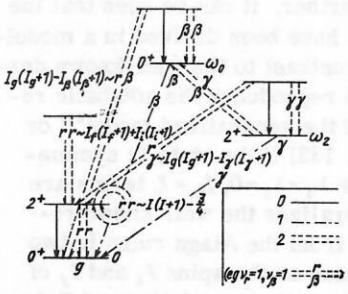

FIG. 5. Statistical and probability effects of the $E2$ moment $\hat{Q}^p_{2M}$ up to second order in the expansion of the density matrix for three bands: the ground-state (g), the beta (β), and the gamma (γ) in even-even nuclei. The matrix element determining the effect is proportional to $\mathrm{Tr}(Q_{2M}\rho^{\nu_r\nu_\beta\nu_\gamma})$, and the order of the effect $\nu=\nu_r+\nu_\beta+\nu_\gamma=0,1,2$ ($\nu_\mu=\nu_\mu^+ + \nu_\mu^-$) and its type (rotation r, β vibration β, and γ vibration γ) (Ref. 191).

the EL moments (43) and Table II, i.e., to the possibility of fairly simple calculations of all energy and probability effects.

As is shown in Ref. 191, the formulas of the zeroth and first order without allowance for the superband completely reproduce the RPA results for vibrations and the cranking model for rotation[40] (see the calculations in Sec. 12). However, allowance for the superband leads to a renormalization of the RPA and the cranking results.[194] Such a renormalization occurs even without the superband if one takes into account the terms of the "direct" coupling with the coefficients χ in the model Hamiltonian (38) (Ref. 196). The second-order formulas make it possible to calculate the effects of rotation–vibration coupling, for example, the anadiabatic corrections to the Alaga rules (see Sec. 13) and the deviations in the internal moments within and between the bands.[191]

12. COLLECTIVE PARAMETERS OF EVEN–EVEN NUCLEI

We consider the following adiabatic parameters, which are related to the energies of the levels and to the $E0$, $M1$, and $E2$ moments for the proton (p) and neutron (n) systems: the mean-square radius r^2, the internal quadrupole moment Q, the moment of inertia J, the collective gyromagnetic ratio g_R, and $B(E2)$, which are the reduced probabilities of the $E2$ transitions $g0\to\beta2\,B_{g\beta}$ and $g0\to\gamma2\,B_{g\gamma}$. They can be calculated[197] in the unified formalism of Sec. 11 by using a deformed Woods–Saxon basis[198] and a pairing-plus-quadrupole interaction.[40] We classify, in accordance with Fig. 5, r^2 and Q as effects of zeroth order, and the remainder, J, g_R, $B_{g\beta}$, and $B_{g\gamma}$, as first-order effects. As is shown at the end of Sec. 11, for them such an approach will not differ from the standard RPA and cranking approaches, except for the individual choice of the interaction parameters (see Sec. 13).

Calculations of r^2 and Q have frequently been made,[40] and the result is related to the choice of the parameters of the Woods–Saxon potential well[198] and to the problem of the relationship between the size and deformations of the potential well with respect to the

charge. Empirical information can be obtained for r^2 from Ref. 199 and for Q from Ref. 200. We shall not here give the results of the calculations of Ref. 197, but merely say that the theoretical values are systematically lower than the experimental ones by 10–15%. Nor shall we dwell on the results of calculations of $B_{g\beta}$ and $B_{g\gamma}$. Empirical information can be found in Refs. 69, 23, and 201. Quantitative agreement can be achieved by introducing effective charges, the physical reasons for which and the numerical aspects of which are considered in detail in Ref. 40. In the calculations made by Solov'ev's group, there are indications that one can also manage without charges by introducing a quadrupole interaction $\varkappa_\mu^{pp} = \varkappa_\mu^{nn} \neq \varkappa_\mu^{pn}$.

On the basis of the cranking model, calculations have been made of the moment of inertia and the collective gyromagnetic ratio. For them, empirical information can be obtained: for J from the energies of the 2^+ states,[202] and for g_R from Ref. 203. Calculations in the single-particle Nilsson basis showed that the large discrepancy (by a factor 2–3) of the moment of inertia from the experimental value can be eliminated by the introduction of pairing, though the theoretical values are systematically (by 10–30%) below the experimental ones.[204-206] Calculations in the more realistic Woods–Saxon basis (Refs. 206a, 206b, and 197) showed that, compared with the Nilsson basis, the theoretical values of J are even more underestimated, on the average by 30% with respect to the experimental values (Table III); the collective gyromagnetic ratios g_R have also been calculated. In contrast to J, which represents the behavior of both systems of protons (p) and neutrons (n), g_R is sensitive to the ratio of the p moment of inertia to the total moment of inertia in the absence of spin polarization.

Thus, the old problem of the moment of inertia has still not been solved in the 15 years up to now. Because of the time parity of the multipole operator, the multipole interactions do not influence the result. Spin–multipole interactions, which make a correction of the order of the discrepancy,[207] actually make matters worse rather than better, as is asserted in Ref. 207, because of the incorrect sign of the constant. On the other hand, quadrupole pairing leads to an improvement, again of the same order.[51] However, the agreement with the experiment of Ref. 51 is an illusion, since the two effects are compensated when taken into account consistently.[208] On the other hand, the correction in Ref. 209 is equivalent to allowance for the rotational correlations in the ground state[210,211] and again leads to an illusory improvement, which is compensated by a deterioration of the same order when allowance is made for rotation anadiabatically.[211,212] In connection with the compensation of interactions of different type, we mention the new paper of Wakai and Faessler (see Sec. 15), in which changes in the picture are reported but there are no changes in the final conclusions.

TABLE III. Moment of inertia J and collective gyromagnetic ratio g_R.

Nucleus	ThWS			ThN		Experiment	
	J	g_R^{free}	g_R^{pol}	J	g_R^{pol}	J	g_R
$^{152}_{62}$Sm	18.922	0.429	0.425	19.9	0.44	24.637	0.370
$^{154}_{62}$Sm	22.494	0.437	0.432	25.75	0.38	36.563	0.377
$^{154}_{64}$Gd	18.649	0.426	0.422	19.6	0.48	24.363	0.375
$^{156}_{64}$Gd	23.009	0.388	0.389	25.2	0.39	33.720	0.373
$^{158}_{64}$Gd	26.088	0.387	0.389	29.4	0.36	37.731	0.342
$^{160}_{66}$Dy	21.225	0.366	0.372	25.85	0.37	34.566	0.364
$^{162}_{66}$Dy	23.454	0.334	0.345	26.15	0.38	37.193	0.350
$^{164}_{66}$Dy	25.833	0.265	0.283	26.05	0.39	40.876	0.342
$^{164}_{68}$Er	21.156	0.362	0.369	25.9	0.38	32.826	0.352
$^{166}_{68}$Er	24.536	0.317	0.329	27.9	0.36	37.235	0.316
$^{168}_{68}$Er	26.940	0.325	0.333	29.8	0.34	37.593	0.324
$^{170}_{68}$Er	28.693	0.276	0.289	31.6	0.31	37.831	0.332
$^{170}_{70}$Yb	24.185	0.334	0.342	30.0	0.36	35.604	0.334
$^{172}_{70}$Yb	26.492	0.311	0.319	32.8	0.34	38.387	0.324
$^{174}_{70}$Yb	26.397	0.304	0.315	33.45	0.32	39.241	0.333
$^{176}_{70}$Yb	27.119	0.291	0.304	30.45	0.35	36.527	0.325
$^{174}_{72}$Hf	22.704	0.283	0.294	30.5	0.34	32.963	—
$^{176}_{72}$Hf	24.088	0.268	0.281	31.45	0.30	33.967	0.266
$^{178}_{72}$Hf	23.601	0.283	0.298	28.05	0.32	32.199	0.267

Note. The calculation (Th) for free nucleons g_R^{free} ($g_S - g_S^{free}$) and with renormalization for polarization effects g_R^{pol} ($g_S = 0.6 g_S^{free}$) (Ref. 206) in the Woods–Saxon (WS) basis (Ref. 197) and Nilsson basis (N) (Ref. 206). The average experimental errors are 0.05–0.3% for J and 2–5% for $2g_R$.

13. ANADIABATIC EFFECTS IN EVEN–EVEN NUCLEI

In the literature, various anadiabatic effects have been taken into account in the cranking model; these result in a variation of the moment of inertia, or the higher coefficients of the expansion (8), with the spin and with it anadiabatic corrections to the energies. The main effect was found to be Coriolis antipairing (see Sec. 15), on the basis of which allowance was made for the breaking of the pairing with the spin and B was calculated, and sometimes also the following coefficients in (8) (Refs. 213–217) and the coefficients of the variable-moment-of-inertia model.[218] This was also done for odd nuclei.[219] Some of these papers took into account other effects as well, such as centrifugal stretching and the higher orders of the cranking model, which were calculated together in the most complete form in Ref. 220. In some papers, phenomenological arguments were used to calculate the anadiabatic effects not only in the energies but also in the transition probabilities (Refs. 221–223). Subsequently, the cranking model was compared with the projection method in the language of Green's functions[224] and used for calculations of the anadiabatic variations with the spin of the nuclear radii (and thus Mössbauer and muonic isomer shifts)[225,226] and the quadrupole moments (and thus the transition probabilities in the ground-state band).[227] The model was also developed for the transition probabilities between bands.[228] This model is unsatisfactory because of its quasiclassical nature (classical rotation of the potential well or conservation of the spin on the average) and two dimensionality (neglect of the quantum uncertainty of the rotation axis).

Here, we shall consider in more detail calculations of the anadiabatic parameters[197] in accordance with the unified formalism of Sec. 11; these parameters are associated with the $E0$ and $E2$ moments of the nuclei, which characterize the static charge and mass distributions and the probabilities of $E2$ transitions. In accordance with the classification of Fig. 5, these are

second-order effects: $\rho = \delta r^2/r^2$, the relative variation of the mean-square radius between the 0^+ ground state and the first 2^+ state (for experimental results, see Ref. 229; theory and additional experimental data can be found in Refs. 225 and 226), and the parameters of the anadiabatic corrections to $B(E2)$ within the ground-state band (21): $\alpha - \delta/\sqrt{6}$, the axial deformability with the spin (for experiments on α, see Refs. 230 and 23; for the theory, Refs. 227, 228, and 88), δ, the nonaxial deformability [an indirect experiment evaluated here from the branching ratios[69,23,201] and the data on z_2 in accordance with formula (27)], and between the g and β,γ bands (22), which are characteristics of the rotation–vibration coupling, z_0 and z_2 (the experiment is presented here as the means of the error-weighted values collected in Refs. 223 and 23 and on the basis of our evaluation of the branching ratios[69]; for the theory, see Refs. 228 and 88). Some calculations of Refs. 88 and 197 are compared in Ref. 231.

The calculations of Ref. 197 were made in two variants: 1) ThS with the Standard Woods–Saxon potential, the same for groups of nuclei near $A = 155, 165, 173, 181$, as in Ref. 198, and 2) ThV, in which Woods–Saxon parameters were varied individually to describe r^{2p}, Q^p, and the single-particle levels. The pairing, G_σ, and quadrupole-interaction, $\varkappa_\mu$, constants were determined individually by fitting the odd–even mass differences[232] and the energies of the β and γ levels[202] without the usual smoothing over a group of nuclei,[40] it being assumed that $\varkappa_\mu^{\sigma\sigma'} = \varkappa_\mu$, $\omega_1 = 0$.

The results of the calculations of Ref. 197, together with the additional calculations of Ref. 232a, presented here for the first time only for the p system, are presented and compared with the re-evaluated experiment in Figs. 6–10.

Calculations of the parameters ρ, α, and δ within the ground-state band cannot be easily compared with experiment, since there are few data for ρ and α, and for

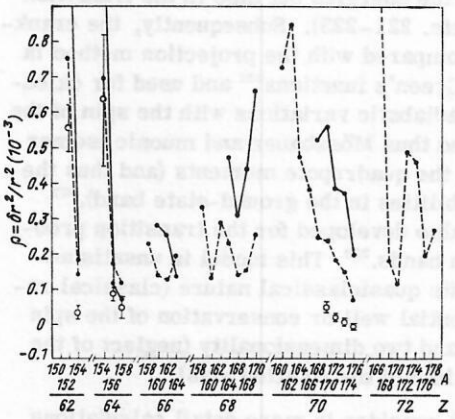

FIG. 6. Relative changes in the mean-square radius $\rho = \delta r^2/r^2$ from the 0^+ ground state to the 2^+ state calculated in two variants. The dashed lines represent ThS (standard values of the Woods–Saxon potential with the experimental value of J); the continuous lines represent ThV (varied Woods–Saxon potential with experimental value of J); the points are experimental values. The experimental data are taken from the papers described in detail in Sec. 13.

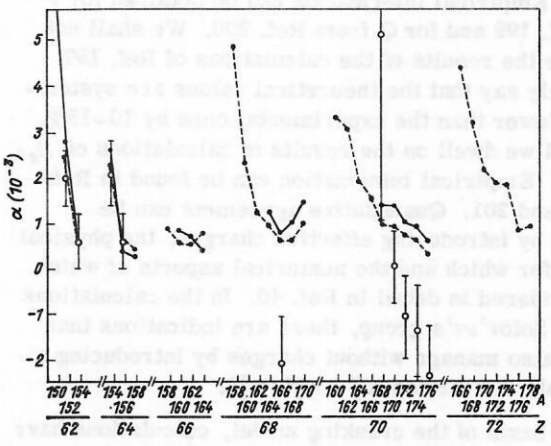

FIG. 7. Parameter α of the anadiabatic, predominantly axial changes of the $E2$ moment within the g band; the remaining notation is as in Fig. 6.

δ there are no direct measurements. Nevertheless, one gets the impression that in the region of the nuclei $_{62}$Sm and $_{64}$Gd the values of ρ, α, and δ are well reproduced, including the increase in soft nuclei. This is natural, since the soft nuclei have a higher deformability. With regard to the region around $_{70}$Yb, one can say here the same for δ, but not for ρ and α, for which the experiment can give negative values, and the theory does not reproduce this sign. The reason for the $\rho<0$ effects can be seen in Ref. 225, in which density-dependent δ forces reproduce this sign. Then the discrepancy here may be due to the fact that the schematic quadrupole interaction does not reproduce well the effective forces in the particle–particle channel. With regard to $\alpha<0$, the experiment in the region of $_{70}$Yb is not direct and therefore is not particularly reliable. We shall return to this question below in connection with the discussion of direct lifetime experiments. The positive sign of δ indicates a contraction along y and an elongation along x (x is the rotation axis), which contradicts the expectations drawn from analogy with the behavior of a solid, but corresponds to the expectations for the behavior of a superfluid.[155] It is also interesting that whereas δ is an order of magnitude smaller than α

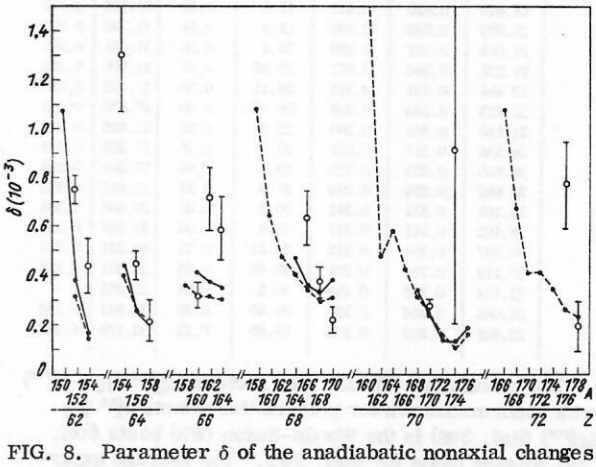

FIG. 8. Parameter δ of the anadiabatic nonaxial changes in the $E2$ moment within the g band; the remaining notation is as in Fig. 6.

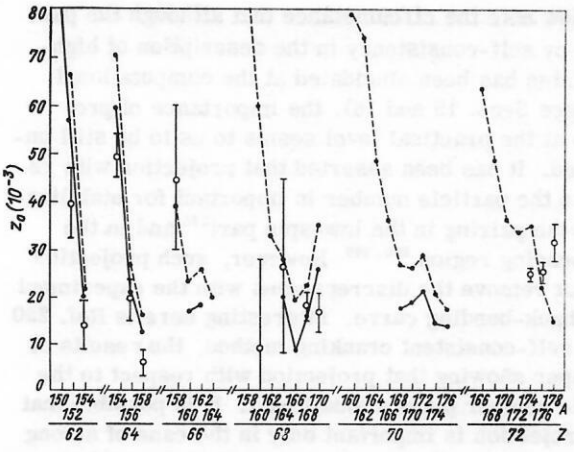

FIG. 9. The parameter z_0 of the anadiabatic changes of the $E2$ moment between the g and β bands; the remaining notation is as in Fig. 6.

for the soft nuclei, for the well-deformed nuclei these two are comparable. Thus, in the deformed nuclei the nonaxial deformability with the spin may play an important part.

The calculations of the anadiabatic effects between the bands, z_0 and z_2, reveal good reproduction of the values and the systematic tendencies. It can be seen that the corrected Woods–Saxon variant ThV reproduces the experimental results better. It is hard to make a comparison with other investigations, since the calculation depends, as the present investigations have shown, on the type of microscopic model and its parameters. Comparison with the semiphenomenological calculations of Marshelek[223] shows that they reproduce correctly the order of magnitude of z_0 and z_2. Note the excellent reproduction (see Fig. 10) of one of the best experiments (see Fig. 4) on z_2 for $^{166}_{68}$Er.

Thus, the well-known microscopic model of Ref. 40 does in general correctly reproduce the experiment when applied to the small anadiabatic effects within and between bands. The remaining discrepancies are evidently due to the shortcomings of this model when allowance is made for the interaction in the particle–particle channel.

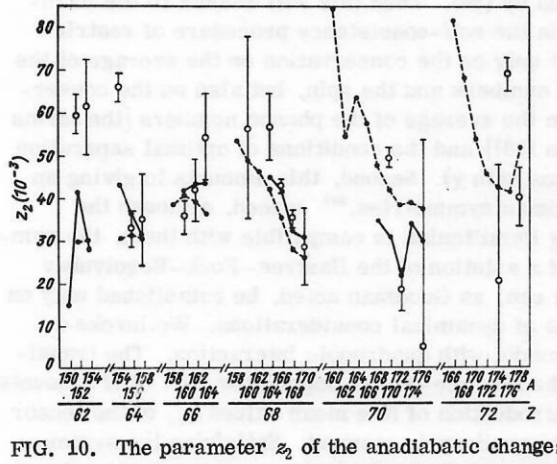

FIG. 10. The parameter z_2 of the anadiabatic changes of the $E2$ moment between the g and γ bands; the remaining notation is as in Fig. 6.

14. SELF-CONSISTENT CRANKING AND PROJECTION

In the microscopic theory of high-spin states and band crossing, new difficulties arose. We are here concerned with the need for a theory capable of treating simultaneously all the "phase-transition" mechanisms described in Sec. 15 so as to be able to make a choice between them. There are developments of different schools that use the self-consistent cranking method—a combination of the cranking model with the Hartree–Fock–Bogolyubov method—at high spins with allowance for conservation of the spin and the particle number on the average, nonaxial shape being taken into account depending on the circumstances. We have here the papers of Mang *et al.*, who developed the self-consistent cranking method together with projection with respect to the spin,[233,234] and subsequently applied it to high-spin states (Refs. 235–237 and 103). The projection methods with respect to the spin and particle number were developed in Ref. 80. Faessler's group used the same self-consistent cranking method, together with projection for the particle number (and in some of the papers with projection as well for the spin; see Refs. 238–241 and the references there to other papers). Calculations in accordance with the self-consistent cranking method without projection were also made in Refs. 242–244. On the other hand, calculations with projection with respect to the particle number and the spin, but without self-consistency, were made in Ref. 245.

Before we turn to the latest development of these methods and to the results of calculations obtained with them (see Secs. 15 and 16), let us consider the self-consistent cranking method. A very important question is that of the symmetries of the nucleon density calculated by means of self-consistent methods. As was noted by Goodman in the first paper of Ref. 242, there is a difference between the case of a nucleus at rest and a rotating nucleus. For the ground state with $I=0$ of an even–even nucleus in a fairly general case one can assume invariance under time reversal T, spatial inversion P, and rotations $R_{x,y,z}$ about the three coordinate axes through π. However, in the case $I\neq 0$, because of the replacement of the Hamiltonian $\hat{H}$ by $\tilde{H}=\hat{H}-\omega\hat{I}_x$, it should be noted that the cranking term is invariant under P, R_x, and $TR_{y,z}$, but not under T and $R_{y,z}$. This amounts to violation of time-reversal symmetry and triaxiality. It is helpful to go over from the basis of the spherical shell model to a new basis before carrying through the Hartree–Fock–Bogolyubov procedure,[240] the new basis being composed of linear combinations of the single-particle j,m and $j,-m$ states. The new basis states are eigenfunctions for R_x with eigenvalues or signatures $r=\exp(-i\pi j_x)=\pm i$. For this choice, the Hartree–Fock–Bogolyubov matrix, independently of the violation of T symmetry, again reduces by half its dimension in accordance with the theorem considered in Ref. 246. For an even number of particles, the signatures are $r=\pm 1$, and they can lead to splitting of a rotational band into two parts[8] with only even or only odd spins (see below). The single-quasiparticle levels in rotating nuclei are also split with signature r (Fig. 11).

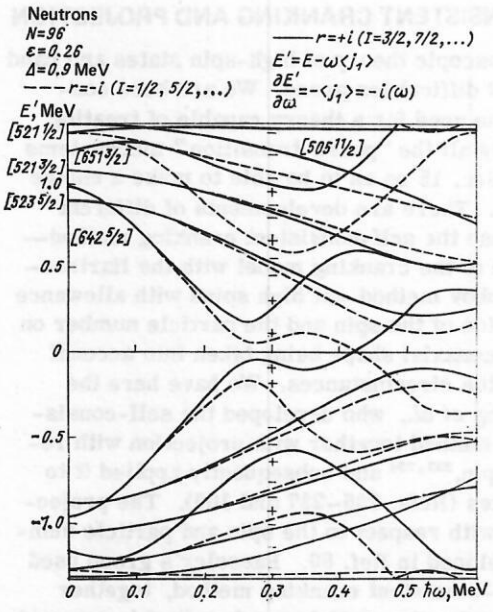

FIG. 11. Quasiparticle energies E' as a function of the angular velocity ω (from Ref. 8).

The problem of the consistency with ($P = P_p, P_n, P_{IM}$) or without ($P = 1$) the operator P of projection with respect to the numbers of protons and neutrons and (or) with respect to the spin is solved as a search for the minimum of

$$\mathcal{H} = \langle | \hat{H} P | \rangle / \langle | P | \rangle \tag{58}$$

with conservation on the average of the spin projection $\hat{I}_x$ and the particle numbers $\hat{N}_p$ and $\hat{N}_n$. The problem is divided into 1) diagonalization with respect to a complete Bogolyubov transformation[40]

$$\alpha_j^+ = \sum_i [a_i^+ A_{ij} + a_i B_{ij}] \tag{59}$$

of the Hartree–Fock–Bogolyubov matrix for $\tilde{H}$ ($\tilde{\Gamma}$ is the matrix of the coefficients of the terms a^+a and $\tilde{\Delta}$ $-aa$ of the Hartree–Fock–Bogolyubov part of the operator $\tilde{H}$):

$$\begin{pmatrix} \tilde{\Gamma}-\varepsilon & \tilde{\Delta} \\ -\tilde{\Delta}^* & -\tilde{\Gamma}^*-\varepsilon \end{pmatrix} \begin{pmatrix} A \\ B \end{pmatrix} = 0 \tag{60}$$

and 2) self-consistency, i.e., the determination of the parameters of the pairings and the multipole moments (deformations),

$$p_{\lambda\mu}^{\sigma} = \langle | \hat{P}_{\lambda\mu}^{\sigma} | \rangle \quad q_{\lambda\mu}^{\tau\sigma} = \langle | \hat{Q}_{\lambda\mu}^{\tau\sigma} | \rangle, \tag{61}$$

that arise on the transition from the Hamiltonian $\hat{H}$ to its Hartree–Fock–Bogolyubov part together with K, the frequency ω, and the chemical potentials λ_p and λ_n. The self-consistent method can be carried out either by successive iterations with repetition of the steps 1) and 2) or by direct minimization of (58), when, in particular, the projection P is included.[240]

We recall the formula for spin projection[247]

$$P_{IM} = \prod_{\lambda \neq I} \frac{\hat{I}^2 - \lambda(\lambda+1)}{I(I+1) - \lambda(\lambda+1)} \prod_{\mu \neq M} \frac{\hat{I}_0 - \mu}{M - \mu} \tag{62}$$

and the comparison in Ref. 248 of the different projection procedures.

We now note the circumstance that although the part played by self-consistency in the description of high-spin states has been elucidated at the computational level (see Secs. 15 and 16), the importance of projection at the practical level seems to us to be still unresolved. It has been asserted that projection with respect to the particle number is important for stabilization of the pairing in the low-spin part[245] and in the back-bending region.[240,249] However, such projection does not remove the discrepancies with the experiment in the back-bending curve. Interesting here is Ref. 250 on the self-consistent cranking method, the results of this paper showing that projection with respect to the particle number plays a small part. It is possible that such projection is important only in the case of strong changes in the behavior of the neighboring nuclei as, for example, in the well-known case of the presence or absence of back-bending in the nuclei $^{166,168,170}_{70}$Yb. In Ref. 238, projection with respect to the spin was also made, but it was later found that nonaxiality is very important,[240] and the technical complexities here meant that it had to be given up for the time being. Recently, Faessler's group has developed a procedure for dealing with this and thus hopes to eliminate the shortcomings of cranking in the back-bending region.[104-107]

It is necessary to develop methods that take into account bands based on quasiparticle states,[241] but to describe not only the yrast line; it is necessary to develop a description of side bands such as, for example, the negative-parity bands in $^{156}_{68}$Er (Ref. 251) and the $I=K$ traps in $^{176}_{72}$Hf (Ref. 252), and to develop a microscopic model of ultrahigh spins[253,254] with inclusion of hexadecapole forces.[254,255] We mention also the microscopic model of Ref. 256, which takes into account as usual (Refs. 240 and 253) pairing and quadrupole interactions but better than in the cranking model the rotational correlations and, therefore the fluctuations of the rotation axis.

We consider finally the possibilities of two important, in our view, developments of the microscopic theory of high-spin states. The first is to go over to the so-called[232a] method of self-consistent coupled modes, which is a generalization of self-consistent cranking. For this, we replace $\tilde{H} = \hat{H} - \omega \hat{I}_x$ by $\tilde{H} = \hat{H} - \hat{h}$, where $\hat{h}$ is given by (38). Then this will amount to the introduction in the self-consistency procedure of restrictions not only on the conservation on the average of the particle numbers and the spin, but also on the conservation on the average of the phonon numbers [the terms with ω in (38)] and the conditions of optimal separation (the terms with χ). Second, this amounts to giving up the Goodman symmetries.[242] Indeed, although the cranking Hamiltonian is compatible with them, the symmetry of a solution of the Hartree–Fock–Bogolyubov problem can, as Goodman noted, be established only on the basis of dynamical considerations. We invoke a simple model with quadrupole interaction. The transition to the Hartree–Fock–Bogolyubov part of $\hat{H}$ amounts to the introduction of five mean values $q_{2\mu}$ of the tensor $\hat{Q}_{2\mu}$ of the quadrupole moment. Satisfying the symmetries T, P, and $R_{x,y,z}$ presupposes a known transition to an intrinsic coordinate system with two nonzero com-

ponents q_{20} and $q_{22}=q_{2-2}$. In the case of the cranking method, there are added three further mean values i_μ of the angular momentum vector I_μ, $\mu=x,y,z$, or altogether eight shape and spin parameters. If the Goodman symmetries are to be satisfied, three of them must remain nonzero, and in an appropriate coordinate system these are the same two components q_{20} and $q_{22}=q_{2-2}$ and the one component i_x. In contrast to the suggestions of Ref. 242, one could imagine an important (for high spins) critical reorientation situation with respect to the quadrupole moment when the two moments have an arbitrary relative orientation. If this is so, then by the choice of an appropriate coordinate system one could reduce to zero only three of the eight components. Among the nonvanishing five one could choose, for example, any two q_0 and $q_{22}=q_{2-2}$ and three i_μ in the intrinsic system for $q_{2\mu}$, or four $q_{2\mu}$ and i_x in the system in which i_μ is directed along the x axis.

15. BACK-BENDING MECHANISMS

The proposed mechanisms can be classified as follows: 1) Coriolis antipairing, i.e., the disruption of the superfluidity by rotation, which was predicted long ago [Ref. 257, and also Ref. 258 and other references there to earlier work]; 2) the rotational alignment of a nucleon pair (Refs. 259, 260, and 6); a similar mechanism was proposed even earlier in Ref. 260a); it arises on the basis of a different, weak-coupling scheme[261] in the rotator model; such alignment was predicted in Ref. 262, and this scheme was then discovered experimentally and developed in Ref. 263; 3) an abrupt change in the deformation due to changes in the potential energy surface resulting from the rotation,[264,265] including the occurrence of nonaxial deformations.[138]

We mention also the estimates of the transition probabilities in the back-bending region in accordance with the Coriolis antipairing mechanism[5,266] and rotational alignment,[259] which predict a 10–20% hindrance compared with a rigid rotator, and also the more microscopic estimates of Ref. 267 on the basis of the Hartree–Fock–Bogolyubov method. There is an interpretation[267a,104] on the basis of gapless superfluidity.[267b] There are also models which assert the possibility of strong hindrances, namely, the model of a particle plus a variable-moment-of-inertia rotator[268] and the two-phase model.[269] There has been proposed a semimicroscopic approach to back-bending, which aims, not at a quantitative description, but at an understanding of the mechanism of the phenomenon on the basis of a model of a particle plus a rotator or two levels generalized to n levels and to allowance for quadrupole pairing.[270]

The question of the physical nature of the phenomena at high spin, i.e., the choice of a particular mechanism, and of the structure of the coupled bands can be solved only by a microscopic theory and by experiments (see below). In general, it may be concluded that in the microscopic theory of self-consistent cranking (the only exception is Ref. 244) preference is given to the rotational alignment effect as being responsible for back-bending; the Coriolis antipairing mechanism gives only a smooth component in the increase in the moment of

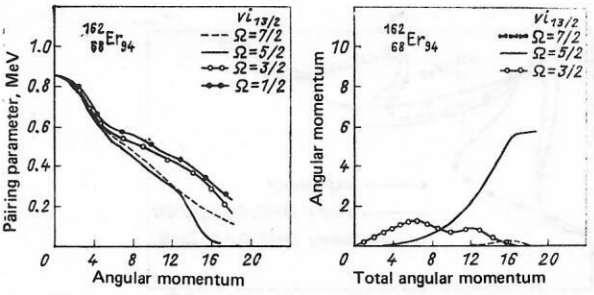

FIG. 12. Dependence of the change in the pairing (on the left) and the angular momentum of the quasiparticle states with respect to the retation axis (on the right) on the spin I (Refs. 4 and 240).

inertia, while the third mechanism, the abrupt change in the deformation, is hardly considered at all, or at least not for rare-earth elements.[240] This can be seen directly in Fig. 12, which shows that the pairing decreases smoothly, whereas the pair of $i_{13/2}$ neutrons is abruptly aligned. Such a calculation leads to the conclusion that the Coriolis antipairing mechanism is responsible for a smooth increase in the moment of inertia, this beginning at low spins, whereas rotational alignment is responsible for an abrupt increase and, therefore, the back-bending.

In Ref. 249, the influence of other interactions—monopole pairing and quadrupole interaction[240]—was considered. It was found that quadrupole pairing through the $(\lambda,\mu)=(2,0)$ components improves the agreement with the experimental curve around the point of back-bending. However, the improvement is a small fraction of the total discrepancy, so that there is still no quantitative agreement. The spin–quadrupole interaction improves the agreement with the experiment above the point of back-bending, reducing the moment of inertia to a value below the rigid-body value (the experiment is described below; some general theoretical arguments for such a difference are given in Ref. 270a). The conclusions converning the moment of inertia at low spins differ from those known hitherto (see Sec. 12): Once again, the total effect of the quadrupole pairing and the spin–quadrupole interaction is zero, though in contrast to Ref. 208 it is assumed that the spin–quadrupole interaction has no influence, and the increase by 20% due to the (2, 1) component of the quadrupole pairing[51] is compensated by the decrease of its (2, 0) component. In the same way, the second back-bending in the nucleus $^{158}_{68}Er$ (Ref. 24) can be associated with alignment of a pair of $h_{1/2}$ protons, but again the agreement is only qualitative (Fig. 13).[271] Sometimes, the $h_{9/2}$ protons can act only as catalyzers of the first back-bending, it being again $i_{13/2}$ neutrons that are aligned.[272]

In nuclei close to the spherical $_{78}Pt$ and $_{80}Hg$, phenomena that simulate back-bending are observed. For example, in the light isotopes $^{184-188}_{80}Hg$ the irregular behavior of the yrast line, which is similar to back-bending, is a shape effect, and this follows from theoretical[273] and experimental studies.[274] The situation is different in the heavier $^{190-198}_{80}Hg$ and in $^{190,192}_{78}Pt$, in which the 10^+ and 12^+ levels of the yrast lines are iso-

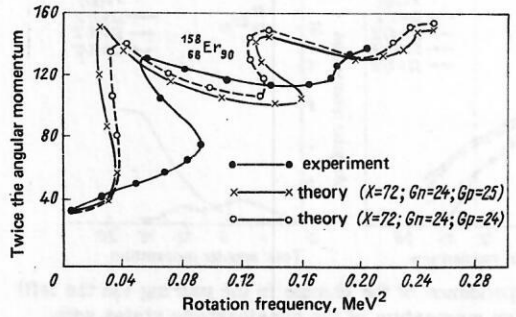

FIG. 13. Diagram of double back-bending in $^{158}_{68}$Er (Ref. 271) with two variants of calculation from Ref. 271 compared with the experiment of Ref. 24.

mers and may have a different, for example, rotationally aligned, nature (Refs. 4, 275, and 276). Such phenomena may also be observed in the nuclei $_{56}$Ba and $_{58}$Ce (Ref. 268).

With regard to side bands with, for example, negative parity in the isotopes $_{68}$Er (Refs. 31–34) and $_{72}$Hf, and also in the lighter nuclei $_{56}$Ba and $_{58}$Ce and the heavier $_{78}$Pt and $_{80}$Hg (see the experiment described below), two mechanisms have been considered in the literature: Octupole vibrations[277] and rotational alignment,[278] with also a generalization to a departure from axial shape.[279] The different effects of Coriolis antipairing in bands with different K have been considered.[279a] In the microscopic approach, one can also understand the double back-bending in bands of negative parity, for example, in $^{156}_{68}$Er (Ref. 251).

16. MECHANISMS OF TRAP FORMATION

In accordance with the predictions of a special behavior of the yrast line at ultrahigh spins,[7] calculations were made by groups at Dubna,[280,281] Warsaw,[282,283] and Jülich.[284,285] This was first done in the Nilsson basis, Strutinsky's procedure being used, and then in the Woods–Saxon basis (Refs. 286, 287, and 255). A microscopic approach with self-consistency was also used, the point of departure being a spherical basis with pairing and quadrupole interaction[52] in Refs. 240 and 253, and subsequently with the introduction of hexadecapole interaction.[254,255] At ultrahigh spins, the pairing is usually assumed to be broken, although approximately one quarter of the pairing energy remains in the nucleus $^{158}_{68}$Er at spin 30 (Ref. 271). Additional calculations can be found in the papers of the following groups: Lund–Warsaw,[288-290] Copenhagen,[291] and Warsaw–Dubna.[292] We note that in Ref. 290 pairing was taken into account. In Ref. 252, an explanation is given of the high-spin traps in the nucleus $^{176}_{72}$Hf, and in Refs. 255 and 289–291 a theoretical search is made for traps or isomers of ultrahigh spins.

The traps on or near the yrast line in the nucleus $^{176}_{72}$Hf with spins 14–22 (see Ref. 35) can be explained by the crossing of between two and six quasiparticle bands (with large K) and the ground-state band (with $K=0$) at $I=K$, which entails rotation about an elongated symmetry axis.[252] We shall see below that such a situation can also arise at ultrahigh spins.

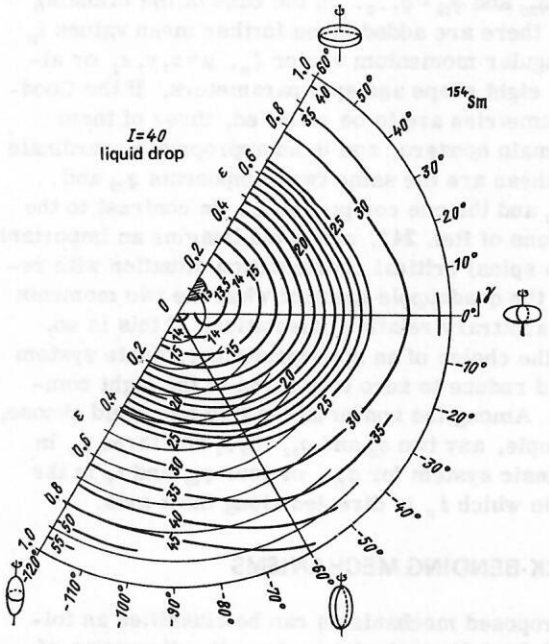

FIG. 14. Energy surfaces of rotating $^{154}_{62}$Sm nucleus at spin $I=40$ in the liquid-drop model[283] and γ with sign opposite to what we have chosen in Secs. 4 and 13.

The behavior of nuclei at ultrahigh spins is governed by effects of special shapes, the breaking of pairing, and a far-reaching rearrangement of the entire quasiparticle structure (see Sec. 14). One can also mention the changes of other global characteristics of the nucleus.[23] All effects are associated with deviations from the predictions of the liquid-drop model[293] (see Fig. 14) due, on the one hand, to shell effects and, on the other, to departure from rigid-body behavior.[155] The predictions made in Ref. 293 are shown in Fig. 15a, which shows that from spherical shape at $I=0$ there arises rotation about an oblate symmetry axis at high and ultrahigh spins; the shape of the nucleus in this model can become prolate at the maximally high spins. In real nuclei, there exists a variety of shapes; these begin with a deformed shape at $I=0$ and pass through different degrees of triaxiality, sometimes returning to an axial shape, but for different cases, both oblate and prolate shapes (see Figs. 15b and 15c).[283] In spherical nuclei near $_{62}$Sm, an oblate shape is reproduced, and in transuranium elements at spins of order 50 there may be an abrupt change to a prolate shape with large deformation,[287] which leads to the so-called *giant back-*

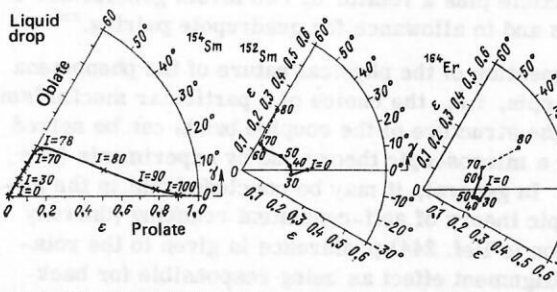

FIG. 15. Equilibrium shape of rotating nuclei as a function of the spin[283] in the liquid-drop model for $^{154}_{62}$Sm and with allowance for shell effects for $^{152}_{62}$Sm and $^{164}_{68}$Er.

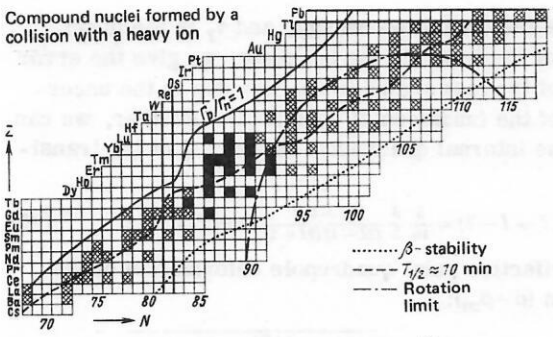

FIG. 16. Island of ultrahigh-spin traps.[39] The hatched regions show the composite systems obtained as a result of searches in reactions with $^{40}_{18}$Ar, $^{50}_{22}$Ti, and $^{65}_{29}$Cu (for the final nuclei, the most probable values of Z are the same and those of N are 3–5 units smaller); the discovered examples of traps (1.5 to 700 nsec) are densely populated.

bending. There has also been proposed a simple model of various effects associated mainly with the shape of rapidly rotating nuclei.[294]

In Refs. 280 and 281, the possibility of stabilization of a shape with large deformation at ultrahigh spins in the region of nuclei around $Z = 66$ and $N = 88$ is demonstrated. In this connection, one may suspect the existence of isomers at such spins. As a trap criterion, use has been made of selection rules for the transitions $I \to I-1, I-2$ along the yrast line of multipolarities $E1$, $E2$, $M1$, and $M2$ (Refs. 291 and 255). Two trap mechanisms have been proposed: 1) statistical,[283] associated with stabilization of quasiparticle structures,[291] and 2) MONA (Ref. 285): maximization of the overlapping of nucleon wave functions by alignment. The statistical mechanism has the consequence that the traps are a relatively rare phenomenon, not only because of the inclination of the yrast line but also because of the softness with respect to γ vibrations.[290] The MONA mechanism leads to traps associated with rotation around an oblate symmetry axis at the beginning of shell filling and around a prolate axis at the end.[254,255] In the last quoted papers, calculations were made of deformations and traps in the nuclei $^{148}_{62}$Sm, $^{150}_{64}$Gd, and $^{158}_{70}$Yb (Ref. 254), and also deformations in $^{186}_{76}$Os, $^{188}_{78}$Pt, $^{190-196}_{80}$Hg, and $^{192-198}_{82}$Pb and traps in $^{188}_{78}$Pt and $^{194,198}_{82}$Pb (Ref. 255). In Ref. 291, the predictions for the island of traps of ultrahigh spins in the region $62 \leqslant Z \leqslant 70$, $80 \leqslant N \leqslant 88$ are compared with the traps discovered experimentally (see also Sec. 32) at Darmstadt[39] in the region $64 \lesssim Z \lesssim 71$, $82 \lesssim N \lesssim 88$ (Fig. 16). However, it is noted that the second predicted island $74 \leqslant Z \leqslant 82$, $98 \leqslant N \leqslant 110$ has not been found experimentally.

17. INTRODUCTORY COMMENTS ON EXPERIMENTS IN THE REGION OF THE YRAST BAND

The possibility of using heavy ions as suitable probes for nuclear physics was realized about 20 years ago, first for the synthesis of new elements at Berkeley and at Dubna,[295] and later for detailed investigations of nuclear structure and the mechanisms of nuclear reactions by Coulomb excitation,[16] many-nucleon transfer reactions,[296] and (HI, xn) reactions (see Ref. 19, and also the review of reaction mechanisms in Ref. 297). Such possibilities arise through several basic features of heavy ions: 1) the strong magnetic fields produced by the large charge; 2) the large number of nucleons; 3) the large angular momenta; and 4) the large momenta introduced or transferred in collisions. These properties are particularly important for the excitation of collective and coupled modes. They have made it possible to develop not only the older off-line experiments[298] but also the most modern in-beam[299] nuclear spectroscopy investigations, especially of high-spin states. We have in fact: 1) Coulomb excitation, which excites preferentially collective levels[300] multiply[301,302]; 2) the possibility of reaching nuclides far from the stability band,[299] in which the back-bending effect is mainly observed,[6,4] and compound-nucleus reactions can be realized[303,304]; particular possibilities will be opened up in this direction if the expected acceleration of radioactive ions is achieved; there is also the possibility of observing new collective modes, for example, pairing and α-vibration modes[305-307] in reactions involving the transfer of two and four nucleons[308]; 3) the possibility of investigating high-spin states, in which interesting band coupling effects such as back-bending are observed[4] and yrast band features leading to so-called *traps* are predicted: isomer high-spin and ultrahigh-spin (superdizzy) states[7]; 4) the possibility of making a much more detailed study of high-spin states through the determination of not only their energies but also characteristics that depend on the wave functions such as, for example, the $E2$ moments, which are related to the lifetimes.

Let us consider briefly the now classical model of population[309] of the yrast band region (the levels of the yrast line[310] and lines close to it) in compound-nucleus reactions with the evaporation of neutrons (HI, xn) (Refs. 303 and 304), which was tested experimentally in Ref. 311 (Fig. 17). This population can be called population "from above" from a "cloud" corresponding to the distribution of the final nuclei over the energy and spin after evaporation of neutrons and before deexcitation by γ emission. Initially, there is a continuous statistical cascade,[4] consisting primarily of high-energy $E1$ transitions, but carrying away virtually no spin, so that in Fig. 17 it is directed vertically downward; the cascade consists of between two and six, on the average four, transitions.[312,313] Then follows the

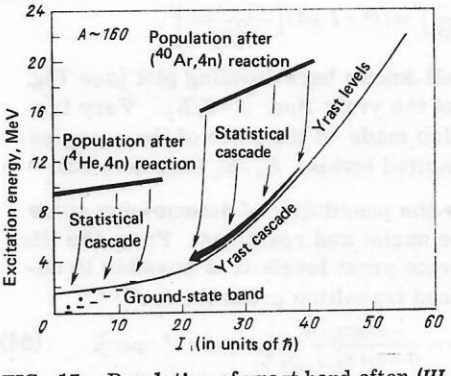

FIG. 17. Population of yrast band after (HI, xn) reaction.[309]

yrast cascade,[4] which consists of a continuum and a discrete spectrum and has approximately ten transitions; it is assumed that these are predominantly aligned $E2$ transitions,[311-313] although more detailed investigations also reveal a dipole component.[314] In Fig. 17, these transitions are parallel with and close to the yrast line. This population mechanism determines the importance of the (HI, xn) reactions for the investigation of the yrast band region. As we shall see below, the main information comes from the discrete and continuous γ-ray yrast cascade; although the total excitation energies are not small, the energies of internal excitation (above the yrast line) are not great (cold nuclei). Therefore, we obtain the possibility of observing a good quantum structure that is not washed out by a large accumulation of levels but is at high rates of rotation, and therefore of an unusual type (see Fig. 1).

Wide use has also been made of Coulomb excitation,[300-302] which in Fig. 17 can be regarded as excitation "from below," initially along the yrast line and then also possibley along paths close to it. However, in the region of sufficiently high-spin states Coulomb excitation may lead to preferential occupation of levels different from those reached in (HI, xn) reactions. Indeed, it is known that these are levels coupled to low-spin levels by enhanced transition probabilities. It is of especial interest to test the situation in the few cases when fairly strongly neutron-deficient but stable nuclei are obtained, it being then possible to have excitation both from above by the (HI, xn) reaction and from below by Coulomb excitation.[315]

It is only in the very recent past that deep inelastic transfer reactions[316] have started to be used for a more detailed study of the angular momentum transfer mechanism[317-319]; in the future, this may give information about the structure of the high-spin region.

Finally, let us consider some of the procedures used to obtain derived information about the structure of the yrast band region and the mechanism of its population from the first experimental data on the discrete and continuous γ-ray spectrum.[320] From the energies and spins of discrete yrast levels, one can obtain the moment of inertia J and the angular frequency as measured by ω by means of the expressions[21]

$$2J=\left[\frac{dE_I}{dI\,(I+1)}\right]^{-1}=\left[\frac{E_I-E_{I-2}}{4I-2}\right]^{-1};$$
$$\omega^2=\left[\frac{dE_I}{d\sqrt{I\,(I+1)}}\right]^2=(I^2-I+1)\left[\frac{E_I-E_{I-2}}{2I-1}\right]^2, \quad (63)$$

which give the well-known back-bending plot (see Fig. 1). At the start of the yrast line, $J=3/E_2$. Very frequently, use is also made of the ratio of the energies of the first two excited levels: E_4/E_2 (see Sec. 23).

Let us consider the possibility of determining some parameters of the nuclei and reactions. From the lifetimes of the discrete yrast levels it is possible to determine the reduced transition probabilities[40,300]

$$B(E2; I\to I-2)=\frac{0.0816235\,(11)}{(1+\alpha_T)\,E^5_{I-I-2}\tau_I}\left[e^2\cdot b^2\cdot \mathrm{MeV}^5\cdot \mathrm{psec}\right]. \quad (64)$$

where α_T is the total coefficient of internal conversion, $E_{I\to I-2}$ is the transition energy, and τ_I is the mean lifetime of the level (in the brackets, we give the error in units of the last significant figure due to the uncertainties of the fundamental constants). Further, we can deduce the internal quadrupole moment Q of the transition,

$$B(E2; I\to I-2)=\frac{5}{16}\,\frac{3}{2}\,\frac{(I-1)\,I}{(2I-1)\,(2I+1)}\,e^2Q^2\,(I\to I-2) \quad (65)$$

and the effective axial quadrupole deformation of the transition ($\beta=\beta_{20}$):

$$\beta\,(I\to I-2)=\frac{1}{0.32}\left[\sqrt{1+0.64\,\frac{\sqrt{5\pi}}{3ZR^2}\,Q\,(I\to I-2)}-1\right]. \quad (66)$$

For the radius of the nucleus, we can take $R=1.2A^{1/3}\mathrm{F}$; Z and A are the charge and mass numbers.

In the investigation of the continuous spectra, using the statistical theory for the number $N(E)$ of γ rays as a function of the energy E, we obtain the formula[4]

$$N(E)=E^{2L+1}S(E, L)\exp\left[-(E_0-E)/T\right], \quad (67)$$

where L is the multipolarity of the radiation, E_0 is the energy of the doorway state, and T is the temperature of the nucleus. It is assumed that the strength function is constant, $S=\mathrm{const}$, for $L=2$ and proportional to E^2 for $L=1$. From this E_0 and T can be extracted.

As we shall see below, the in-beam methods for investigating the population and structure of the yrast-band region are in a period of advance.[4] The results for high- and ultrahigh-spin states, right up to the stability limits of the nuclear system, have opened up to us in recent years more and more details of a new physical picture. The picture is attractive because under the experimental conditions of high rotation velocities the nuclei change their structure strongly but can still preserve simplicity of their quantum properties. One can also have transitions between structures associated with not only changes in the shape and the superfluidity but also a more radical change in the coupling scheme of the nucleons, and therefore of great physical interest.[8]

18. IN-BEAM ENERGY MEASUREMENTS

Energy measurements of high-spin states have been described frequently in reviews (Refs. 321, 3, and 4). These measurements have led to the compilation of tables of the energies of the yrast levels[322] and back-bending diagrams (Fig. 18). We shall consider this question here briefly.

Such measurements encounter two main problems[21,3]: 1) the suppression of the background, since here the discrete transitions between the yrast levels (the discrete yrast cascade) have not only the ordinary accelerator backgrounds but also a continuous background of γ rays that follow the evaporation of neutrons (statistical and continuous yrast cascade; see Fig. 17); 2) the identification of the γ transitions. The γ rays are detected by Ge(Li) spectrometers, and the identification is achieved through measurements of: a) the excitation functions that characterize these reactions and determine the A number of the observed nuclide; b) the spin distributions or the intensities of side popu-

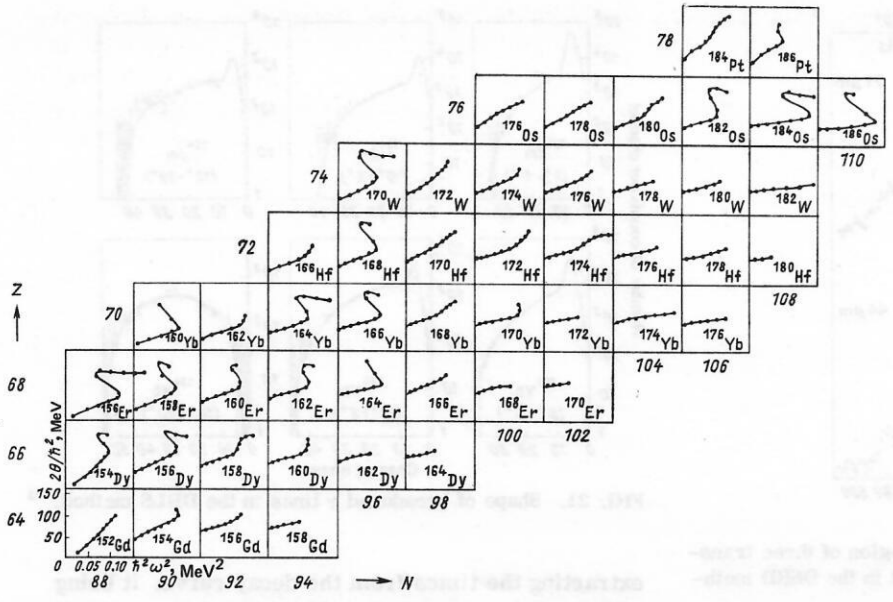

FIG. 18. Systematics of back-bending diagrams.[4]

lation, which exhibit a characteristic shape with a maximum in the back-bending region and indicate that the γ-ray lines belong to the yrast cascade and what is the most probable position in it; c) $\gamma\gamma$ coincidences, which prove that a γ-ray line belongs to the yrast cascade and gives its exact position in it; d) the angular and polarization distributions and correlations. As an example of the combined use of such methods, we mention Ref. 323, which exploited the methods a), b), and d) fully, including polarization measurements. In the $N=87$ nuclei $^{149}_{62}$Sm, $^{151}_{64}$Gd, and $^{153}_{66}$Dy it was possible by means of ($^4_2$He, $3n\gamma$) reactions to prove in this manner the presence of a strongly deformed collective $h_{11/2}$ band in contrast to the other $\Delta I=2$ bands $i_{13/2}$, $h_{9/2}$, and $f_{7/2}$ (see Sec. 27).

Also made are classical lifetime measurements with electronic timing in the nanosecond region ($>10^{-10}$ sec) using coincidences or accelerator pulses.[324] This time range is not suitable for the high-spin region. Data on transition intensities are compiled in Ref. 201. In this connection, we mention an interesting method that makes it possible to penetrate into the subnanosecond region,[325] which is called the *recoil shadow method*. In this method, one detects electrons that are emitted by the recoil nuclei only after they have been in flight for some time.

19. IN-BEAM DOPPLER-SHIFT LIFETIME METHODS OF MEASUREMENT

There have been proposed two Doppler-shift methods that have given basic direct information on the transition probabilities in the region of high-spin states. These have used: 1) the Doppler shift of the γ rays from recoil nuclei with a definite time of flight (RD) in vacuum, or the "plunger" method [DSRD, RD(M)]; 2) analysis of the broadened line shape (BLS) due to the gradual attenuation (A) of the velocity of the recoil nuclei in a medium [DBLS, DSA(M)]. The DSRD method has long been known,[326,327] but was developed for the yrast levels of heavy nuclei in the case of (HI, xn) reactions in Ref. 328 or Coulomb excitation in Ref. 329. It was established that Coulomb excitation gives the lifetimes in a pure form and is therefore more accurate, whereas the (HI, xn) reaction gives the total effect of the lifetime and the time of side population, with, however, the advantage of doing this in cases that are not accessible with Coulomb excitation. The typical range of times is 10^{-8} to 10^{-12} sec. The DBLS method has also been known for quite a long time,[326,330] but was developed for heavy nuclei in the case of Coulomb excitation in Ref. 331. The typical range of times is from 10^{-10} to 10^{-14} sec. Both methods are considered fairly fully from the methodological side in the review of Ref. 324 and from the point of view of the results in the high-spin region in Refs. 4 and 332. We shall return to the results of the measurements obtained by means of them in Secs. 28, 29, and 31.

The DSRD method is based on the following idea [Fig. 19, the variant of the (HI, xn) reaction[324]]. In the target, there is a reaction in which the heavy ion fuses with the target nucleus and neutrons are evaporated, after which the reaction product moves forward as a recoil nucleus. Some of the recoil nuclei emit in the stopper, and the others while still in flight, with the consequence that one observes two γ-ray lines, one unshifted (u) and one shifted (s); the unshifted line has energy E_u and intensity N_u, and the Doppler-shifted line

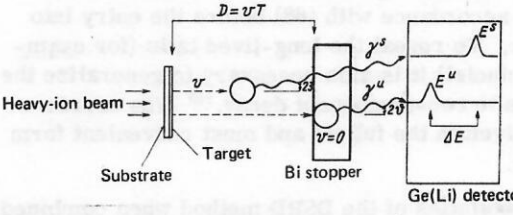

FIG. 19. Principle of the DSRD method.

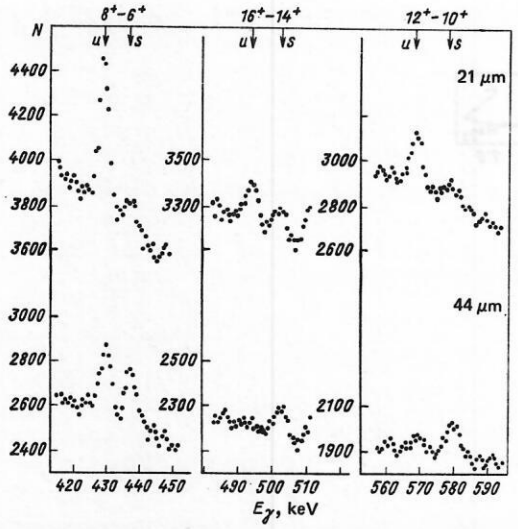

FIG. 20. Gamma spectra of $^{166}_{70}$Yb in the region of three transitions for two target-stopper times of flight in the DSRD method.[366]

has E_s and N_s, respectively, with

$$E_s = E_u \sqrt{\frac{1+v/c}{1-v/c}} \approx E_u (1+v/c). \tag{68}$$

From this, one can deduce the intensities of the total population N_I and the side population P_I:

$$N_I = [N_u + N_s]_{I \to I-2}; \; P_I = N_I - N_{I+2} \tag{69}$$

as the intensity ratio

$$R_I = [N_u/(N_u + N_s)]_{I \to I-2} \tag{70}$$

for the transition $I \to I-2$ as a function of the time of flight t of the recoil nuclei from the target to the stopper. A typical variation of the intensity ratio with the time of flight is shown in Fig. 20 for the ($^{40}_{18}$Ar, $4n$) reaction. The dependence $R_I(t)$ gives the characteristic decay curve from 1 to 0 (see Sec. 21).

The intensities of the γ-ray lines are corrected to the total transition intensities by multiplying by $1+\alpha_T$, where α_T is the total coefficient of internal conversion.[333,334] In addition, it is necessary to introduce a correction to the energies and intensities for a number of effects that distort the simple decay curves $R_I(t)$. The corrections were discussed in Ref. 324 on the basis of the well-known formulas[335] and data of Ref. 336; however, they were augmented to seven and were given in a form convenient for calculation in Ref. 337. In the high-spin region, the main correction was found to be due to the finite time $2t_r$ of stopping of the recoil nuclei in the stopper (Ref. 338): $t = t_{corr} = t_{unc} + t_r$, where $t_r = r/v$, r is the range of the recoil nuclei in the stopper in accordance with the tables given in Ref. 339, and v is the velocity in accordance with (68) before the entry into the stopper. To reveal the long-lived tails (for example in $_{72}$Hf nuclei) it is also necessary to generalize the corrections to two-component decay.[340] The corrections are given in the fullest and most convenient form in Ref. 320.

The uncertainties of the DSRD method when combined with the (HI, xn) reaction are related to the problem of

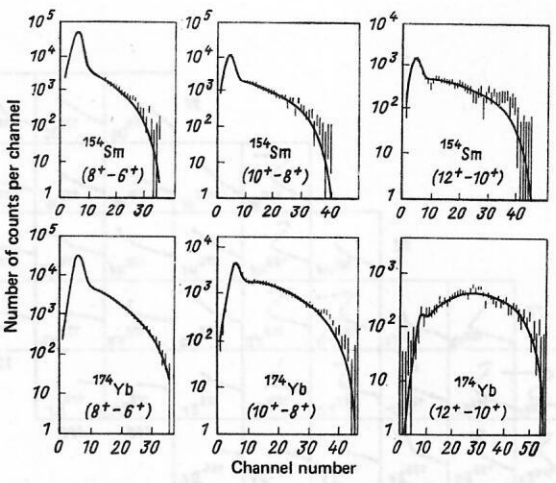

FIG. 21. Shape of broadened γ lines in the DBLS method.[341]

extracting the times from the decay curve, it being necessary to separate the effects associated with the reaction, i.e., the intensities P_I and the side feeding (population) times φ_I. We shall consider this question specially in Sec. 21.

The DBLS method is based on the fact that in the process of stopping of the recoil nuclei lines Doppler-shifted in accordance with (69) are emitted, the final shape being obtained as the total effect of the emission at different velocities from the initial to the final zero velocity. An example of such broadened lines is shown in Fig. 21 in the case of Coulomb excitation by $^{56}_{26}$Fe and $^{84}_{36}$Kr ions.[341] The main problem is associated with extracting the times from the line profile, for which model calculations of the stopping process, which lead to some uncertainties, are used. This is done on the basis of a model for calculating the electron and nuclear stopping,[342] to which modifications[343] and new approaches[344] are applied. Usually, the semiempirical tables of Ref. 339 are used. The stopping of the recoil

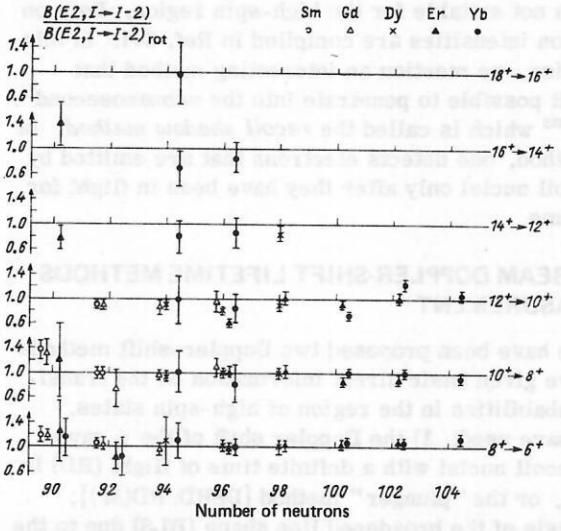

FIG. 22. Plot of results for the enhancement factors from lifetime measurements by Doppler methods.[4] The data for the spins 16⁺ and 18⁺ for $^{158}_{68}$Er$_{90}$ are from Ref. 364 and for $^{164-6}_{70}$Yb$_{94-6}$ from Ref. 338.

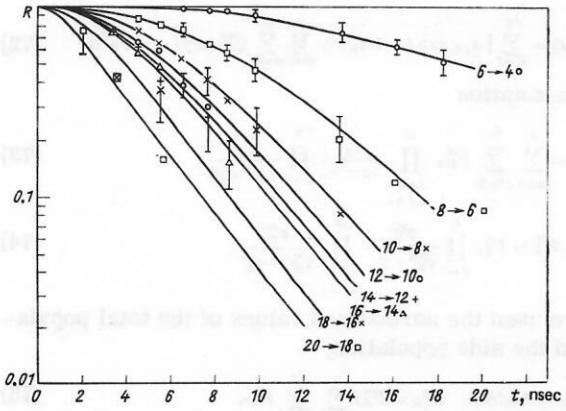

FIG. 23. Decay curves of R_I plotted against t for $^{166}_{70}$Yb (Ref. 338).

nuclei is improved by comparison with measurements of the DBLS times and measurement by the DSRD method (Refs. 341, 345, and 346). In Refs. 345 and 346, it is assumed that the tables given in Ref. 339 must be corrected by a factor 1.25 with normalization to $^4_2$He ions,[347] whereas in Ref. 341 the tables are assumed to be correct and these corrections are not introduced. Note also that in the tables given in Ref. 348 some partial improvements have been made compared with the tables of Ref. 339. The DSRD method with ions up to $^{40}_{18}$Ar was used to measure lifetimes of levels up to 18^+; the DBLS method was used up to 12^+ (Ref. 4). The results are given in Fig. 22. New data, including some for higher spins, will be given belwo. The decay curves of states with record high spins up to 20^+ (Ref. 338) are shown in Fig. 23. Recently, without a change in the method of measurement, the use of very heavy ions has made it possible to obtain the following results: up to 24^+ by the DSRD method after the $(^{136}_{54}\text{Xe}, 4n)\,^{158}_{66}$Dy reaction[349] (these results are shown in Fig. 24), and up to 14^+ in $^{174,176}_{70}$Yb (Ref. 350) and 18^+ in $^{232}_{90}$Th (Ref. 351) after Coulomb excitation by the ions $_{36}$Kr and $_{54}$Xe.

We mention a new method, the so-called *charge-plunger method* (Ref. 352), which was used to determine the quadrupole moment of $^{239}_{94}$Pu from the lifetime of levels in the second potential well.

20. MAGNETIC IN-BEAM MEASUREMENTS

Measurement of the g_R factors of high-spin states in the back-bending region would give new possibilities

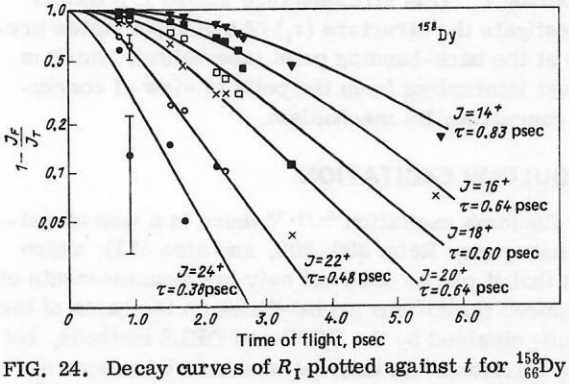

FIG. 24. Decay curves of R_I plotted against t for $^{158}_{66}$Dy (Ref. 349).

for experimental separation of different mechanisms of back-bending.[353,354] Among the many methods of measurements of the magnetic moments of excited states,[355] only the methods[356] of attenuation of the angular distributions[357,358] because of the interaction of the nuclear magnetic moment with a magnetic field outside the nucleus in the case of recoil in vacuum, gas, or a ferromagnetic medium are effective at lifetimes of order 10^{-12} sec. For example, in the case of recoil in vacuum the characteristic attenuation times are of order 10^{-11} sec (Ref. 336).

However, there have been very few such measurements and only in the low-spin region $I \leq 8$ (Refs. 4 and 332) or for fairly long-lived isomer states, for example, the 12^+ in the isotopes $^{192,194,196}_{78}$Pt (Ref. 359). Such measurements do not contradict constancy of g_R as the spin changes[360] in $_{66}$Dy nuclei. In some cases, such effects are observed[336] in $_{68}$Er nuclei; these can be given different interpretations[4] in terms of a decrease in g_R with the spin, a change in the attenuation mechanism with the spin, or constancy of both but the existence of population from nonyrast states with a smaller g_R factor.[361]

Most recently, there has been a report of application of the recoil technique in a gas (see Ref. 362 and references there) after the $(^{136}_{54}\text{Xe}, xn)\,_{68}$Er reaction with very heavy ions at Darmstadt, measurements being made up to spins 14^+–18^+ (Ref. 363). Unfortunately, the data have not yet been evaluated, and it is not yet known to what extent it will be possible to separate the effects discussed above.

21. METHODS FOR SEPARATING STRUCTURE AND REACTION EFFECTS

We are here concerned with the problem of extracting from the decay curves of the DSRD method after the (HI, xn) reaction (see Figs. 23 and 24) information about effects associated with the structure, i.e., information about the lifetimes τ_I of the yrast levels, and information about effects associated with the process of de-excitation of the compound nucleus, i.e., the intensities P_I and times φ_I of side population. In the back-bending region, where the intensities P_I of side population are maximal,[338] this becomes the main problem. It can be solved in two ways,[332] the first of which is to eliminate the effects of the reaction by making coincidences between lower transitions and some highest observed transition and obtaining a pure cascade. The first measurements of the lifetimes were made in this manner in the back-bending region for $^{158}_{68}$Er by a Canadian group.[364] However, in this case the statistics are very poor, and it is difficult to find an effect exceeding the experimental errors.

The second method to be discussed here is as follows. We attempt to separate the two effects on the basis of a model of the decay curves $R_I(t)$ with allowance for side feeding. This method was used by the Canadian group for $^{130}_{58}$Ce up to 12^+ (Ref. 365) with determination of only the lifetime τ_I and by a Dubna group (Refs. 338, 340, 366, and 367) for the nuclei $_{70}$Yb, $_{72}$Hf, and $_{68}$Er up to 20^+ with determination of the lifetime τ_I and the side

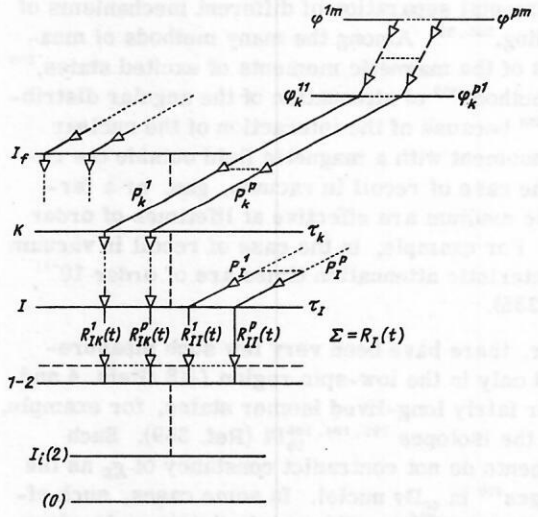

FIG. 25. Scheme of levels and their population. The spin I of the yrast level, with lifetime τ_I, changes from the lowest I_i to the highest I_f observed experimentally. The decay curve $R_I(t)$ of level I is made up of the partial decay curves $R_{IK}^{\varkappa}(t)$ of the cascades which populate the yrast levels $K = 1, I+2, \ldots, I_f$ through the side components $\varkappa = 1, 2, \ldots, p$ with the weight intensities $P_K^{\varkappa}$ of side population; each component of the side population proceeds through a cascade of side levels with side feeding times $\varphi_K^{\varkappa 1}, \varphi_K^{\varkappa 2}, \ldots, \varphi_K^{\varkappa m}$.

feeding time φ_I. This method was also adopted by a West-German group and applied to the nuclei $_{58}$Ce (Ref. 368) and $^{158}_{68}$Dy (Ref. 349). The calculation model without side feeding corresponds to a cascade of successive transitions between yrast levels I and is similar to the model of a radioactive decay chain. It was also used earlier[328] and is described in Refs. 337 and 369. The generalization to side feeding was made in Ref. 338. The most general case of cascade side feeding by many paths[320] is described below.

Consider Fig. 25, which represents the model for calculating $R_I(t)$ with allowance for side feeding in the most general case. Each level with spin I and lifetime τ_I is populated through many parallel cascades, which populate from the side each level with spin K, $I \leqslant K \leqslant I_f$ (I_f is the highest or final level of the yrast line observed experimentally), and then pass downward along the yrast line. The side population of a level with spin K with intensity P_K proceeds through several components (parallel cascades) with intensities $P_K^{\varkappa}$, so that

$$P_K = \sum_{\varkappa=1}^{p} P_K^{\varkappa}. \tag{71}$$

In practice, under normal conditions the number of such components of the nuclei $_{68}$Er and $_{70}$Yb was taken to be $p = 1$, and $p = 2$ was taken only for the long-lived tails of the decay curves of $_{72}$Hf nuclei for some levels. Each cascade that populates the yrast level K from the side with intensity $P_K^{\varkappa}$ passes through several successive side levels with side feeding times $\varphi_K^{\varkappa\mu}$, $\mu = 1, 2, \ldots, m$. In practice, only one level $m = 1$ was taken, and for test calculations $m = 2$ and 3 were taken (double and triple side feeding cascade).

The theoretical formula for the decay curve is then

$$R_I(t) = \sum_{K=I}^{I_f} \left[A_{IK} \exp(-t/\tau_K) + \sum_{\varkappa=1}^{p} \sum_{\mu=1}^{m} B_{IK}^{\varkappa\mu} \exp(-t/\varphi_K^{\varkappa\mu}) \right] \tag{72}$$

with the notation

$$A_{IK} = \sum_{\varkappa=1}^{p} \sum_{M=K}^{I_f} P_{IM}^{\varkappa} \prod_{\substack{L=I \\ (L \neq K)}}^{M} \frac{\tau_K}{\tau_K - \tau_L} \prod_{\mu=1}^{m} \frac{\tau_K}{\tau_K - \varphi_M^{\varkappa\mu}}; \tag{73}$$

$$B_{IK}^{\varkappa\mu} = P_{IK}^{\varkappa} \prod_{L=I}^{K} \frac{\varphi_K^{\varkappa\mu}}{\varphi_K^{\varkappa\mu} - \tau_L} \prod_{\substack{\lambda=1 \\ (\lambda \neq \mu)}}^{m} \frac{\varphi_K^{\varkappa\mu}}{\varphi_K^{\varkappa\mu} - \varphi_K^{\varkappa\lambda}}. \tag{74}$$

We have used the normalized values of the total population and the side population,

$$N_{IK} = N_K / N_I; \quad P_{IK}^{\varkappa} = P_K^{\varkappa} / \sum_{\varkappa'=1}^{p} \sum_{K'=I}^{I_f} P_{K'}^{\varkappa'}, \tag{75}$$

which are derived in Ref. 320.

The problem of extracting the lifetime τ_I and the side feeding time φ_I can in principle be solved by fitting to the experimental data by the least-squares method. Such fitting was programmed for computer calculations and carried out in two independent ways:

1) χ^2 minimization or analogs of it by means of regularized iterative processes on a large computer of the type CDC-6200 (Ref. 370);

2) χ^2 minimization by means of a "maximal descent spiral" on a minicomputer of the type TPA and IZOT-0310 (unpublished program); the principle here is a direct comparison of the minimized functional for χ^2 at the mesh points of a system of embedded multidimensional parallelepipeds, only a suitable "spiral" of these points being chosen.[320]

In the back-bending region, τ_I (structure effect) and φ_I (reaction effect) are usually strongly correlated. Numerical experiments showed that the experimental decay curves $R_I(t)$ are strongly sensitive to the choice of τ_I and weakly sensitive to φ_I at low spins, where the normalized side populations P_{II} (75) are small. Conversely, they are weakly sensitive to τ_I and strongly sensitive to φ_I at high spins, where P_{II} are large. This makes the method good for investigating structure (τ_I) at low spins and more suitable for investigating the population mechanism (φ_I) at high spins (see below). Nevertheless, at the back-bending point, because of the weak variations of $B(E2)$ and the strong dependence of τ_I on the transition energy $\sim E_{I\to I-2}^{-5}$ (64), the decrease of E leads to an appreciable increase of τ_I and thus to much cleaner determinations of it than for neighboring I. This circumstance makes it possible to investigate the structure (τ_I) of high-spin states precisely at the back-bending point (see below), which is the most interesting from the point of view of conclusions concerning its mechanism.

22. COULOMB EXCITATION

For Coulomb excitation[13,14,16] there is a well-developed theory (see Refs. 300–302, and also 371), which means that it can be used not only for measurements of the reduced transitions probabilities on the basis of the lifetimes obtained by the DSRD and DBLS methods, but also to determine the internal moments by measurement of the excitation probabilities (cross sections).

It is also possible to measure the angular distributions in order to obtain information about the spins and the coefficients of multipole mixing.

In Coulomb excitation, a fundamental part is played by the so-called *Coulomb barrier*:

$$E_c = \frac{1.44}{r_0}\frac{Z_i Z_t}{A_i^{1/3}+A_t^{1/3}}(1+A_i/A_t),\ \text{MeV}\cdot\text{F}, \tag{76}$$

where $r_0 = 1.41$F; Z_i and A_i refer to the ion and Z_t and A_t to the target. As will be seen in Sec. 23, the cross sections of nuclear reactions decrease strongly if the ion energy E_i falls below the barrier E_c, so that $E_i \ll E_c$ is then the condition for observing Coulomb excitation in a pure form. Simultaneously, this condition ensures the validity of the quasiclassical description.[371] The corresponding cross section in the first order of perturbation theory is[300]

$$d\sigma_{EL} = (Z_t e/\hbar v_i)^2 a^{-2L+2} B(EL;\ i\to f)\, df\, d_{EL}(\theta\xi\eta_i) \tag{77}$$

with the notation

$$a = \frac{Z_i Z_t e^2}{M v_i v_f};\quad \eta_{i,f} = \frac{Z_i Z_t}{\hbar v_{i,f}};\quad \xi = \eta_f - \eta_i, \tag{78}$$

where θ is the scattering angle, M is the reduced mass of the ion and target nuclei, and v_i and v_f are the velocities of the ions before and after the collision. For a magnetic transition, it is necessary to substitute $EL \to ML$ and multiply the right-hand side of (77) by $v_i v_f/c^2$. The functions f_{EL} have been tabulated. Multiple excitation takes into account virtual excitations through intermediate states, and its description reduces to a coupled system of differential equations.[371] There exist programs for computer calculations.

As some examples of recent applications in the region of low spins, we mention only the completion of the systematics of the $E2$ and $E4$ moments and, in particular, the hexadecapole β_{40} deformations for nuclei from $_{60}$Nd to $_{76}$Os (Refs. 372–374). It turns out that β_{40} are positive for nuclei from $_{60}$Nd to $_{66}$Dy, pass through zero near $_{68}$Er, and are negative for nuclei from $_{70}$Yb to $_{76}$Os. There may be a difference between the deformation of the charge and of the complete nucleus.[373] In Refs. 375–377, vibrational 2^+ and 3^- states were excited in the nuclei $_{64}$Gd, $_{68}$Er, $_{72}$Hf, and $_{74}$W. In Ref. 378, the transition probabilities between the γ bands of $^{162}_{66}$Dy and $^{168}_{68}$Er were determined.

We shall return to high spins in combination with lifetime measurements in Secs. 28 and 29. Here we mention investigations of a different nature using the ions $_{54}$Xe, $_{82}$Pb, and $_{92}$U. In Ref. 379, $^{136}_{54}$Xe ions were used to achieve spins 16^+ (18^+) in $^{164}_{68}$Er. In Ref. 380, levels of the ground-state band up to 10^+ and a γ-ray band up to 8^+ were excited by $^{136}_{54}$Xe ions in $^{192,194,196}_{78}$Pt nuclei and their γ softness was determined. We mention the record attainment of 28^+ levels in $^{238}_{92}$U by $^{238}_{92}$U and $^{208}_{82}$Pb ions and the simultaneous excitation of a negative-parity band up to 15^- by $^{208}_{82}$Pb ions.[381] It has already been established that, in contrast to population "from above" in the (HI, xn) reaction, Coulomb excitation "from below" excites preferentially, not the yrast band, but the continuation of the ground-state band, this depending on the reduced probabilities of transitions coupling the levels, i.e., a different branch in the picture of band crossing.[315] We shall consider the significance of this circumstance for our understanding of the back-bending mechanism in Sec. 26. In recent cases of Coulomb excitation to achieve record spins, an interesting particle–γ-ray coincidence device was used to correct the Doppler shift.[382]

23. COMPOUND-NUCLEUS REACTION

Experiments using the (HI, xn) reaction are planned and analyzed on the basis of semiempirical theoretical approaches.[303,304] The compound-nucleus reaction is divided into two stages associated with the formation (entrance channel) and decay (exit channel) of the compound system:

$$\sigma(E_f, I) = \sum_{J=0}^{J_{\max}} \sigma_c(E_i, J)\, G(E_f, I; J)/g(J), \tag{79}$$

where $\sigma(E_f, I)$, multiplied by the level density of the final nucleus, determines the cross section per unit interval of the excitation energy for obtaining a final nucleus with excitation energy E_f and spin I; $\sigma_c(E_i, J)$ is the cross section for production of a compound nucleus with spin J at ion energy E_i (entrance channel); $G(E_f, I; J)$ and $g(J)$ are the partial and total decay widths of the compound nucleus (exit channel); σ_c is parametrized by the so-called *transmission coefficient* $T_l(E_i)$ for the entrance channel; G and g are parametrized in terms of $T_l(E_f)$ for the exit channel.[303] In the analysis of the entrance channel, it is important, first, to know the total reaction cross section, which is estimated in the model of a black nucleus.[383] The cross sections and angular momenta are given in the most convenient form in Ref. 384. Characteristic features are the zero cross section below the Coulomb barrier ($E_i < E_c$), the very strong growth in the region of the potential barrier ($E_i \sim E_c$), and the smooth growth, which slows down, above that barrier ($E_i > E_c$) [see (76)].

However, only part of the total cross section corresponds to the complte-fusion reaction; the remaining part is associated with *peripheral reactions*. This part is determined by the critical angular momentum J_{cr}, which is replaced by the J_{max} of the black-nucleus model in (79). This is an already well-established experimental fact,[385] which is due to the fact that when $E_i > E_c$ the growth is replaced by a decrease.[386] The peripheral reactions reduce basically to transfer reactions[387] and change somewhat the Z of the target nucleus. Recently, various methods have been proposed for estimating J_{cr} on the basis of two mechanisms: dynamical effects in the entrance channel[388,389] and instability of the compound system (Refs. 293, 390, and 391). The two methods lead to approximately the same estimates.[4] There has also been proposed a method of experimental determination based on the spin selectivity of the reaction.[392]

In Ref. 393 there is a review of the problem of preequilibrium processes. In Ref. 394, there is a discussion of the problem of the different critical angular momenta (in addition to that of complete fusion) for, for example, fission in reactions induced by $^{40}_{18}$Ar and $^{86}_{36}$Kr and leading to the compound nuclei $^{154\text{-}164}_{68}$Er. In connection with the problem of the possible absence of fusion

with evaporation of particles at small transfers of the angular momentum for the fairly heavy $^{86}_{36}$Kr ions, the absence of such behavior has been established. It is concluded that there are pre-equilibrium processes with the emission of charged particles at high excitation energies because of the dependence of their probabilities on the energy and the ion, in contrast to the predictions of (79). In Ref. 395, a second pre-equilibrium neutron is assumed. From data on multiplicity measurements,[396] one can conclude that more than one pre-equilibrium neutron is emitted in the reaction with $^{4}_{2}$He; in other cases of the heavier ions $^{20}_{10}$Ne and $^{40}_{18}$Ar, that there is a compound-nucleus type reaction.

24. DE-EXCITATION OF THE COMPOUND NUCLEUS

Statistical and empirical considerations are used in analyzing the exit channel. After a time of the order of several units on the 10^{-18} sec scale,[397,398] the compound nucleus decays basically with the evaporation of neutrons.[399,400] We mention the new technique of time measurement in the previously inaccessible region 10^{-16} sec (Ref. 401) based on the displacement of X lines because of the emission of protons. It is only at higher energies that there is increased competition from the emission of charged particles,[402] in particular, protons[404] and α particles[404,396]; nevertheless, in reactions with carbon[403] the evaporation of up to 12 neutrons was observed (Fig. 26). For heavier nuclei and higher energies, competition from fission is important[405,406]; in Ref. 395, later results have been considered.

The process of evaporation of neutrons is considered in a simple statistical model,[407] which gives the excitation function, i.e., the cross sections as a function of the excitation energy E^*:

$$E^*_{\text{lab}} = E^*_{\text{cms}}(1 + A_i/A_t); \quad E^*_{\text{cms}} = \Delta E_t + \Delta E_i - \Delta E_c, \tag{80}$$

where ΔE_t, ΔE_i, and ΔE_c are the rest-energy excesses of the target nuclei, the ion, and the compound nucleus relative to the sum of the rest energies of the nucleons; these energies can be calculated by means of the mass tables given, for example, in Refs. 408 and 409. Maxima $\sigma_{\max}$ are obtained at energies $E^*_{\text{cms},\max}$ that increase with the number of neutrons x. They can be determined from

$$E^*_{\text{cms,max}} = \sum_{i=1}^{x} B_i + x\varepsilon, \tag{81}$$

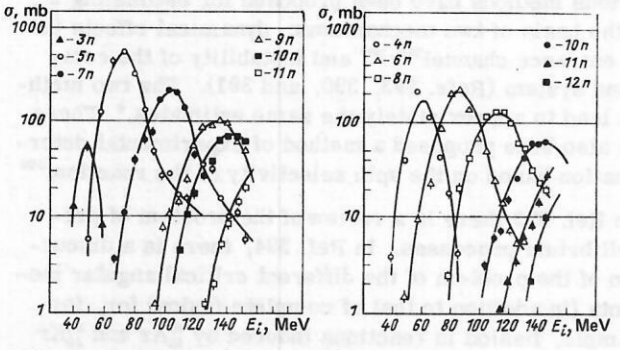

FIG. 26. Excitation functions of the reaction $^{130}_{52}\text{Te}(^{12,13}_{6}\text{C}, xn)^{142,143-x}_{58}\text{Ce}$: on the left for ^{12}C and on the right for ^{13}C (Ref. 404).

where B_i is the binding energy of the ith neutron[408,409]; ε is the mean energy lost in the emission of one neutron in the form of kinetic energy and the energy of the γ rays. All this facilitates the identification of the products.[410] In the determination of $E^*_{\max}$, an important part was played by the empirical Simonoff–Alexander rule,[411] which subsequently was made more precise on the basis of extensive empirical data by Neubert[412]:

$$\varepsilon = 9.0 - 2.4 \cdot 10^{-2} A_c, \text{ MeV}, \tag{82}$$

where A_c is the mass number of the compound nucleus. For the use of the statistical model to estimate the competition from the emission of charged particles and from fission, see Refs. 413 and 414, respectively.

In the process of evaporation of neutrons, as the first stage in the de-excitation of the compound nucleus, the initial distribution of the spins J of the compound nucleus changes and goes over into a narrower distribution of the spins I of the final nucleus, which can be obtained by a statistical theory[415,416] and also by a simple graphical calculation.[391] It is found that the neutrons carry away a small fraction of the angular momentum—up to $(1-2)\hbar$ each—and that a greater fraction is carried away in the second stage of de-excitation by γ rays in two stages: the statistical cascade (principally $E1$ transitions) and the yrast cascade (principally $E2$ transitions) in accordance with the combined model of population of the yrast band,[309] which has been confirmed experimentally[311] and is shown in Fig. 17. The problem of the distribution of the angular momentum in the final nucleus and its removal is also considered in Ref. 414. By measuring the multiplicity of the continuum γ rays and its spin distribution one can experimentally reconstruct[417] the spin distribution I of the final nucleus before the statistical cascade (Fig. 27) for lighter nuclei as well.[418]

The distribution of the γ rays for the statistical cascade ($E1$) and the continuous yrast cascade ($E2$) with respect to the spin carried away (roughly 0 or, respectively, 2 in one transition) is found principally in experimental studies, which were considered above. From this there follows an empirical relationship between the mean multiplicity $\langle M \rangle$ of the γ rays and the mean spin $\langle l \rangle$ carried away:

$$\langle l \rangle = 0\,\langle k \rangle + 2\,(\langle M - k \rangle), \tag{83}$$

where $\langle k \rangle$ is the mean number of γ rays of the statis-

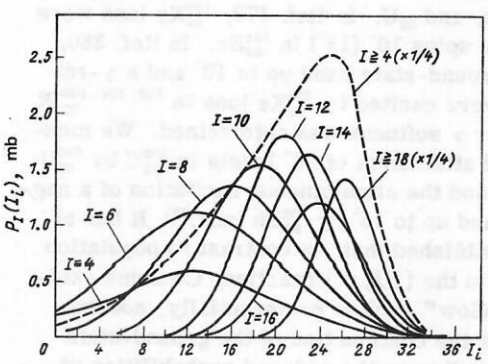

FIG. 27. Distribution of the spins I of the final nucleus after the reaction $^{150}_{60}\text{Nd}(^{16}_{8}\text{O}, 4n)^{162}_{68}\text{Er}$ (Ref. 417).

tical cascade. It can be taken equal to four,[312,313] although there are indications[400] for a value 2.5–4. The factor 0 follows from the fact that k for a transition of E_1 type is statistically distributed with respect to the change in the spin, and the factor 2 follows from the fact that $M-k$ for an $E2$ type transition is stretched,[311-313] although there is a dipole component.[314] The statistical treatment gives formula (67) for the energy distribution, but with restrictions that will be considered below.[4] Reference 419 is devoted to the theory of this problem in terms of the competition between the statistical (noncollective) and rotational (collective) de-excitation modes. The paper of Ref. 419 somewhat changes the classical picture[309] of de-excitation by γ rays shown in Fig. 17, since the competition can begin fairly high, 3–5 MeV above the yrast line; thus, this competition may be responsible for a de-excitation trajectory that is inclined on the average and more complicated than in Fig. 17.

25. SYSTEMATICS OF QUASIROTATIONAL ENERGIES AND INTERNAL E2 MOMENTS OF EVEN–EVEN NUCLEI: BOUNDARIES OF THE TRANSITION REGION

There exists well-developed schematics of quasirotational energies[202] and internal $E2$ moments and deformations (Refs. 69, 200, 201, 372, 373, and 420) as well as theoretical calculations of deformations (Refs. 40 and 421–423) and anadiabatic effects.[23] Although we shall not consider light nuclei here, we also mention Ref. 424, which leads to a self-consistent systematics of $B(E2)$ values in sd nuclei. Our task here is restricted, namely, using data for the nuclei $_{68}$Er (Ref. 367), $_{70}$Yb (Ref. 338), and $_{72}$Hf (Ref. 340) on the probabilities of the $E2$ transitions to the yrast line with the lowest spins, 2^+-0^+ and 4^+-2^+, to elucidate the systematics of the effects mentioned above. This region of nuclei is far from the stability band and is somewhat unusual, as will be seen below.

Table IV contains all data on the internal ($E2$) moments Q and the effective deformations β obtained on the basis of measurements of the lifetime τ_I of levels with $I=2$ and 4 (see below) extracted from their reduced transition probabilities $B(E2)$ in accordance with Eq. (64) in conjunction with the coefficients of internal conversion[333,334] and the further extraction of Q in accordance with (65) and β in accordance with (66). For comparison, in Table IV we also give the energy characteristics[202]: the moment of inertia J and the ratio E_4/E_2 of the energies of the first two levels. This last is, as is well known, a measure of the deviation of the nucleus from spherical shape through the deviation from a harmonic vibrator, $E_4/E_2=2$, and from deformed shape through the deviation from a rigid rotator, $E_4/E_2=10/3$. Such a comparison is of interest, since the probability parameter β gives direct indications of a transition in the shape, while the energy ratio E_4/E_2 gives only indirect indications. For comparison, we also give the Berkeley literature data for $^{156,158,160}_{68}$Er on the basis of our calculation of the data of Ref. 328. The reactions used to obtain these data are

$$^{120,122,124}_{50}\mathrm{Sn}\,(^{40}_{18}\mathrm{Ar},4n)\,^{156,158,160}_{68}\mathrm{Er}; \quad (84)$$

$$^{124,126,128,130}_{52}\mathrm{Te}\,(^{40}_{18}\mathrm{Ar},4n)\,^{160,162,164,166}_{70}\mathrm{Yb}; \quad (85)$$

$$^{122,124}_{50}\mathrm{Sn}\,(^{48,50}_{22}\mathrm{Ti},4n)\,^{166,168,170}_{72}\mathrm{Hf}. \quad (86)$$

From Table IV, we can draw the following conclusions:

1) the probability parameters—the internal $E2$ moment Q and the effective quadrupole axial deformation β, reveal the same tendency to decrease with decreasing number N of nucleons when the magic value 82 is approached as the energy parameters, i.e., the moment of inertia J and the ratio E_4/E_2. This tendency is readily understood from the point of view of a transition from a deformed to a spherical shape;

2) the observed transition with decreasing N is fairly abrupt in all three cases of the nuclei $_{68}$Er, $_{70}$Yb, and $_{72}$Hf but still takes place, roughly speaking, within a range of variation of N of approximately four units;

3) if the boundary of the transition region is fixed where the sharp decrease of all the parameters is observed, it can be seen from Table IV that it passes through the nuclei $^{158}_{68}\mathrm{Er}_{90}$, $^{162}_{70}\mathrm{Yb}_{92}$, $^{166}_{72}\mathrm{Hf}_{94}$. Thus, a somewhat unexpected effect is observed: The boundary is moved from the magic number $N=82$ with increasing number Z of protons from 8 neutrons for $_{68}$Er through 10 neutrons for $_{70}$Yb to 12 neutrons for $_{72}$Hf.

This may be related to the well-known problem of the boundary of the transition region,[48] due to competition between the effects of deformation by nucleons in unfilled shells and stabilization of the spherical shape by pairing. Then such an effect can be explained by the correlation between the deviations from the magic values in the numbers of neutrons N and protons Z. Indeed, the increase of Z from $_{68}$Er to $_{72}$Hf means that the magic number of protons, $Z=82$, is approached, although from below, namely, from 14 protons for $_{68}$Er through 12 protons for $_{70}$Yb to 10 protons for $_{72}$Hf. Thus, the discovery of this effect means that we have traced the bending of the boundary of the transition region around the point $Z=82, N=82$. In the case of $_{68}$Er, the transition is due to the neutrons, while for $_{70}$Yb and $_{72}$Hf the neutrons and protons are equally important for the transition. At even higher Z, the protons must play the main part.

TABLE IV. Moments of inertia $J=3/E_2$, energy ratios E_4/E_2, internal $E2$ moments $Q=Q(2\rightarrow 0)$, and effective quadrupole deformations $\beta=\beta(2\rightarrow 0)$.

Nucleus	J, MeV^{-1}	E_4/E_2	Q, b	β
$^{156}_{68}$Er$_{88}$	8.7	2.32	$\left\{\begin{array}{l}4.1\pm0.1^{a}\\4.020\pm0.073\end{array}\right.$	$\begin{array}{l}0.185\pm0.005^{*}\\0.182\pm0.003\end{array}$
$^{158}_{68}$Er$_{90}$	15.6	2.74	$5.3\pm0.15^{*}$	$0.235\pm0.01^{*}$
$^{160}_{68}$Er$_{92}$	23.8	3.10	$\left\{\begin{array}{l}6.5\pm0.15^{*}\\6.54\pm0.11\end{array}\right.$	$\begin{array}{l}0.28\pm0.01^{*}\\0.286\pm0.005\end{array}$
$^{160}_{70}$Yb$_{90}$	12.34	2.626	4.81 ± 0.08	0.207 ± 0.003
$^{162}_{70}$Yb$_{92}$	18.02	2.924	6.07 ± 0.45	0.257 ± 0.019
$^{164}_{70}$Yb$_{94}$	24.29	3.128	6.79 ± 0.13	0.284 ± 0.006
$^{166}_{70}$Yb$_{96}$	29.33	3.228	7.26 ± 0.18	0.301 ± 0.008
$^{166}_{72}$Hf$_{94}$	18.90	2.966	5.94 ± 0.14	0.241 ± 0.005
$^{168}_{72}$Hf$_{96}$	24.25	3.114	6.49 ± 0.14	0.261 ± 0.006
$^{170}_{72}$Hf$_{98}$	29.91	3.202	7.14 ± 0.30	0.284 ± 0.012

*Ref. 328.

26. BACK-BENDING AND BAND CROSSING

A compilation of data on the energies of yrast levels associated with back-bending is shown in Fig. 18. It is the compilation of Ref. 322 augmented in the review of Ref. 4. The review of Ref. 4 gives diagrams of the eight nuclei $^{124\text{-}130}_{56}$Ba and $^{128\text{-}134}_{58}$Ce (see Fig. 11 in Ref. 4), which are not given here. There have recently been published new data on $^{172,174,176}_{74}$W (Refs. 425 and 426), $^{178,180,182}_{74}$W (Ref. 427), and $^{154}_{68}$Er (Ref. 428) and repeated measurements of the yrast levels of $^{164,166}_{68}$Er (Ref. 429); in Ref. 429, there is a discussion of the connection with the measurements of the lifetimes. New data have been obtained on the yrast levels of $^{164}_{68}$Er (Refs. 428 and 429) and there have been repeated measurements of the yrast levels of $^{172}_{72}$Hf (Refs. 33 and 34) in connection with the discovery of many side bands in these two nuclei.

It can be seen from Fig. 18 that back-bending is observed predominantly in neutron-deficient nuclei. This was already discussed in connection with back-bending mechanisms, but we can now say that it is evidently due to the method of excitation. Indeed, neutron-deficient nuclei far from the stability band are excited in (HI, xn) reactions, whereas Coulomb excitation can naturally be used for stable nuclei. On the other hand, it has been shown experimentally[315] that the (HI, xn) reactions populate mainly the yrast line, whereas Coulomb excitation populates the ground-state band. According to the model of band crossing,[144,145] they differ above the back-bending point, it being the yrast line that exhibits back-bending (see below). It can also be seen from Fig. 18 that an irregularity is sometimes observed in the back-bending phenomenon: It is absent in $^{168}_{70}$Yb but present in the neighboring even–even nuclei $_{70}$Yb or, conversely, in $^{154}_{64}$Gd. In theoretical studies (for example, Ref. 238 and the references there for $_{70}$Yb nuclei) such irregularities are attributed to features of the scheme of single-particle levels near the Fermi surface.

It can now be regarded as proved[4] that back-bending is a property of the yrast line, which is identified with the ground-state band (g) below the back-bending point and with the superband (s) above it, as has been demonstrated by the investigations of $^{154}_{64}$Gd, $^{154,156}_{66}$Dy (Refs. 25–30 and 150). This can be clearly seen in Fig. 28. It is particularly convincing after population of the low-

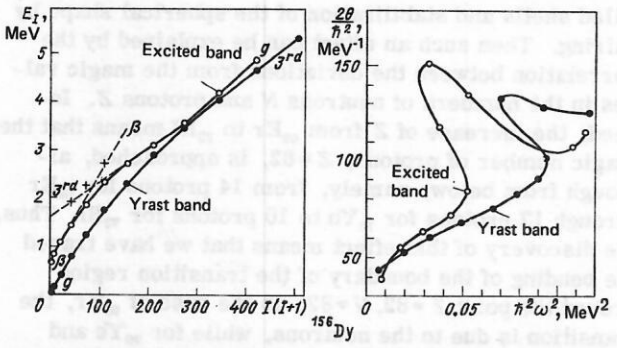

FIG. 28. Experimental confirmation that the back-bending effect is due to crossing of bands: for crossing of the g and β bands by a third "superband" in $^{156}_{66}$Dy (Ref. 4) according to the data of Refs. 28 and 30.

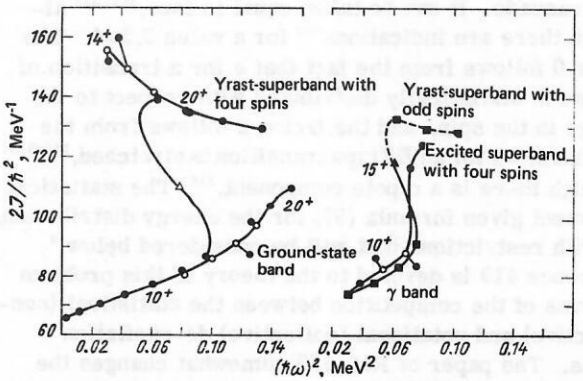

FIG. 29. Back-bending diagram of the nucleus $^{164}_{68}$Er resulting from the crossing of the g, γ, and s bands.[33] The black circles are the experimental points, the open circles are the corrected values, and the black triangles indicate transitions between bands.

spin continuation of the superband in $^{156}_{66}$Dy (Ref. 30). Disagreement with such an identification was voiced in Ref. 432, although in Ref. 433 reference is made to a possible continuation of the superband consisting of the levels (2^+), $4^+, \ldots, 10^+$. There is also disagreement with regard to the properties of the superband: In the original papers of the model of band crossing[145] it was ascribed quantum numbers $K^\pi = I^+$, whereas it is assumed in Ref. 434 that 0^+ and 1^+ equally well describe the data if the γ band is taken into account. It is difficult to prove this exactly in an experiment,[433] and for the purpose of orientation we can take the values $K^\pi = 0^+$.

In the literature there are already the first indications of a superband with odd spins, besides a superband with even spins, and of the intersection of the γ band with these two superbands.[33,34] A curious situation has arisen: An yrast band of positive parity with odd spins is situated 500 keV higher than an yrast band with even spins (Fig. 29). This is all explained by the mechanism of rotational alignment (see Sec. 15).

In reactions of even–even nuclei with α particles and heavier ions, levels that differ from those of the yrast line and also from the positive-parity levels that cross it are excited. These are side bands of negative parity

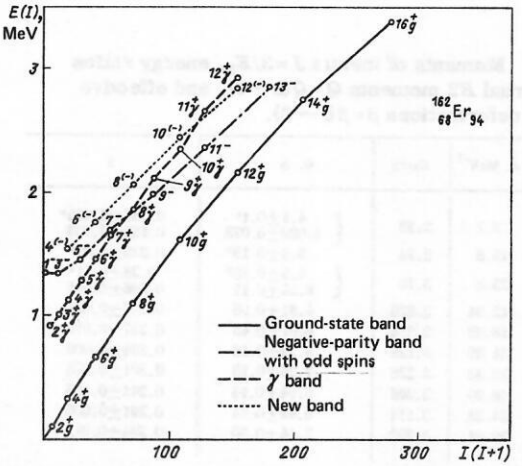

FIG. 30. Bands of different parity in the nucleus $^{162}_{68}$Er (Ref. 32).

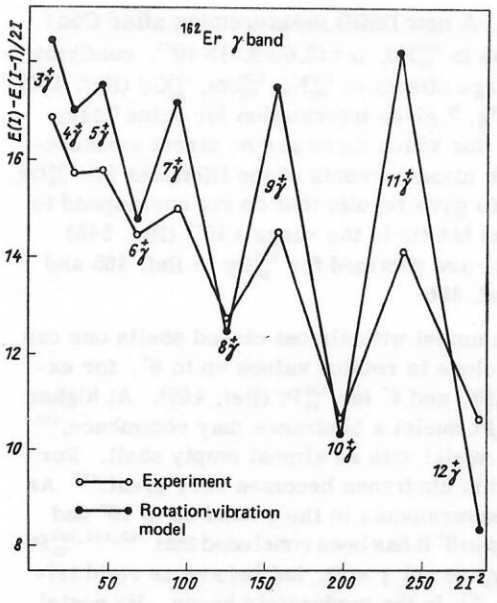

FIG. 31. Zigzag effect in the γ band of the nucleus $^{168}_{68}$Er (Ref. 32). The experiment is the lower zigzag. The calculations are the upper zigzag and are in accordance with the rotation-vibration model of Ref. 147.

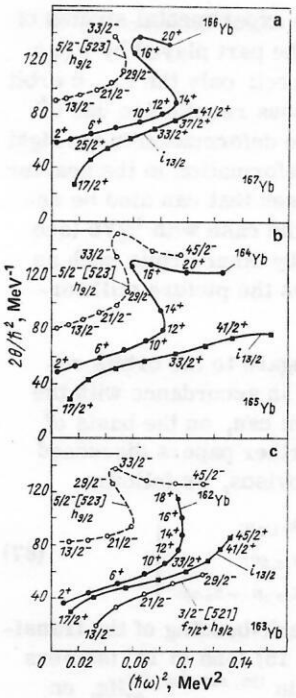

FIG. 32. Back-bending diagram of odd and even $_{70}$Yb nuclei (Ref. 444). c) is the rigid-rotator limit.

with odd spins,[4] and they appear systematically[435] in the isotopes $^{186\text{-}194}_{78}$Pt and $^{190\text{-}200}_{80}$Hg and have been studied in detail in $_{78}$Pt (Refs. 436 and 437) and $_{80}$Hg (Refs. 438 and 439). They are also manifested in the nuclei $^{172,174,176}_{74}$W (Ref. 426), $^{182}_{74}$W (Ref. 428), $^{172}_{72}$Hf (Refs. 430 and 431), and also in lighter nuclei, for example, $^{156}_{68}$Er (Ref. 31), $_{58}$Ce, and $_{56}$Ba, as in $^{126,128}_{56}$Ba (Ref. 449), and in heavier nuclei such as $^{238}_{92}$U (Ref. 441), in which one observes an octupole-vibrational band $K=0$, $I^{\pi}=1^-, 3^-, \ldots, 19^-$. Sometimes, one also observes an even part of the band, raised in energy relative to the odd part, as, for example, $I^{\pi}=2^-, 4^-, \ldots, 12^-$ in $^{162}_{68}$Er (Ref. 32) (Fig. 30) and also in the nucleus $^{164}_{68}$Er (Refs. 33 and 34). The zigzag effect in the γ bands of positive parity is shown in Fig. 31. The mechanisms of occurrence of the side bands are octupole vibrations[277] and rotational alignment,[278] which were mentioned in Sec. 15. A combination of the mechanism of octupole vibrations at low spins with alignment at spins above 11^- is assumed in $^{150}_{64}$Gd for the negative-parity band with odd spins.[442]

27. BACK-BENDING IN ODD NUCLEI AS A TEST OF ROTATIONAL ALIGNMENT

We now consider the interesting suggestion of using the presence or absence of back-bending in an odd nucleus as a test of the RAL mechanism for back-bending in a neighboring even–even nucleus (Refs. 4, 6, 332, and 443). It is assumed that if a nucleon in an odd nucleus is in an orbit that must be used in accordance with the RAL mechanism in the alignment of two nucleons, the even nucleus will exhibit back-bending, while the odd one will not because of the blocking of the orbit by the odd nucleon. Investigating the $\Delta I=2$ bands of the odd nucleus based on different single-quasiparticle states, one can "feel out" the orbit responsible for the back-bending in the even–even neighbor. This is shown in Fig. 32 (Ref. 444). For the example of $^{167,165}_{70}$Yb it can be seen that precisely the $i_{13/2}n$ orbit does not exhibit back-bending in the odd nuclei and is therefore responsible for the back-bending in the neighboring even $_{70}$Yb nuclei.

Such an approach has been implemented experimentally[4] in a number of cases. For example, in the isotopes $^{154\text{-}160}_{66}$Dy and $^{156\text{-}160}_{68}$Er it is concluded on the basis of the positive result of the test of the participation of the $i_{13/2}n$ orbit in the back-bending[445] and the negative result for $h_{11/2}p$ (Ref. 446) that the neutron orbit $i_{13/2}$ is responsible for the back-bending from the left-hand edge of the deformed region $82<N<126$. At the right-hand end of the same region at the isotopes $^{182,184}_{76}$Os and $^{184}_{78}$Pt there is a test that the proton orbit $h_{9/2}$ is responsible (Refs. 4, 447, and 448). In the so-called *new deformation region* $Z>50, N<82$, for example, for $^{126,128}_{56}$Ba and $^{128,130}_{58}$Ce protons are again responsible, but with the $h_{11/2}$ orbit.[449,450]

However, papers have been published which question whether only one orbit is responsible or whether it is at least two, for example, $h_{9/2}p$ and $i_{13/2}n$ for the back-bending in $^{182,184}_{76}$Os (Ref. 451) and in $^{178,180}_{74}$W (Refs. 427 and 452), the $i_{13/2}n$ orbit again apparently being predominant in these last nuclei.[452] A similar situation is observed in the middle of the region $82<N<126$ for $^{164}_{68}$Er and $^{164,166}_{70}$Yb in the tests of the neighbors with odd N, $^{165}_{70}$Yb (Ref. 453), and odd Z, $^{167}_{71}$Lu (Ref. 454) and $^{165}_{69}$Tm (Ref. 455). Here again there are indications of the participation of both the $i_{13/2}n$ and $h_{9/2}p$ orbits. This then means that one must question whether the RAL effect is manifested in a pure form.

Theoretical attempts have been made to show that this is not so. In one attempt,[272] it is asserted that $i_{13/2}n$ is the responsible orbit in the region of $_{70}$Yb and $h_{9/2}p$ is only a catalyst (see Sec. 15), while in Ref. 456 it is

said that the conclusions of the experimental studies of Refs. 447 and 451 concerning the part played by $h_{9/2}p$ in the region of $_{76}$Os are incorrect; only the $i_{13/2}n$ orbit is responsible, and the ambiguous results are due to the part played by hexadecapole deformation in the light isotopes of $_{76}$Os and nonaxial deformation in the heavier isotopes. In contrast to the cases that can also be regarded as transitional cases, the case with $^{163}_{70}$Yb (see Fig. 32) reveals a part played by other orbits such as $(f_{7/2}+h_{9/2})n$, which complicates the picture still further.[444]

The general situation with regard to the orbits responsible for the back-bending in accordance with the rotational alignment mechanism can, on the basis of the review of Ref. 4 and the further papers discussed here, be represented, with provisos, as follows:

$$\left.\begin{array}{ll} ^{126,\,128}_{56}\mathrm{Ba},\ ^{128,\,130}_{58}\mathrm{Ce}: & h_{11/2}p; \\ ^{154-160}_{66}\mathrm{Dy},\ ^{156-160}_{68}\mathrm{Er},\ ^{162-166}_{70}\mathrm{Yb}: & i_{13/2}n; \\ ^{178,\,180}_{74}\mathrm{W}\rightarrow\ ^{182,\,184}_{76}\mathrm{Os},\ ^{184}_{78}\mathrm{Pt}: & i_{13/2}n\rightarrow h_{9/2}p. \end{array}\right\} \quad (87)$$

The phenomena simulating back-bending of the transition region $_{78}$Pt, $_{80}$Hg (see Sec. 15) lead to 12^+ isomers in $^{190,\,192}_{78}$Pt and to 10^+ isomers in $^{190,\,192,\,194,\,196}_{80}$Hg, on which there is based a band with energy intervals similar to the energy intervals at the start of the ground-state band.[4] There are theoretical indications[4] that bands with responsible orbits $i_{13/2}n$ and $h_{11/2}p$ are based on 12^+ in $_{78}$Pt and 10^+ in $_{80}$Hg, respectively. A transition to $i_{13/2}n$ in $^{198}_{80}$Hg is possible.[275] For $_{80}$Hg nuclei, there are also experimental indications of what we have said above.[4] For the $_{78}$Pt nuclei, there is also an experiment, but of a different kind, namely, measurement of the g factors of 12^+ isomers.[359]

Besides considering these phenomena in the framework of the usual model of the coupling of quasiparticles to an asymmetric rotator,[457] another approach is possible in the framework of the alternative model of coupling of quasiparticles to a vibrator.[458] These models penetrate into the transition region from different sides, deformed and spherical, respectively, with equal success.[4] This can be concluded from the theoretical[459] and experimental[460] investigations in the transition nuclei $_{78}$Pt and $_{80}$Hg.

28. LIFETIMES AND PROBABILITIES OF E2 TRANSITIONS BELOW THE YRAST BAND: ANADIABATIC EFFECTS

From information on the lifetimes τ_I one can extract the reduced probabilities $B(E2;\ I\rightarrow I-2)$, the internal $E2$ moments $Q(I\rightarrow I-1)$, and the effective quadrupole deformations $\beta(I\rightarrow I-2)$ in accordance with Eqs. (64)–(66). Further, if a limitation is made to data for the low-spin region $I\leqslant 8$, where the anomalies associated with back-bending are not yet manifested, one can extract the parameter α of the anadiabatic deviations by means of (21).

Experimental information about α is given in Fig. 7 and, as can be seen, it is very small (see also Refs. 4 and 332). The DSRD measurements of the lifetime after Coulomb excitation of levels up to 10^+ (Refs. 158, 230, 346, and 461–463) for the $_{62}$Sm and $_{64}$Gd nuclei are the most reliable. A new DSRD measurement after Coulomb excitation in $^{150}_{60}$Nd, $\alpha=(2.6\pm0.5)\times10^{-3}$, confirms the regular large effects in $^{150}_{60}$Nd, $^{152}_{62}$Sm, $^{154}_{64}$Gd (Ref. 464). In addition, Fig. 7 gives information for some heavy $_{70}$Yb isotopes, for which there are no direct measurements.[230] Such measurements of the lifetimes for $^{164}_{66}$Dy, $^{170}_{68}$Er, and $^{174}_{70}$Yb gave results that do not correspond to negative values but lie in the range $\pm10^{-3}$ (Ref. 345). Similar results are obtained for $^{162}_{66}$Dy in Ref. 465 and for $^{164}_{66}$Dy in Ref. 466.

In transition nuclei with almost closed shells one can obtain values close to rotator values up to 6^+, for example, for $^{192}_{78}$Pt, and 4^+ for $^{194}_{76}$Pt (Ref. 467). At higher spins in the $_{78}$Pt nuclei a hindrance may commence,[468] in contrast to nuclei with an almost empty shell. For the 10^+ level this hindrance becomes very great.[437] As a result of measurements in the g band up to 10^+ and in the γ band up to 8^+ it has been concluded that $^{192,194,196}_{78}$Pt most probably are not γ soft, but behave as rigid triaxial rotators.[380] In the moderately heavy $_{80}$Hg nuclei, such hindrances are at first ($^{190}_{80}$Hg) associated with a two-hole $h_{11/2}p$ nature. They gradually disappear with the consequence that in $^{198}_{80}$Hg the rigid-rotator behavior is preserved up to 12^+ (Ref. 275).

Additional information has been obtained for a number of the neutron-deficient $_{68}$Er, $_{70}$Yb, and $_{72}$Hf nuclei by a lifetime measurement by the DSRD method after the (HI, xn) reactions (84)–(86) in Refs. 338, 340, and 367. A least-squares evaluation of formula (21) gives the internal $E2$ moment at 0 spin, $Q=Q(0)$, and the parameter α. They are given in Table V and compared with the microscopic calculations from Sec. 13 and Fig. 7.

In Table V, we also give calculations of α in accordance with the formulas (27) of the phenomenological model of the coupling of the β and γ bands with the g band[159] and on the basis of our microscopic calculations of z_0 and z_2 and the $B(E2)$ branching ratios. The agreement with the independently calculated microscopic values of α indicates a fact known from other studies[23]; namely, coupling to the β band (α_0) makes the main contribution to the coefficient α of the anadiabatic deviations within the g band.

TABLE V. Internal $E2$ moments Q and parameters α of the anadiabatic deviations.

Nucleus	Theory					Experiment	
	Q, b	α (10^{-3})	α_0 (10^{-3})	α_2 (10^{-3})	α_{02} (10^{-3})	Q, b	α (10^{-3})
$^{156}_{68}$Er$_{88}$	—	3.26[a]	—	—	—	3.99±0.09	4.28±2.75
$^{158}_{68}$Er$_{90}$	6.33	4.71	3.38	0.28	3.66	5.24±0.15[b]	3.76±2.30[b]
$^{160}_{68}$Er$_{92}$	6.34	2.26	2.48	0.25	2.73	6.54±0.11	0.32±1.03
$^{160}_{70}$Yb$_{90}$	6.33	3.24	1.65	0.43	2.08	4.79±0.09	2.51±1.57
$^{162}_{70}$Yb$_{92}$	6.33	3.04	3.28	0.16	3.44	6.10±0.45	1.24±4.17
$^{164}_{70}$Yb$_{94}$	6.34	1.82	2.24	0.27	2.51	6.85±0.12	0.05±0.88
$^{166}_{70}$Yb$_{96}$	6.34	1.47	1.74	0.23	1.97	7.24±0.14	−0.50±0.82
$^{162}_{72}$Hf$_{90}$	6.36	4.33	4.42	0.38	4.80	5.96±0.15	0.58±1.99
$^{168}_{72}$Hf$_{96}$	6.36	3.13	3.66	0.30	3.96	6.47±0.14	0.06±0.92
$^{170}_{72}$Hf$_{98}$	6.36	2.11	2.08	0.20	2.28	6.90±0.39	0.29±1.52

Note. The variant of calculations ThS has $\alpha_{02}=\alpha_0+\alpha_2$, where α_0 and α_2 are the parts of α calculated from the coupling to the β and γ bands, respectively. The superscript a indicates Ref. 269 and the superscript b indicates Ref. 364.

Let us consider the experimental data on the parameter α. Although it is equal to zero in the majority of cases within the experimental errors, cases are found when α is positive and outside the errors. Now these are in fact the cases of the soft transition nuclei $^{156}_{68}$Er and $^{160}_{70}$Yb. Therefore, here, as in Fig. 7, we again see the part played by softness in the occurrence of large positive anadiabatic deviations α. We note also the agreement between the tendency for α to increase with decreasing N and the theoretical calculations when they are at our disposal. On the other hand, we draw attention to a different behavior observed on the transition from the region of $_{68}$Er to the region of $_{72}$Hf. One here observes a decrease in the importance of softness, since in the $_{72}$Hf nuclei α has very small values even for soft nuclei. At the same time, one also observes an increase in the discrepancy with the calculations. The negative experimental values of α for the heavy $_{70}$Yb isotopes in Fig. 7 also fit into both these tendencies well, but here caution must be exercised.

The physical meaning of the increase in α in soft transition nuclei is obvious. It indicates an increase in the longitudinal deformability of the nuclei. On the other hand, these data for α confirm the general conclusion of Sec. 13 that calculations with the Hamiltonian of the model with pairing and quadrupole interaction for effects of second order in the rotation give, in this region of nuclei, better results for smaller Z and worse results for larger Z. This last circumstance may have the same origin as for ρ in Fig. 6 (see Sec. 13), namely, the effective forces in the particle–particle channel may not be reproduced well by the schematic interaction of Ref. 225.

29. LIFETIMES AND PROBABILITIES OF E2 TRANSITIONS IN THE REGION OF BAND CROSSING: THE BACK-BENDING MECHANISM

Measurements by the DBLS method after Coulomb excitation make it possible to obtain $B(E2)$ in the yrast lines of a number of stable isotopes[4, 332] (see Fig. 22) of rare-earth elements up to 12^+, and in the two cases of $^{162,164}_{66}$Dy up to 14^+ (Refs. 341 and 469), which approaches the point of crossing of the bands. In some cases, for example, for $^{162}_{66}$Dy, $^{164}_{68}$Er, $^{170}_{70}$Yb, there are reported to be hindrances in $B(E2)$ relative to a rigid rotator by 20–40%, and in $^{158}_{64}$Gd, $^{160,164}_{66}$Dy there is a similar tendency for hindrances of ~10%. For $^{164}_{68}$Er, the presence of a 37 ± 5% hindrance and the absence of such hindrance in $^{166}_{68}$Er is attributed[429] to the presence and absence, respectively, of back-bending (see Fig. 18). We note, however, that, as can be seen from Fig. 18, such measurements do not reach the point of back-bending, and it is therefore difficult to interpret them. In Ref. 466, the DSRD method after Coulomb excitation was used up to 12^+ in $^{164}_{66}$Dy; no deviations were observed, but the inaccuracies at high spins make it impossible to compare these data with the results of Ref. 341.

Recently, the Doppler-shift methods after Coulomb excitation were used in the heavy nuclei $^{232}_{90}$Th up to 10^+ (Ref. 470), $^{236}_{92}$U up to 12^+ (Ref. 471), and also in $^{174,176}_{70}$Yb with $_{86}$Kr and $_{54}$Xe ions up to 14^+ (Ref. 350) and in $^{232}_{90}$Th up to 18^+ (Ref. 351). No back-bending effect was observed, nor are there any deviations from the rotator model. Because Coulomb excitation excites the ground-state band predominantly, and not the continuation of the yrast line at high spins (see Sec. 20), this is not surprising.

TABLE VI. Transition energies $E_{I\text{-}I\text{-}2}$ and lifetimes τ_I.

Nucleus	Level I	$E_{I\to I-2}$, keV tabulated data	τ_I, psec	
			Experiment	Rigid rotator*
$^{158}_{68}$Er$_{88}$	2	344.2	50.05±1.81	50.05
	4	452.7	7.25±0.73	9.062
	6	543.3	2.93±0.45	3.329
	8	618.5	2.35±0.85	1.678
	10	674.4	2.25±1.00	1.061
	12	682.1	4.26±2.60	0.986
	14	522.7	8.1±4.8	3.665
$^{160}_{68}$Er$_{92}$	2	125.6	1326±45	1326
	4	263.8	46.67±1.52	47.43
	6	375.3	7.78±0.41	7.866
	8	463.7	2.44±0.61	2.646
	10	531.7	1.26±0.31	1.311
	12	579.2	0.84±0.21	0.841
	14	592.2	0.90±0.22	0.744
	16	533.9	1.57±0.20	1.236
	18	556.1	0.98±0.28	1.003

*Calculation in accordance with (64) and (65) with constant Q and normalization to the experimental τ_I of the lowest I.

When the DSRD method is used after (HI, xn) reactions, the region of band crossing can be reached (see Sec. 21). This method has been used to make measurements in nuclei of rare-earth elements up to spins 18^+–20^+ in $^{158}_{68}$Er (Ref. 364), $^{156,160}_{68}$Er (Ref. 367), $^{(160,162)164,166}_{70}$Yb (Ref. 338), and $^{166,168,170}_{72}$Hf (Ref. 340) in the reactions (84)–(86). The results of the last three investigations are given in Table VI for $_{68}$Er, in Table VII for $_{70}$Yb, and in Table VIII for $_{72}$Hf. In Ref. 349, the preliminary result of a similar measurement with $^{136}_{54}$Xe ions for $^{158}_{66}$Dy is reported. From these measurements, using the formulas (64)–(66), one can obtain derived quantities: the reduced transition probabilities $B/(E2; I\to I-2)$, the matrix elements of the internal $E2$ moment $Q(I\to I-2)$, and the effective $E2$ deformation $\beta(I\to I-2)$ (Refs. 338, 340, and 367).

TABLE VII. Transition energies $E_{I\to I-2}$ and lifetimes τ_I.

Nucleus	Level I	$E_{I\to I-2}$, keV		τ_I, psec	
		Tabulated data	Present paper	Experiment	Rigid rotator
$^{160}_{70}$Yb$_{90}$	2	243.0	243.1	182±6	182
	4	395.3	395.4	11.6±0.60	12.38
	6	508.8	508.8	2.73±0.30	3.235
	8	588.7	588.7	1.29±0.30	1.498
	10	(636)	636	0.87±0.50	0.993
$^{162}_{70}$Yb$_{92}$	2	166.5	166.5	578±85	578
	4	320.2	320.3	20.3±3.0	21.71
	6	436.2	436.2	4.6±0.9	4.352
	8	521.4	521.4	2.0±0.7	1.720
$^{164}_{70}$Yb$_{94}$	2	123.3	123.5	1272±50	1272
	4	262.4	262.8	42.8±1.5	44.54
	6	374.7	375.0	7.24±0.25	7.298
	8	463.0	463.0	2.20±0.70	2.472
	10	530.9	530.9	1.19±0.40	1.222
	12	576.9	576.9	0.80±0.30	0.794
	14	569.7	569.7	1.05±0.30	0.836
	16	490.0	490.0	2.53±0.50	1.748
	18	543.2	543.0	1.07±0.50	1.042
$^{166}_{70}$Yb$_{96}$	2	102.26	102.3	1789±90	1789.0
	4	228.05	227.9	76.3±2.5	75.10
	6	337.3	337.7	11.24±0.40	10.64
	8	430.4	430.2	3.09±0.35	3.109
	10	507.5	~507.3	1.46±0.70	1.339
	12	569.3	569.8	0.93±0.47	0.737
	14	603.3	603.5	0.73±0.42	0.547
	16	494.5	494.1	1.65±0.39	1.467
	18	509.1	~509.2	—	1.253
	20	588.8	588.4	—	0.608

TABLE VIII. Transition energies $E_{I\to I-2}$ and lifetimes τ_I.

Nucleus	Level I	$E_{I\to I-2}$, keV	τ_I, psec	
		Tabulated data	Experiment	Rigid rotator
$^{166}_{72}Hf_{94}$	2	158.7	717.4±33	717.4
	4	312.0	24.3±1.5	25.65
	6	426.9	5.41±0.68	5.053
	8	509.5	1.80±0.66	2.014
	10	564.0	0.95±0.70	1.185
	12	593.8	1.29±1.02	0.901
$^{168}_{72}Hf_{96}$	2	123.7	1278±54	1278.0
	4	261.5	51.5±5.2	49.57
	6	371.2	8.51±0.83	8.397
	8	456.6	2.86±0.27	2.898
	10	522.0	1.45±0.22	1.455
	12	569.8	0.75±0.26	0.925
	14	551.6	1.21±0.26	1.074
	16	452.9	2.62±0.29	2.845
$^{170}_{72}Hf_{98}$	2	100.3	1771±396	1771.0
	4	220,9	89.8±9.5	88.35
	6	320.4	15.6±1.3	13.88
	8	400.2	4.57±0.44	4.578
	10	462.0	2.19±0.27	2.196
	12	510.7	1.46±0.19	1.314
	14	550.6	0.95±0.21	0.894
	16	584.4	~ 0.64	0.659
	18	614.1	~ 0.50	0.511
	20	653.6	~ 0.34	0.373

The values of Q are shown in Fig. 33, from which it can be seen that in the complete range of measured nuclei the $B(E2)$ and Q values are close to the corresponding ones in the rigid-rotator model. One notes, however, a tendency for there to be no hindrance in the absence of back-bending, as in $^{170}_{72}$Hf, and for there to be hindrance at the point of back-bending when it is present. Particularly striking are the data on $^{164}_{70}$Yb. The $^{156}_{68}$Er data also indicate the possible existence of appreciable hindrance. Such a conclusion is confirmed by the observation of hindrance of the same order as in $^{164}_{70}$Yb for $^{158}_{66}$Dy in Ref. 349.

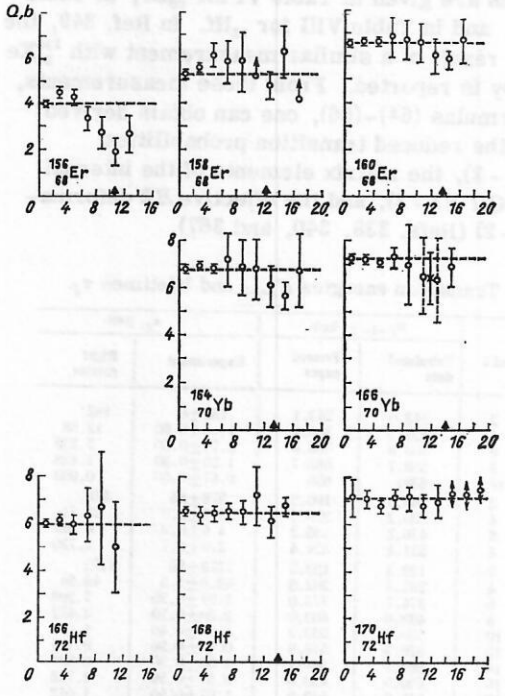

FIG. 33. Dependence of the internal $E2$ moment $Q=Q(I+1\to I-1)$ on the spin I for the nuclei $_{68}$Er, $_{70}$Yb, and $_{72}$Hf (data of Sec. 29 (Ref. 338, 340, and 367) except for $^{158}_{68}$Er (Ref. 364)). On the abscissas, the arrows indicate the points of back-bending when the effect is present. The crosses are for $^{166}_{70}$Yb, the total effect of two neighboring transitions to reduce the errors. The dashed horizontal straight lines correspond to a rigid rotator.

For $^{156}_{68}$Er, it is necessary to exercise caution. Evaluation of the data revealed the possibility of a second solution for τ_I and φ_I with values for τ_I much closer to the rotator values. The values given in Table VI and Fig. 33 and their errors were chosen only on the basis of additional arguments, which use the circumstance that for the chosen solution the side feeding times φ_I of the low-spin levels (see Sec. 31) correspond to the transition times to them from the side bands. This means that the chosen solution with respect to φ_I does not contradict side feeding through known side bands,[31] in contrast to the second solution.

We now consider what these measurements can tell us about the back-bending mechanism in the sense of distinguishing between the mechanisms of the three types considered earlier: abrupt change in the deformation due to changes in the potential energy surface (DEJ), Coriolis antipairing (CAP), and rotational alignment of a nucleon pair (RAL) (see Sec. 15):

1)The DEJ mechanism, understood as a change in the deformation, would entail simultaneously changes in the moment of inertia J and the internal $E2$ moment Q. As can be seen by comparing Figs. 18 and 33, there is no trace of this. The moment of inertia J has a strong growth at the point of back-bending and remains constant above it; Q remains approximately the same below and above the point, with a possible small reduction near it.

2) From the point of view described above, the CAP mechanism appears to be a suitable explanation of the effect. In fact, as is known from many calculations, the moment of inertia J depends strongly on the pair breaking and must increase as a result by a factor 2–3 (Refs. 40 and 48). In contrast, the internal $E2$ moment Q depends weakly on the pair breaking, as is also shown, in particular, by our calculations. However, many calculations[197,240] have shown that the pairing is broken not abruptly but smoothly with increasing spin. This means that the hindrance of the transitions must be not only small but also spread over a large range of spins. However, in Fig. 3 hindrance in the neighborhood of the point of back-bending is observed.

3) The rotational alignment mechanism (RAL) satisfies all the requirements. Breaking of one pair has little influence on a diagonal matrix element of Q, and therefore Q preserves its almost rotator values above the point of back-bending as well. However, the alignment takes place abruptly[6,240]; see Fig. 12. Moreover, near the point of back-bending there is an abrupt change in the structure of the internal state. Then a nondiagonal $Q(I\to I-2)$ matrix element must be hindered precisely for a transition with a value of I in the back-bending region.

We can therefore conclude that among the back-bending mechanisms of these three types the RAL mechanism gives the best explanation of the experiment for the transition probabilities. This agrees with the general conclusion of experiments on the energies of aligned bands in odd nuclei (see Sec. 27) and with theoretical

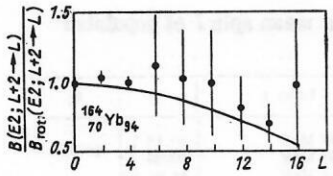

FIG. 34. Dependence of the enhancement factors $B(E2; L+2 \to L)/B_{rot}(E2; L+2 \to L)$ on the spins L for the nucleus $^{164}_{70}$Yb (Ref. 143). The calculation of this paper is compared with the experiments of Ref. 338.

investigations[240] (see Sec. 15). For the sake of caution, we note, however, that the experiment in the neighborhood of the back-bending point, in contrast to one at the point itself, is not so accurate. Moreover, there have been proposed model descriptions of the experiment on $^{164}_{70}$Yb (Ref. 338) in the framework of the model of interacting bosons (Fig. 34)[143] or on $^{156}_{68}$Er (Ref. 367) in the framework of the two-phase model (Table IX).[269] Unfortunately, Fig. 34 does not reproduce the increase after the back-bending point, which is indicated by many measurements (see Fig. 33), albeit with large errors. In Table IX, in contrast, the position and depth are reproduced reasonably, but not the width of the minimum.

An experiment in the "new" deformation region on the nuclei $^{130,132,134}_{58}$Ce (Ref. 365) has given a result similar to that for $^{130}_{58}$Ce (Ref. 365), but indicates a greater hindrance on the transition to $^{134}_{58}$Ce. For this last nucleus, $B(E2)$ is reported to be hindered for $10^+ \to 8^+$ by a factor 25 compared with the rigid-rotator value. If this result is confirmed, it will signify a different situation with regard to back-bending in this region of nuclei. Figure 35 shows the results of Ref. 368 for $_{58}$Ce nuclei in conjunction with the theoretical model of a particle plus a variable-moment-of-inertia rotator.[268] As in the region of the nuclei $_{78}$Pt (Ref. 380 and 437) and $_{80}$Hg (Ref. 275), there may exist appreciable hindrances, which are associated with the differences in the nature of the quasi-back-bending in this region of nuclei, namely, transitions to two-quasiparticle states[275,437] or to a rigid triaxial rotator.[380]

30. INTENSITIES OF THE POPULATION OF YRAST STATES: REGION OF POPULATED LEVELS

From the classical model of population of the yrast line[309] after a (HI, xn) reaction it has long been known that although heavy ions introduce a fairly large angular momentum I_0 into the compound system,[383,384] yrast levels with appreciably lower spin are populated.[3,4] In

TABLE IX. Enhancement factors of $E2$ transitions along the yrast line of the nucleus $^{156}_{68}$Er.

Transition $I \to I-2$	$B(E2; I \to I-2)/B_{rot}(E2; I \to I-2)$		Transition $I \to I-2$	$B(E2; I \to I-2)/B_{rot}(E2; I \to I-2)$	
	Experiment[a]	Theory[b]		Experiment	Theory
$2 \to 0$	1 ± 0.036	1	$10 \to 8$	0.472 ± 0.210	1.294
$4 \to 2$	1.250 ± 0.126	1.080	$12 \to 10$	0.231 ± 0.141	0.150
$6 \to 4$	1.136 ± 0.174	1.168	$14 \to 12$	0.452 ± 0.268	0.899
$8 \to 6$	0.714 ± 0.258	1.265			

Note. The superscript *a* indicates Ref. 367 and the superscript *b*, Ref. 269.

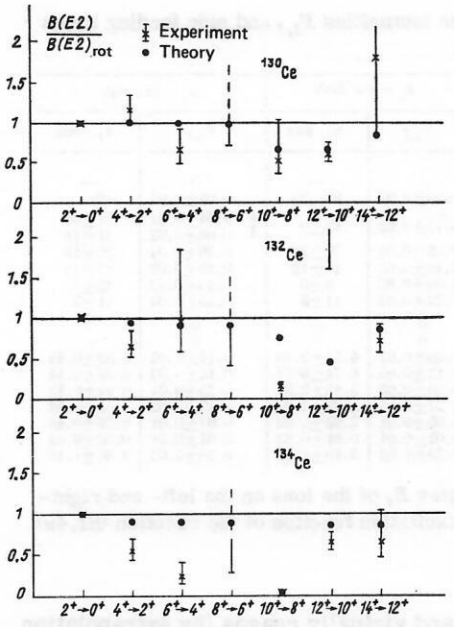

FIG. 35. Dependence of the enhancement factors $B(E2)/B_{rot}(E2)$ on the spins of the transitions $I_i \to I_f$ for $_{58}$Ce nuclei (Ref. 268). The calculation of Ref. 268 is compared with the experiments of Ref. 368.

addition, it is known that an increase in the energy of the $^4_2$He ions or transition to the heavier $^{40}_{18}$Ar ions (in both cases, this entails a larger transferred angular momentum) shifts the region of populated yrast levels to higher spins.[3,4] This occurs because of the shift upward of the "cloud" of final nuclei after evaporation of neutrons and before emission of γ rays (see Fig. 17).

Nevertheless, the systematics of reactions with ions up to $^{40}_{18}$Ar (Ref. 391) has shown that although the mean spin $\bar{I}$ of the populated levels,

$$\bar{I}^2 = \sum_{I=2}^{\infty} P_{2,I}\, I(I+1), \tag{88}$$

still increases with increasing mass A_i of the ion, the ratio $\bar{I}/I_0$ decreases. A weakening of the dependence of I on I_0 with increasing A_i is observed. Therefore, the simple model in Fig. 17 does not answer the following questions: 1) Where does the yrast cascade go over predominantly from a cascade along a band parallel to the yrast line to a cascade along the yrast line itself? 2) To what extent does this depend on quantities associated with the reaction such as the mass A_i and the energy E_i of the ion, and to what extent on the structure of the yrast band? This problem concerns not only the theoretical question of the excitation mechanism of the nucleus, but also a practical question: How high are the spins of the discrete yrast levels that can be populated in (HI, xn) reactions?

Our aim is to extend the systematics of the intensities of side population to higher ion masses A_i by going over from reactions with $^{40}_{18}$Ar (85) (Ref. 338) to reactions with $^{48}_{22}$Ti (86) (Ref. 340), and also to investigate the dependence on the energy E_i at a sufficiently large mass A_i in the reactions (84) (Ref. 367). These data are given in Tables X–XII.

It can be seen that the population of the yrast levels

TABLE X. Relative intensities $P_{2,I}$ and side feeding times φ_I.

Nucleus	Level I	$E_i = 150$ MeV		$E_i = 168$ MeV	
		$P_{2,I}$	φ_I, psec	$P_{2,I}$	φ_I, psec
$^{156}_{68}Er_{88}$	2	0	—	0	—
	4	0.10±0.02	65±39	0.04±0.02	~60
	6	0.15±0.02	15±9	0.04±0.01	91±54
				0.06±0.02	31±18
	8	0.35±0.04	29±21	0.36±0.04	22±15
	10	0.10±0.02	17±12	0.15±0.02	17±13
	12	0.08±0.02	8±6	0.10±0.02	10±7
	14	0.22±0.04	11±5	0.25±0.04	11±7
$^{160}_{68}Er_{92}$	2	0	—	0	—
	4	0	—	0	—
	6	0.08±0.02	4.52±2.10	0.11±0.02	4.53±0.44
	8	0.12±0.03	6.74±6.72	0.14±0.03	5.58±0.44
	10	0.20±0.03	5.12±2.82	0.25±0.04	6.94±0.43
	12	0.27±0.04	3.39±2.02	0.13±0.02	3.01±0.43
	14	0.05±0.01	2.93±2.22	0.07±0.01	4.76±0.44
	16	0.05±0.01	0.61±0.53	0.04±0.01	0.50±0.42
	18	0.23±0.03	3.10±1.30	0.26±0.03	2.86±1.10

Note. At two energies E_i of the ions on the left- and right-hand slopes of the excitation function of the reaction $(HI, 4n)$, $4n)$.

begins at $I \approx 6$–8 and virtually ceases (by extrapolation of the populations to higher spins) at $I \approx 20$–26. Moreover, contrary to the expectation, the spin distribution of the population $P_{2,I}$ is shifted very little upward in the spin I with increasing ion energy E_i and with increasing ion mass A_i. In this respect the heavy ions differ from light ions, in which such dependences are

TABLE XI and XII. Relative intensities $P_{2,I}$ and side feeding times φ_I.

Nucleus	Level	$P_{2,I}$	φ_i, psec
$^{164}_{70}Yb_{94}$	2	0	—
	4	0	—
	6	0	—
	8	0.16±0.01	6.5±5.3
	10	0.17±0.01	5.1±4.2
	12	0.14±0.01	4.8±3.2
	14	0.06±0.01	2.3±1.1
	16	0.12±0,015	1.3±0.5
	18	0.35±0.035	5.3±1.5
$^{166}_{70}Yb_{96}$	2	0	—
	4	0	—
	6	0	—
	8	0.13±0.02	3.8±1.8
	10	0.16±0.04	3.7±3.1
	12	0.09±0.03	2.5±2.2
	14	0,09±0.03	3.0±2.2
	16	0.13±0.03	3.0±1.5
	18	0.14±0.04	2.0±2.3
	20	0.26±0.05	2.8±2.1
$^{166}_{72}Hf_{94}$	2	0	—
	4	0.21±0.05	10.5±4.2
	6	0.18±0.05	14.1±5.3
	8	0.10±0.03	5.0±3.7
	10	0.07±0.03	16.4±13.3
	12	0.44±0.05	8.9±2.0
$^{168}_{72}Hf_{96}$	2	0	—
	4	0	—
	6	0	—
	8	0.11±0.04	~200
		0.06±0.03	3.0±2.4
		0.07±0.04	~200
	10	0.14±0.03	3.9±1.2
	12	0.12±0.03	9.2±3.2
	14	0.10±0.04	3.0±1.1
$^{170}_{72}Hf_{98}$	16	0.40±0.08	3.2±0.5
	2	0	—
	4	0	—
	6	0.15±0.04	~50
		0.15±0.04	~6000
	8	0.13±0.02	8.9±4.8
	10	0.06±0.03	2.7±2.2
	12	0.13±0.03	1.0±0.5
	14	0.08±0.03	0.8±0.7
	16	0.09±0.03	~0.2
	18	0.05±0.02	~0.2
	20	0.16±0.04	~0.8

Note. At the ion energy E_i corresponding to the maximum of the excitation function of the reaction $(HI, 4n)$.

TABLE XIII. Dependence of the mean spin $\bar{I}$ of populated levles on the reaction.

Reaction	Level I	$\bar{I}$	I_b
$^{120}_{50}Sn$ ($^{40}_{18}Ar$, $4n$) $^{156}_{68}Er$	$E_i = 150$ MeV	10.19	10.95
	$E_i = 168$ MeV	10.93	
$^{124}_{50}Sn$ ($^{40}_{18}Ar$, $4n$) $^{160}_{68}Er$	$E_i = 150$ MeV	14.00	13.93
	$E_i = 168$ MeV	14.30	
$^{128}_{52}Te$ ($^{40}_{18}Ar$, $4n$) $^{164}_{70}Yb$	—	15.61	13.58
$^{130}_{52}Te$ ($^{40}_{18}Ar$, $4n$) $^{166}_{70}Yb$	—	15.91	14.10
$^{122}_{50}Sn$ ($^{48}_{22}Ti$, $4n$) $^{166}_{72}Hf$	all components	11.89	(12.41)
	only short-lived components	13.24	
$^{124}_{50}Sn$ ($^{48}_{22}Ti$, $4n$) $^{168}_{72}Hf$	all components	14.44	14.08
	only short-lived components	15.64	
$^{24}_{50}Sn$ ($^{50}_{22}Ti$, $4n$) $^{170}_{72}Hf$	all components	13.08	(17.40)
	only short-lived components	13.97	

Note. The back-bending point I_b is obtained as the point of inflection in the dependence of $E_{I+1} - E_{I-1}$ on I; in the cases when there is no back-bending, the obtained value is placed in brackets.

manifested more strongly[3,4] and in which the onset of population sinks from $I \approx 8$ to low spins. Results on this saturation effect of the spin distribution, which is independent of the spin introduced by the reaction, are also shown in Table XIII. It can be seen that the dependence of $\bar{I}$ on A_i is saturated and that $\bar{I}$ depends very weakly on E_i. Note that this fact is, in a certain sense a pessimistic answer to the practical question posed at the beginning, namely: how high can discrete yrast levels be populated? Nevertheless, this does not imply the complete impossibility of populating levels with $I > 24$, since we do not know how far the $P_{2,I}$ tail extends to the high-spin states, and this cannot be guessed by simple extrapolation. The observation of levels up to 32^+ in $^{158}_{68}Er$ (see Ref. 24, Fig. 13) shows that an additional special technique may work in the region of this tail.

One can make a conjecture[338] concerning the transition of the yrast cascade from a cascade along the band into a cascade along the line. For sufficiently heavy ions, this transition occurs predominantly in the region of crossing of the bands. It is therefore primarily associated with the structural properties of the yrast band, and not with the reaction mechanism. The reaction mechanism only slightly distorts the picture. It is clear from this conjecture why the saturation effect was not noted earlier in reactions with lighter ions. When an ion and its energy are such that an appreciable fraction of the statistical cascade descending almost vertically downward in Fig. 17 arrives at the yrast band in the region of or below the point of back-bending, levels of the yrast line near and below that point will be populated. This reduces the mean spin $\bar{I}$ of the populated levels observed in reactions with lighter ions.[391]

31. TIME OF POPULATION OF YRAST STATES: HIGH-SPIN TRAPS

We shall dwell here on the problem of the quasiparticle isomer states in the even–even hafnium nuclei, not because a good systematics has been established for them in recent years, but because it has been possible through them to approach two interesting questions:

1) the structural question, with the discovery of high-spin traps near and on the yrast line itself;

2) the population mechanism, i.e., the extent to which such states are populated by heavy ions and thus can indeed appear as traps.

It is known that in (HI, xn) reactions the time of the continuous (statistical and yrast) cascade, which is effectively equal to the side feeding time of the yrast line, is of order 10^{-11}–10^{-12} sec (Refs. 332, 391, and 472). In reactions with the not very heavy neon ions, fairly long-lived traps in the yrast band were not observed[472] in the hafnium nuclei $^{166,168,170}_{72}$Hf. It is interesting to compare this time with the time obtained in reactions with very light particles, namely, α particles[473] or deuterons,[474] but in the different isotopes $^{168}_{70}$Yb and $^{174,176}_{72}$Hf. In this case, one does observe hindered components of order 10% with a time of tens of nanoseconds and more.

In reactions with α particles, and sometimes with slightly heavier (but not too heavy) ions, levels different from the yrast line, of a different nature, are populated (see Sec. 26). We consider here the fact that in a number of the heavy $_{72}$Hf isotopes levels are known that differ from the yrast line but also from the bands discussed above by having a larger K, so that they are isomer lines because of the K selection rule. We have, for example, 8^-, the superposition of $[7/2^+(404)p, 9/2^-(514)p]$ and $[7/2^-(514)n, 9/2^+(624)n]$ and 6^+, the superposition of $[7/2^+(404)p, 5/2^+(402)p]$ and $[7/2^-(514)n, 5/2^-(512)n]\,2qp$ (two-quasiparticle) isomer states (Refs. 36, 69, 430, 431, 473, and 475–477) with the half-lives

$^{180}_{72}$Hf:	8^- (5.5 h)	$^{174}_{72}$Hf:	6^+ (2.1 μsec)	(89)
$^{178}_{72}$Hf:	8^- (4 sec), 6^+ (78 ns)	$^{172}_{72}$Hf:	6^+? (155 ns)	
$^{176}_{72}$Ht:	8^- (9.8 μsec) 6^+ (9.6 μsec)			

(The K^π values of the isomer in $^{172}_{72}$Hf are not given in Ref. 430, and we have given them here on the basis of the preliminary data of a private communication. Later there was published the paper of Ref. 431, which ascribes to this isomer the preliminary values 8^-.) Also known are $4qp$ isomers: 14^- (401 μsec) (Ref. 478), 19^+ (34 nsec) and $6qp$: 22^- (43 μsec) (Ref. 35) in $^{176}_{72}$Hf, and also $4qp$: 14^- (68 μsec) and 16^+ (31 years) in $^{178}_{72}$Hf (Ref. 36). In reactions with α particles, they can appear as traps near the yrast line, and the $6qp$ isomer 22^- in $^{176}_{72}$Hf (Ref. 35) and $4qp$ isomers 14^- and 16^+ in $^{178}_{72}$Hf (Ref. 36) as traps on the yrast line. The $2qp$ isomers 8^- and 6^+ populate the yrast levels 8^+, 6^+, and 4^+ by the transition $8^-\,2qp \to 8^+ g$ in $^{180}_{72}$Hf or by $6^+\,2qp \to 6^+ g, 4^+ g, 8^-\,2qp \to 8^+ g$ in $^{178}_{72}$Hf or $8^-\,2qp \to 6^+\,2qp \to 6^+ g, 4^+ g$ in $^{176}_{72}$Hf. Frequently, this occurs with a low probability, for example, of order 1% in $^{172}_{72}$Hf (Ref. 430), but one also encounters cases with α particles[473] and deuterons,[474] in which the population takes place with a greater probability of order 10%, as discussed above.

Such cases in reactions with α particles are beginning to be discovered in the $_{74}$W nuclei, in which, for example, one observes the $4qp$ isomer 14^- (~3 μsec) in $^{180}_{74}$W, which populates the 8^- (5.2 msec) band.[479] We draw attention to the interesting communication of Ref. 452 on the odd nucleus $^{179}_{74}$W, in which one of the isomers $5qp$ (710 nsec) does not manifest the expected strong suppression through the K selection rule and is coupled by transitions directly to the back-bending region. We note as a side result the population of the lowest excited 3^- (1 nsec) octupole state[480] and the discovery of the lowest 2^+ state above the 3^- in $^{146}_{64}$Gd (Ref. 481). This suggests that the shell is closed at $Z = 64$.

An interesting question is whether the isomer levels described above can also be populated in (HI, xn) reactions with heavier ions and act as traps. Investigation of the feeding times is an experimental method capable of answering such a question. For, as is shown in Sec. 23, the lifetime of the compound nucleus is of order 10^{-18} sec and is much shorter and will not interfere. In addition, the evaporation of neutrons and the statistical γ cascade will, on account of the high-energy $E1$ transitions (see Sec. 24), make an insignificant contribution to the feeding times, which are 10^{-11}–10^{-12} sec. Thus, the feeding time is a characteristic of the continuous part of the yrast cascade, the de-excitation by transitions near the yrast line.

For the nuclei $_{68}$Er (Ref. 367), $_{70}$Yb (Ref. 338), and $_{72}$Hf (Ref. 340), experimental material has been obtained on the side feeding time φ_I; this material was identified by the method described in Sec. 21, and, moreover, at two energies E_i for two $_{68}$Er nuclei. The material is given in Tables X–XII. From the theoretical point of view, this feeding time is a cleaner parameter than the total feeding times θ_I used in Refs. 328 and 472 and determined by the value of t for which the decay curve reaches $R_I(t) = e^{-1}$. It is clear that θ_I depends not only on φ_I but also on τ_I and on the lifetime τ_K and the side feeding time φ_K of all the preceding levels with $K > I$ (see Sec. 21). In the same sense, the intensity P_{I_f} and the time φ_{I_f} of the uppermost observed level I_f in Tables X–XII are also not side or total: φ_{I_f} depends not only on φ_I but also on the τ_K and φ_K of all the unobserved levels $K > I_f$. On the other hand, the definition of the time θ_I relates it to experiments directly, and therefore their errors are much smaller. We give this time for the cases mentioned above together with the case of $^{158}_{68}$Er (see Ref. 364 and Table XIV).

The systematics of Table XIV shows that θ_I increases for given I with decreasing N, i.e., as the magic number 82 is approached from above. It can be seen from Table XIV that such an effect can be established in a pure form precisely at high spins, whereas for low spins $I \leqslant 8$ this population effect, despite being noted earlier,[328,472] may be masked because of the strong influence of the longer lifetime τ_I. Conversely, it can be seen that changes in Z for fixed N have little influence on θ_I. We shall return to consider the possible connection between this effect and the ultrahigh-spin traps (see Sec. 16) in Sec. 32.

We now compare φ_I (see Table X) and θ_I (see Table XIV) of each of the nuclei $^{156,160}_{68}$Er at two different ion energies E_i—on the left- and right-hand slopes of the excitation function. One could assert that in the second case at higher E_i there should occur, because of the higher spin I_0 introduced by the reaction and then (see

TABLE XIV. Dependence of the time θ_I of total population of the yrast levels on the reaction.

Reaction	Level I	θ_I, psec							
	E_I, MeV	20	18	16	14	12	10	8	6
$^{120}_{50}$Sn ($^{40}_{18}$Ar, $4n$) $^{156}_{68}$Er	150	—	—	—	20.5±0.7	21.5±0.5	22.9±0.5	~26	28±0.7
	168	—	—	—	20.7±0.5	22.5±0.5	23.4±0.5	25.3±0.5	29.4±0.7
$^{130}_{52}$Te ($^{32}_{16}$S, $4n$) $^{158}_{68}$Er		—	2.2	4.8	6	7.5	8.6	10	14
$^{124}_{50}$Sn ($^{40}_{18}$Ar, $4n$) $^{160}_{68}$Er	150	—	4.2±0.7	5.4±0.7	6.0±0.5	5.9±0.5	7.1±0.9	9.8±0.5	17.6±0.7
	168	—	4.0±0.7	5.3±0.7	6.2±0.5	6.4±0.5	7.9±0.5	10.3±0.5	18.1±0.7
$^{124}_{52}$Te ($^{40}_{21}$Ar, $4n$) $^{160}_{70}$Yb	—	—	—	—	—	—	13±1.5	14±2	17±2
$^{126}_{52}$Te ($^{40}_{18}$Ar, $4n$) $^{162}_{70}$Yb	—	—	—	—	—	—	—	12±3	16±4
$^{128}_{52}$Te ($^{40}_{18}$Ar, $4n$) $^{164}_{70}$Yb	—	—	6.5±1.5	8.0±1.5	8.3±1.5	8.7±1.5	9.4±2.0	11.8±2.0	19.7±2.0
$^{130}_{52}$Te ($^{40}_{18}$Ar, $4n$) $^{166}_{70}$Yb	—	3.7±2.0	4.9±2.5	6.2±1.5	6.6±1.5	7.2±1.5	8.3±2.5	11.2±2.0	20.9±2.0
$^{122}_{50}$Sn ($^{48}_{22}$Ti, $4n$) $^{166}_{72}$Hf	—	—	—	—	—	10.2±3.0	11.5±3.0	12.5±2.0	18.3±2.2
$^{124}_{50}$Sn ($^{48}_{22}$Ti, $4n$) $^{168}_{72}$Hf	—	—	—	6.2±0.8	7.0±1.0	8.0±1.0	9.0±1.0	12.6±1.1	22.0±2.0
$^{124}_{50}$Sn ($^{50}_{22}$Ti, $4n$) $^{170}_{72}$Hf	—	1.1±0.3	1.4±0.6	1.8±0.5	2.6±0.5	3.8±0.5	6.0±0.5	12.1±1.0	27.0±2.0

Sec. 24) carried away principally by the yrast cascade in units of $2\hbar$ per transition, a greater number of yrast transitions before the population of a given level I. One could then expect the times φ_I and θ_I, respectively, to increase. It can be seen from Tables X and XIV that if such an increase does exist it is very small, and in the majority of cases is within the error limits. This indicates that the main contribution to φ_I and θ_I is made by the lowest transitions to the yrast line, which at different E_i are the same. Such an explanation is confirmed indirectly by another experiment,[312,313] in which it was shown that the moment of inertia of the continuum transitions along the yrast band at ultrahigh spins becomes constant and almost equal to the rigid-body value (see Sec. 32). It is then clear that the transition energy will increase linearly with the spin, and the time will, because of (64), decrease in proportion to its fifth power, so that only the lowest transition will indeed contribute to φ_I and θ_I.

Finally, we consider the long-lived components of side population for the $_{72}$Hf nuclei (see Ref. 340 and Table XII), which are most directly seen from the long-lived tails of the decay curves themselves for $4 \leqslant I \leqslant 8$ in the case of $^{168}_{72}$Hf and $^{170}_{72}$Hf (Fig. 36). They probably also exist for $^{166}_{72}$Hf, but they cannot be separated experimentally from the short-lived components. They indicate directly the existence of traps near the yrast line populating the 8^+, 6^+, and possibly also the 4^+ levels. The lifetimes of the traps decrease systematically with decreasing A:

$$\left.\begin{array}{ll} ^{170}_{72}\text{Hf:} & \varphi_{1/2} = 4200\,\text{psec} \\ ^{168}_{72}\text{Hf:} & 140\,\text{psec} \\ ^{166}_{72}\text{Hf:} & 7\,\text{psec?} \end{array}\right\} \quad (90)$$

[where $\varphi_{1/2}$ are the half-lives for comparability with (89), and not φ_m, the mean times as they are defined in Sec. 21 and used in Tables X–XII]. The traps are populated in reactions with the ions $^{48,50}_{22}$Ti with intensities of order 15% (see Table XII), in contrast to the case of $^{172}_{72}$Hf in reactions with $^{4}_{2}$He, in which the population is only of order 1% (Ref. 430).

All this enables us to suggest that the traps in $^{166,168,170}_{72}$Hf are the systematic extension of the $2qp$ isomer levels 8^- and 6^+ of the heavier nuclei $^{172-180}_{72}$Hf. Such a hypothesis is confirmed by the fact that the trap lifetimes in $^{166-170}_{72}$Hf extrapolate well the systematics of the known isomers in $^{172-180}_{72}$Hf. This is shown in Fig. 37, which is based on the known lifetime of the longer-lived of the 8^- and 6^+ $2qp$ isomer levels of $^{172-180}_{72}$Hf (89) and the data on the feeding time of the $^{166-170}_{72}$Hf long-lived components (90). These last are interpreted as the lifetimes of isomer levels of the same nature populated in (HI, xn) reactions "from above" with a fairly high intensity, so that they act as traps near the yrast line. Which isomer precisely is at present hard to say because of the

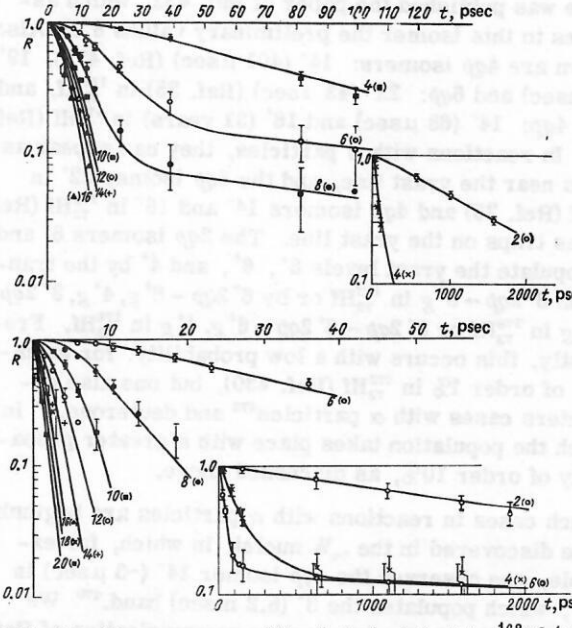

FIG. 36. Decay curves of R_I plotted against t. $^{168}_{72}$Hf (at the top) and $^{170}_{72}$Hf (at the bottom) (Ref. 340).

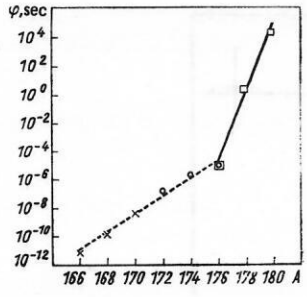

FIG. 37. Schematics of the lifetimes φ (given here not as usual as the mean time φ_m, but as the half-life $\varphi = \varphi_{1/2} = \ln 2 \varphi_m$) as a function of the mass number A of the known $2qp$ 8^- isomers (open squares), the known $2qp$ 6^+ isomers (open circles) [see Eq. (89)], and traps (crosses) [see Eq. (90); data from Ref. 340] in the nuclei $^{A}_{72}$Hf.

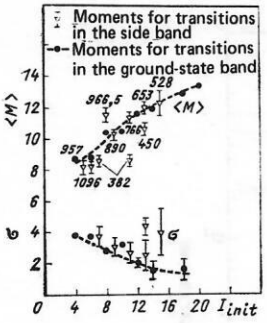

FIG. 38. Dependence of $\langle M \rangle$ and $\sigma(\langle M \rangle$ is the mean multiplicity and σ^2 is the variance of the multiplicity) on the initial spin in the reaction $^{150}_{60}\mathrm{Nd}(^{16}_{8}\mathrm{O}, 4n)^{162}_{68}\mathrm{Er}$ (Ref. 400).

uncertainties in the $^{172}_{72}$Hf decay scheme (Refs. 430 and 431). In constructing Fig. 37, we assumed that the isomer in the final nucleus, 6^+, corresponds better to the systematics of the two straight lines intersecting at the point $A = 176$, these being associated for $A > 176$ with the longer-lived isomer, which is 8^-, and for $A < 176$ with 6^+; the half-lives become equal (10 μsec) at $A = 176$.

For $^{178}_{72}$Hf, the isomer 8^- can also be populated by Coulomb excitation "from below" by the very heavy ions $^{86}_{36}$Kr and $^{136}_{54}$Xe with 1% isomer component relative to direct population of the 8^+ level.[38] In Ref. 38, this population is ascribed to a possible downward branching from higher levels of the yrast band.

32. CONTINUOUS γ CASCADE: ULTRAHIGH-SPIN TRAPS

The experimental technique for investigating the continuous γ cascade after the (HI, xn) reaction has been strongly developed very recently. In principle, we include here measurements of the energy distributions (of an individual γ ray and the sum of the complete cascade) and the spin and angular intensity distributions, the multiplicities of the γ rays, and, for some special purposes, the internal-conversion electrons.

These investigations began with measurements of the energy and angular distributions,[311] were augmented by measurements of the mean multiplicity,[482,483] and were subsequently perfected by the measurement of the energy distribution of the multiplicity (Ref. 484; see also Ref. 4 for some earlier references). Introduction of multiple coincidences and the corresponding extraction of information on the multiplicity distribution represented the next important methodological step.[4,417] In the investigation of γ-ray cascades by multiple coincidences with a Ge(Li) detector that determines a discrete state I with efficiency Ω_G and several NaI(Tl) detectors with efficiency Ω_N, the following formulas are used:

$$N = \sigma_I \Omega_G; \quad N_{np} = \sigma_I \Omega_G (-)^{n+p} \sum_{x=n-p}^{n} (-)^{x+1} \times \binom{p}{n-x} \langle 1 - (1 - x\Omega_N)^{M-1} \rangle. \tag{91}$$

Here, σ_I is the cross section for obtaining a cascade which passes through the state I, N is the rate of singles counting, N_{np} is the rate of counting of coincidences by the Ge detector with p data from all the n NaI detectors, and M is the number of γ rays of the cascade. Hence, in particular, for $n = p$ one can extract different moments of the multiplicity $\langle M^n \rangle$, $n = 1, 2, \ldots$, as, for example, the mean multiplicity $\langle M \rangle$ and the variance $\sigma^2 = \langle (M - \langle M \rangle)^2 \rangle$, usually up to $n = 4$. An example of the spin distribution of $\langle M \rangle$ and σ is shown in Fig. 38. Interesting new possibilities are offered by the measurement of the total energy of all γ rays of a given cascade by a large NaI crystal.[485]

Such measurements are directed, on the one hand, to the elucidation of the mechanism of the (HI, xn) reaction (see Sec. 23 and Ref. 394, in which a measurement of the multiplicity was made in addition to that of the A and Z distributions of the fission products, and Ref. 396). In particular, they are directed toward the investigation of the de-excitation mechanism, with, for example, the aim of establishing the spin distribution of the final nucleus before the γ cascade (see Refs. 400, 417, 486 and Fig. 27). These methods are also used as a means to investigate deep inelastic transfer reactions.[317-319]

The same methods are used for a more detailed investigation of the de-exciting γ cascade (see Sec. 24). By this we mean the decomposition of it into the statistical cascade and the yrast cascade (Fig. 39), and the determination of the numbers and multipolarities of the γ rays of each of them (Refs. 312–314 and 400). It can be seen from the results of Refs. 338, 340, and 367 (see Tables X–XII) that the orders of magnitude of the side feeding φ_I are, if allowance is made for the number of γ rays from the measurements of the multiplicity[417] and their energy from measurements of the energy distributions of the continuum γ rays with the statistical cascade separated from the yrast cascade,[312] compatible with the assertion that the yrast cascade consists predominantly of aligned $E2$ transitions (see Sec. 24 and Refs. 4 and 311). A paper has already been puslished on the direct measurement of the total coefficient of internal conversion of the continuous γ-ray spectrum.[487] In broad agreement with the population model of Ref. 309 and in qualitative agreement with the theory of $E1$ and $E2$ compe-

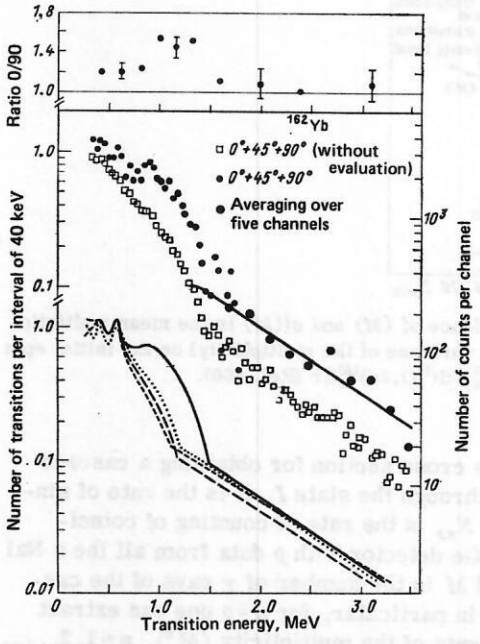

FIG. 39. Continuous γ-ray spectrum of HI, $4n$) reactions in $^{162}_{70}$Yb. $HI = ^{40}_{18}$Ar, with 181 MeV at the top. The schematic spectra are given below. For reactions with $^{40}_{18}$Ar, 181 MeV (continuous curve), 157 MeV (long dashes), $^{86}_{36}$Kr, 331 MeV (dashed curve) and $^{16}_{8}$O, 87 MeV (short dashes) (Ref. 313).

tition[419] in the region of the statistical cascade at energies $E_\gamma > 1$ MeV, $E1$ and $E2$ superpositions are observed, the $E1$ fraction increasing from 45 to 71% with increasing energy. In the region of intermediate energies of the yrast cascade, $E2$ is predominant, but at lower energies the part played by $M1$ transitions increases somewhat unexpectedly. This may be due to transitions through some of the parallel paths, as in the case of observations of $M1$ admixtures in odd nuclei.[323] The enhancement of the $E2$ transitions is the same as for the gound-state band, but in the ultrahigh-spin region $I = 30-50$ it is observed by direct measurement of the time of the continuous γ rays.[488] This shows that even in this region there exist strongly collectivized bands, and it explains the de-excitation through paths parallel to the yrast line.

Somewhat unexpected was another aspect of the use of measurements of the continuum. This relates to their possibility of casting light on the structure of nuclei at ultrahigh spins. We mention the ingenious method of deducing the moment of inertia in accordance with the first of formulas (63) at such spins. Use is made of the hump in the energy distribution associated with the yrast cascade in Fig. 39 [whereas the statistical tail is given by formula (67)] to determine the energy and measure the mean multiplicity and to determine the spin in accordance with Eq. (83) (Refs. 312 and 313). The result of the last quoted papers is given in Fig. 40. A similar method for drawing conclusions about the shape of nuclei has been proposed.[489] Finally, we mention the use of the summing technique[485] in searches for superdeformed nuclei at ultrahigh spins.[490] This exploits the circumstance that this technique makes it possible to measure directly the total energy, and

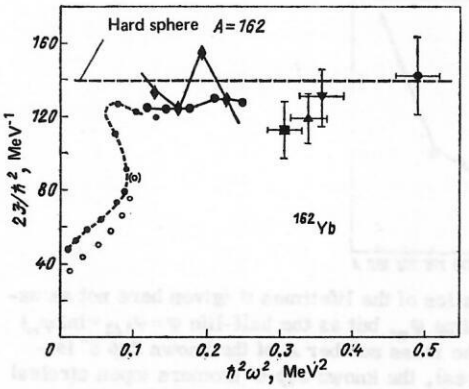

FIG. 40. Back bending diagram for the nucleus $^{162}_{70}$Yb (compared with $^{160}_{68}$Er, shown by the open circles below) with data on the continuum in the ultrahigh-spin part.[313]

measurement of the mean multiplicity gives the spin in accordance with (83), which again makes it possible to determine the moment of inertia.

The theoretically predicted (see Sec. 16) ultrahigh-spin isomers or traps have become a special direction for searches. We mention that strong increase in the time of total population θ_I with decreasing N (see Table XIV) may have a connection with the theoretically expected isomer island (see Sec. 16). For direct searches at Darmstadt, reactions with $^{40}_{18}$Ar, $^{50}_{22}$Ti, and $^{65}_{29}$Cu were used. Searches were made for cascades with a fairly large number of γ rays delayed by a time in the nanosecond range. Discovery of such a cascade would indicate the existence of a nanosecond isomer of fairly high spin. There was found an island of traps with half-lives from 1.5 to 700 nsec in the region $64 \lesssim Z \lesssim 71$ and $82 \lesssim N \lesssim 88$ (see Ref. 39, and also Fig. 16). It can be compared with the theory of Ref. 291. The Z and N of the compound nucleus were identified, but there was no exact identification of the Z and N of the final nucleus or the E and I of the isomer. To determine the E and I of the isomer, it has been suggested[491] that the summing-crystal method should be used.[485]

Detailed searches for isomers (>10 nsec) in $^{150}_{66}$Dy, whose nucleus lies in the middle of the island in Fig. 16, gave a negative result.[492] But searches[493] in the $_{64}$Gd nuclei by means of $^{4}_{2}$He ions gave positive results: In $^{147}_{64}$Gd there was found an isomer $E = 7.50$ MeV, $37/2 \lesssim I \lesssim 49/2$, 560 nsec, and in $^{147}_{66}$Gd an isomer $6.4 < E < 8.3$ MeV, $16 \lesssim I \lesssim 18 \lesssim 20$, 4 nsec. Despite the differences from the lifetimes found in Ref. 39 (in which the lifetimes were 100 nsec and ~1.5 nsec, respectively) and the different reactions, it is assumed that these are the same isomers. In such a case, it is asserted[493] that these are not ultrahigh-spin isomers but are similar to the isomers of the spherical shell model. Examples of such isomers are the five four-quasiparticle isomers found in $^{212}_{86}$Rn (Ref. 494). However, the investigation of Ref. 494 also found four isomers populated by the ($^{13}_{6}$C, $5n$) reaction with spins from 22 to 30 and nanosecond lifetimes. They are attributed in Ref. 494 to the MONA effect,[285] i.e., strong alignment of an excited neutron core with valence protons.

The idea has been put forward that yrast isomers

could decay with the emission of delayed α particles. Preliminary results of searches at Darmstadt with $^{50}_{22}$Ti and $^{132}_{54}$Xe ions in the picosecond and nanosecond ranges[495] by the recoil shadow technique, as in Ref. 325, by $^{40}_{18}$Ar and $^{48}_{22}$Ti ions in the microsecond range,[496] and at Jülich by $^{4}_{2}$He ions in the range from a millisecond to a minute[497] have so far given negative results.

At the time of going to print, there have been published detailed predictions of islands of traps.[498] There have been discovered ultrahigh-spin isomers of $^{152}_{66}$Dy with spins up to 30 and indications of a transition to an oblate shape (Refs. 499 and 500).[2]

CONCLUSIONS

The entire development of the theory (and the experiments relating to high-spin states in recent years) has demonstrated the development of methods of calculation of the detailed characteristics of these states and the mechanisms of their population. On the one hand, there has been a great improvement in the methods of populating these states by heavy ions and, on the other, in the investigation of discrete and continuous transitions by in-beam spectroscopy. Nevertheless, from theory one expects a deeper understanding of the mechanism of formation of elementary excitation modes under the unusual conditions of high rotational velocities, of the mechanisms of transitions between structures of different type, and of the mechanism of population of excited states by heavy ions. From experiment one expects to know whether the predictions of changes in nuclear structure at ultrahigh spins are realized, what are the possibilities for elucidation by means of heavy ions, and how far can one advance by making more detailed measurements of discrete transitions.

[2)] *Publisher's Note.* The last three references are not given in Russian bibliography.

[1]R. K. Sheline, Rev. Mod. Phys. **32**, 1 (1960).
[2]A. Bohr. Rev. Mod. Phys. **48**. 365 (1976); Fys. Tidsskr. **74**, 49 (1976).
[3]A. Johnson, in: Heavy-Ion High-Spin States and Nuclear S Structure, Vol. 1, IAEA, Vienna (1975), p. 317.
[4]R. M. Lieder and H. Ryde, Adv. Nucl. Phys. **10**, 1 (1978).
[5]R. A. Sorensen, Rev. Mod. Phys. **45**, 353 (1973).
[6]F. S. Stephens, Rev. Mod. Phys. **47**, 43 (1975).
[7]A. Bohr and B. R. Mottelson, Phys. Scr. **A10**, 13 (1974).
[8]A. Bohr and B. R. Mottelson, Preprint 77/38, NORDITA, Copenhagen (1977).
[9]M. Goldhaber and A. W. Sunyar, Phys. Rev. **83**, 906 (1951).
[10]A. Bohr, K. Dan, Vidensk, Selsk. Mat.-Fys. Medd. **26**, No. 14 (1952); Rotational States of Atomic Nuclei, Thesis, Munkgaard, Copenhagen (1954).
[11]A. Bohr and B. R. Mottelson, K. Dan, Vidensk. Selsk. Mat.-Fyz. Medd. **27**, No. 16 (1953).
[12]J. Rainwater, Phys. Rev. **79**, 432 (1950).
[13]T. Huss and C. Zupancic, K. Dan, Vidensk. Selsk. Mat.-Fys. Medd. **28**, No. 1 (1953).
[14]C. L. McClelland and C. Goodman, Phys. Rev. **91**, 760 (1953).
[15]F. Asaro and I. Perlman, Phys. Rev. **91**, 763 (1953).
[16]F. S. Stephens, R. M. Diamond, and I. Perlman, Phys. Rev. Lett. **3**, 435 (1959).
[17]H. Morinaga and P. C. Gugelot, Nucl. Phys. **46**, 210 (1963).
[18]G. B. Hansen *et al.*, Nucl. Phys. **47**, 529 (1963).
[19]F. S. Stephens, N. L. Lark, and R. M. Diamond, Phys. Rev. Lett. **12**, 225 (1964); Nucl. Phys. **63**, 82 (1965).
[20]A. Johnson, H. Ryde, and J. Sztarkier, Phys. Lett. **B34**, 605 (1971); A. Johnson, H. Ryde, and S. A. Hjorth, Nucl. Phys. **A179**, 753 (1972).
[21]A. Johnson and Z. Szymanski, Phys. Rep. **C7**, 181 (1973).
[22]J. Krumlinde, Nukleonika **19**, 251 (1974).
[23]I. N. Mikhailov *et al.*, Fiz. Elem. Chastits At. Yadra **8**, 1338 (1977) [Sov. J. Part. Nucl. **8**, 550 (1977)].
[24]I. Y. Lee *et al.*, Phys. Rev. Lett. **38**, 1454 (1977).
[25]D. Ward *et al.*, Phys. Lett, **B44**, 39 (1973).
[26]T. L. Khoo *et al.*, Phys. Rev. Lett. **31**, 1146 (1973).
[27]H. Beuscher *et al.*, in: Reactions between Complex Nuclei (Nashville), Vol. 1, North-Holland, Amsterdam (1974), p. 189.
[28]R. M. Lieder *et al.*, Phys. Lett. **B49**, 161 (1974).
[29]H. R. Andrews *et al.*, Nucl. Phys. **A219**, 141 (1974).
[30]Y. El Masri *et al.*, Z. Phys. **A274**, 113 (1975).
[31]A. W. Sunyar *et al.*, Phys. Lett. **B62**, 283 (1976).
[32]R. Janssens *et al.*, Nucl. Phys. **A283**, 493 (1977).
[33]N. R. Johnson *et al.*, Phys. Rev. Lett. **40**, 151 (1978).
[34]O. C. Kistner, A. W. Sunyar, and E. der Mateosian, Phys. Rev. C **17**, 1417 (1978).
[35]T. L. Khoo *et al.*, Phys. Rev. Lett. **37**, 823 (1976).
[36]T. L. Khoo and G. Lovhoiden, Phys. Lett. **B67**, 271 (1977).
[37]B. Bochev *et al.*, Nucl. Phys. **A282**, 159 (1977).
[38]J. H. Hamilton *et al.*, in: Intern. Conf. on Nuclear Structure, Contributed Papers, Tokyo (1977), p. 421; Intern. Symp. on High-Spin States and Nuclear Structure, ZfK-336, Dresden (1977), p. 96.
[39]J. Pedersen *et al.*, Phys. Rev. Lett. **39**, 990 (1977).
[40]V. G. Solov'ev, Teoriya slozhnykh yader, Nauka, Moscow (1971); English translation: Theory of Complex Nuclei, Pergamon, Oxford (1976).
[41]A. B. Migdal, Teoriya konechnykh fermi-sistem i svoĭstva atomnykh yader, Nauka, Moscow (1965); English translation: Theory of Finite Fermi Systems, Interscience, New York (1967).
[42]T. H. R. Skyrme, Philos. Mag. **1**, 1043 (1956); Nucl. Phys. **9**, 615 (1959).
[43]S. A. Moszkowski, Phys. Rev. **C 2**, 402 (1970).
[44]H. Flocard, in: Nuclear Self-Consistent Fields, North-Holland, Amsterdam (1975), p. 219.
[45]H. S. Kohler, Phys. Rep. **C18**, 217 (1975); P. U. Sauer, in: Nuclear Self-Consistent Fields, North-Holland, Amsterdam (1975), p. 89.
[46]D. Vautherin and D. M. Brink, Phys. Rev. **C5**, 626 (1972).
[47]S. Krewald *et al.*, Nucl. Phys. **A281**, 166 (1977).
[48]D. J. Rowe, Nuclear Collective Motion, Methuen, London (1970).
[49]L. S. Kisslinger and R. A. Sorensen, K. Dan. Vidensk. Selsk. Mat.-Fys. Medd. **32**, No. 9 (1960); Rev. Mod. Phys. **35**, 853 (1963); D. R. Bes and R. A. Sorensen, Adv. Nucl. Phys. **2**, 129 (1969).
[50]D. R. Bes and R. A. Broglia, Phys. Rev. **C3**, 2349 (1971).
[51]I. Hamamoto, Nucl. Phys. **A232**, 445 (1974); Phys. Lett. **B66**, 222 (1977).
[52]M. Baranger and K. Kumer, Nucl. Phys. **A62**, 113 (1965); **A110**, 490 (1968); **A122**, 241 (1968); K. Kumar and M. Baranger, Nucl. Phys. **A110**, 529 (1968); **A122**, 273 (1968).
[53]K. Kumar, Nucl. Phys. **A231**, 189 (1974).
[54]F. Villars, Ann. Rev. Nucl. Sci. **7**, 185 (1957).
[55]N. N. Bogolyubov, Dokl. Akad. Nauk SSSR, **119**, 224 (1958) [Sov. Phys. Dokl, **2**, 273 (1958)]; Zh. Eksp. Teor. Fiz. **34**, 58, 73 (1958) [Sov. Phys. JETP **7**, 41, 51 (1958)]. Usp. Fiz. Nauk **67**, 549 (1959) [Sov. Phys. Usp. **2**, 236 (1959)].
[56]M. Baranger, Phys. Rev. **122**, 992 (1961).
[57]D. L. Hill and J. A. Wheeler, Phys. Rev. **89**, 1102 (1953).
[58]J. J. Griffin and J. A. Wheeler, Phys. Rev. **108**, 311 (1957).
[59]C. W. Wong, Phys. Rep. **C15**, 283 (1975).

[60]P. A. M. Dirac, Proc. Cambridge Philos. Soc. **26**, 376 (1930).
[61]F. Willars, in: Nuclear Self-Consistent Fields, North-Holland, Amsterdam (1975), p. 3: Nucl. Phys. **A285**, 269 (1977).
[62]K. Goeke, A. M. Lane, and J. Martorell, Nucl Phys. **A269**, 109 (1978).
[63]E. R. Marshalek and J. O. Rasmussen, Nucl. Phys. **43**, 438 (1963).
[64]D. Bohm and D. Pines, Phys. Rev. **92**, 609 (1953).
[65]M. Baranger, Phys. Rev. **120**, 957 (1960).
[66]D. J. Thouless, Nucl. Phys. **22**, 78 (1961).
[67]J. Sawicki, Nucl. Phys. **23**, 285 (1961).
[68]M. K. Pal, in: Theory of Nuclear Structure, IAEA, Vienna (1970), p. 547.
[69]E. P. Grigor'ev and V. G. Solov'ev, Struktura chetnykh deformirovannykh yader (Structure of Even Deformed Nuclei), Nauka, Moscow (1974).
[70]S. P. Ivanova, A. L. Komov, L. A. Malov, and V. G. Solov'ev, Fiz. Elem. Chastits At. Yadra **7**, 450 (1976) [Sov. J. Part. Nucl. **7**, 175 (1976)].
[71]R. Arvieu, E. Salusti, and M. Veneroni, Phys Lett. **8**, 334 (1964).
[72]D. R. Inglis, Phys. Rev. **96**, 1059 (1954): **97**, 701 (1955): **103**, 1786 (1956).
[73]D. J. Thouless, Nucl. Phys. **21**, 225 (1960).
[74]D. J. Thouless and J. G. Valatin, Nucl. Phys. **31**, 211 (1962).
[75]S. T. Belyaev, K. Dan Vidensk. Selsk. Mat.-Fys. Medd. **31**, No. 11 (1959); Nucl. Phys. **24**, 322 (1961).
[76]A. B. Migdal, Nucl. Phys. **13**, 655 (1959).
[77]H. J. Lipkin, A. de-Shalit, and I. Talmi Phys. Rev. **103**, 1773 (1956).
[78]R. E. Peierls and J. Yoccoz, Proc. Phys. Soc. London **70**, 381 (1957).
[79]T. H. R. Skyrme, Proc. Phys. Soc., London **70**, 433 (1957).
[80]K. Goeke, J. Garcia, and A. Faessler, Nucl. Phys. **A208**, 477 (1973).
[81]A. Klein and A. K. Kerman, Phys. Rev. B138, 1323 (1965).
[82]A. Klein, L. Celenza, and A. K. Kerman, Phys. Rev. B140, 245 (1965).
[83]A. Klein, Lectures in Theoretical Physics, Gordon and Breach, New York (1968).
[84]C. Dasso and A. Klein, Phys. Rev. C **8**, 2511 (1973).
[85]S. G. Rohozinski, Preprint R4-4108 [in Russian], JINR, Dubna (1968); Acta Phys. Pol. **35**, 783 (1969).
[86]S. T. Belyaev and V. G. Zelevinskiĭ, Preprint IYaF 298 [in Russian], Novosibirsk (1969); Yad. Fiz. **11**, 741 (1970); **16**, 1195 (1972); **17**, 525 (1973) [Sov. J. Nucl. Phys. **11**, 416 (1970); **16**, 657 (1973); **17**, 269 (1973)].
[87]V. G. Zelevinskii and M. I. Shtokman, Preprint IYaF 88-73 [in Russian], Novosibirsk (1973).
[88]M. I. Shtokman, Yad. Fiz. 22, 479 (1975) [Sov. J. Nucl. Phys. **22**, 247 (1975)].
[89]T. Holstein and H. Primakoff, Phys. Rev. **58**, 1098 (1940).
[90]S. T. Belyaev and V. G. Zelevinskiĭ, Zh. Eksp. Teor. Fiz. 42, 1590 (1962) [Sov. Phys. JETP **15**, 1104 (1962)]; Nucl. Phys. **39**, 582 (1962).
[91]T. Matumori, M. Yamamura, and A. Tokynaga, Prog. Theor. Phys. **31**, 1009 (1964).
[92]B. Sorensen, Nucl. Phys. **A97**, 1 (1967); **A119**, 65 (1968); **A142**, 392, 411 (1970); **A217**, 505 (1973).
[93]J. Da Providencia and J. Weneser, Phys. Rev. C **1**, 825 (1970).
[94]E. R. Marshalek, Nucl. Phys. **A161**, 401 (1971); A224, 221, 245 (1974).
[95]T. Kishimoto and T. Tamura, Nucl. Phys. **A192**, 246 (1972); **A270**, 317 (1976).
[96]S. Y. Li, R. M. Dreizler, and A. Klein, Phys. Lett. **B32**, 169 (1970); Phys. Rev. C **4**, 1571 (1971).
[97]E. R. Marshalek and J. Weneser, Ann. Phys. **53**, 569 (1969); Phys. Rev. C **2**, 1682 (1970).
[98]E. R. Marshalek, Phys. Rev. C **3**, 1710 (1971); **11**, 1426 (1975).
[99]G. Holzwarth, Nucl. Phys. **A156**, 511 (1970); **A174**, 97 (1971); **A185**, 268 (1972).
[100]S. G. Lie and G. Holzwarth, Phys. Rev. C **12**, 1035 (1975).
[101]G. Holzwarth, D. Janssen, and R. V. Jolos, Nucl. Phys. **A261**, 1 (1976).
[102]E. R. Marshalek and G. Holzwarth, Nucl. Phys. **A191**, 438 (1972).
[103]H. J. Mang, Phys. Rep. **C18**, 325 (1975).
[104]S. Y. Chu *et al.*, Phys. Rev. C **12**, 1017 (1975).
[105]I. Hamamoto, Nucl. Phys. **A271**, 15 (1976).
[106]E. R. Marshalek and A. L. Goodman, Nucl. Phys. **A294**, 92 (1978).
[107]E. R. Marshalek, Preprint NBI-77-34, Copenhagen (1978); to appear in Nukleonika.
[108]R. J. Glauber, Phys. Rev. **130**, 2529 (1963); **131**, 2766 (1963).
[109]A. M. Perelomov, Commun. Math. Phys. **26**, 222 (1972).
[110]D. J. Rowe, in: Intern. Symp. on Nuclear Structure. Coexistence of Single Particle and Collective Types of Excitation, Balatonfured (1975).
[111]K. Goeke, Nucl. Phys. **A265**, 301 (1976); K. Goeke and P. G. Reinhard, Ann. Phys. (N.Y.) **112**, 328 (1978).
[112]T. Marumori, in: Selected Topics in Nuclear Structure, Vol. 2, JINR D-9920, Dubna (1976), p. 412.
[113]E. M. de Guerra and F. Villars, Nucl. Phys. **A285**, 297 (1977); **A298**, 109 (1978).
[114]E. R. Marshalek, Nucl. Phys. **A266**, 317 (1976); **A275**, 416 (1977).
[115]A. Bohr and B. Mottelson, At. Energ. **14**, 41 (1963).
[116]S. M. Harris, Phys. Rev. B **138**, 509 (1965).
[117]O. Saethre *et al.*, Nucl. Phys. **A207**, 486 (1973).
[118]M. A. J. Mariscotti, G. Scharff-Goldhaber, and B. Buck, Phys. Rev. **178**, 1864 (1969).
[119]A. Klein, R. M. Dreizler, and T. K. Das, Phys. Lett. **B31**, 333 (1970).
[120]H. Ejiri *et al.*, J. Phys. Soc. Jpn. **24**, 1189 (1968).
[121]T. K. Das, R. M. Dreizler, and A. Klein, Phys. Rev. Lett. **25**, 1626 (1970); Phys. Lett. B34, 235 (1971).
[122]S. M. Abecasis and E. S. Hernandes, Nucl. Phys. **A180**, 485 (1972).
[123]S. M. Abecasis, Nucl. Phys. **A205**, 475 (1973).
[124]A. S. Davydov and G. F. Filippov, Nucl. Phys. **8**, 237 (1958).
[125]I. N. Mikhailov, E. Nadzhakov, and R. Kh. Safarov, Preprint R-2866 [in Russian], JINR, Dubna (1966).
[126]I. N. Mikhailov *et al.*, C. R. Acad. Bulg. Sci. **22**, 635 (1969).
[127]E. Nadjakov and I. N. Mikhailov, Preprint IC/71/111, Trieste (1971).
[128]P. Holmberg and P. O. Lipas, Nucl. Phys. **A117**, 552 (1968).
[129]E. Nadjakov and I. N. Mikhailov, Nucl. Phys. **107**, 92 (1968).
[130]S. Wahlborn and R. K. Gupta, Phys. Lett. **B40**, 27 (1972).
[131]R. K. Gupta, S. Wahlborn, and L. Hjertman, Phys. Scr. **6**, 261 (1972).
[132]J. E. Draper, Phys. Lett. **B41**, 105 (1972).
[133]A. N. Mantri and P. C. Sood, Phys. Rev. C **9**, 2076 (1974).
[134]P. C. Sood and A. K. Jain, Phys. Rev. C **12**, 1064 (1975).
[135]Y. P. Varshni and S. Bose, Phys. Rev. C **6**, 1770 (1972).
[136]T. K. Das and B. Banerjee, Phys. Rev. C **7**, 2590 (1973).
[137]A. N. Mantri and P. C. Sood, Phys. Rev. C **7**, 1294 (1973).
[138]B. C. Smith and A. B. Volkov, Phys. Lett. **B47**, 193 (1973).
[139]R. K. Gupta, Phys. Rev. C **7**, 2476 (1973).
[140]H. Toki and A. Faessler, Z. Phys. **A276**, 35 (1976).
[141]A. A. Raduta and R. M. Dreizler, Nucl. Phys. **A258**, 109 (1976).
[142]A. A. Raduta and M. Badea, Z. Phys. **A278**, 51 (1976).

[143]A. Arima and F. Iachello, Ann. Phys. (N. Y.) **99**, 253 (1976); **111**, 201 (1978); **115**, 325 (1978).
[144]A. Molinari and T. Regge, Phys. Lett. **B41**, 93 (1972).
[145]R. A. Broglia *et al.*, Phys. Lett. **B50**, 295 (1974); **B57**, 113 (1975).
[146]A. L. Goodman and A. Goswami, Phys. Rev. C **9**, 1948 (1974).
[147]A. Faessler, W. Greiner, and R. K. Sheline, Nucl. Phys. **70**, 33 (1965).
[148]E. Nadjakov, A. Apostolova, and V. Kitipova, Preprint E4-7753 JINR, Dubna (1974).
[149]E. Nadjakov and R. Nojarov, Preprint IC/75/41, Trieste (1975); Bulg. J. Phys. **3**, 352 (1976).
[150]Y. El Masri *et al.*, Nucl. Phys. **A271**, 133 (1976).
[151]O. Nathan and S. G. Nilsson, Alpha, Beta, and Gamma Rays Spectroscopy, North-Holland, Amsterdam (1965), Ch. 10.
[152]G. Alaga *et al.*, K. Dan. Vidensk. Selsk. Mat.-Fys. Medd. **29**, No. 9 (1955).
[153]A. K. Kerman, K. Dan. Vidensk. Selsk. Mat.-Fys. Medd. **30**, No. 15 (1956).
[154]V. M. Mikhailov, Izv. Akad. Nauk SSSR, Ser. Fiz. **28**, 308 (1964); **30**, 1334 (1966).
[154a]M. I. Baznat, N. I. Pyatov, and M. I. Chernei, Fiz. Elem. Chastits At. Yadra **4**, 941 (1973) [Sov. J. Part. Nucl. **4**, 384 (1973)].
[155]D. Karadjov, I. N. Mikhailov, and I. Piperova, Phys. Lett. B46, 163 (1973); Yad. Fiz. **21**, 964 (1975) [Sov. J. Nucl. Phys. **21**, 495 (1975)].
[156]P. G. Hansen, O. B. Nielsen, and R. K. Sheline, Nucl. Phys. **12**, 389 (1959).
[157]P. O. Lipas, Nucl. Phys. **39**, 468 (1962).
[158]R. M. Diamond *et al.*, Nucl. Phys. **A184**, 481 (1972).
[159]I. A. Fraser *et al.*, Phys. Rev. Lett. **23**, 1051 (1969).
[160]J. H. Hamilton, in: Radioactivity in Nuclear Spectroscopy, Vol. 2, Gordon and Breach, New York (1972), p. 935; in: Nuclear Structure, D-6465, JINR, Dubna (1972), p. 332; Izv. Akad. Nauk SSSR, Ser. Fiz. **36**, 17 (1972).
[161]N. Rud, H. L. Nielsen, and K. Wilsky, Nucl. Phys. **A167**, 401 (1971).
[162]J. P. Elliott, Proc. R. Soc. London **A245**, 128, 562 (1958).
[163]V. Bargmann and M. Moshinsky, Nucl. Phys. **18**, 697 (1969); **23**, 177 (1961).
[164]M. Moshinsky, Fundamentals in Nuclear Theory, IAEA, Vienna (1967), Ch. 12.
[165]I. N. Mikhailov and E. Nadjakov, Preprint E4-4884, JINR, Dubna (1970); Izv. Akad. Nauk SSSR, Ser. Fiz. **34**, 2088 (1970); I. N. Mikhailov, E. Nadzhakov, I. Piperova, and B. Petrov, Preprint R4-6035 [in Russian], JINR, Dubna (1971).
[166]P. P. Raichev, Yad. Fiz. **16**, 1171 (1972) [Sov. J. Nucl. Phys. **16**, 643 (1973)].
[167]L. Weaver and L. C. Biedenharn, Nucl. Phys. **A185**, 1 (1972).
[168]L. Weaver, L. C. Biedenharn, and R. Y. Cusson, Ann. Phys. (N. Y.) **77**, 250 (1973).
[169]O. L. Weaver, R. Y. Cusson, and L. C. Biedenharn, Ann. Phys. (N. Y). **102**, 493 (1976).
[170]G. Rosensteel and D. J. Rowe, Phys. Rev. Lett. **38**, 10 (1977).
[171]G. N. Afanas'ev, Yad. Fiz. **12**, 1175 (1970) [Sov. J. Nucl. Phys. **12**, 645 (1971)].
[172]V. Vanagas, E. Nadjakov, and P. Raychev, Bulg. J. Phys. **2**, 558 (1975).
[173]B. G. Wybourne, Classical Groups for Physicists, Wiley, New York (1974).
[174]C. Dasso *et al.*, Nucl. Phys. **A210**, 429 (1973).
[175]D. Janssen, R. V. Jolos, and F. Dönau, Nucl. Phys. **A224**, 93 (1974).
[176]J. F. Dyson, Phys. Rev. **102**, 1217, 1231 (1956).
[177]D. Janssen *et al.*, Nucl Phys. **A172**, 145 (1971).
[178]R. V. Jolos and D. Janssen, Fiz. Elem. Chastits At. Yadra **8**, 330 (1977) [Sov. J. Part. Nucl. **8**, 138 (1977)].
[179]R. M. Dreizler and A. Klein, Phys. Rev. C **7**, 512 (1973).
[180]Yu. A. Simonov, Yad. Fiz. **3**, 630 (1966); **7**, 1210 (1968) [Sov. J. Nucl. Phys. **3**, 461 (1966); **7**, 722 (1968)].
[181]A. I. Baz' *et al.*, Fiz. Elem. Chastits At. Yadra **3**, 275 (1972) [Sov. J. Part. Nucl. **3**, 137 (1972)].
[182]Yu. F. Smirnov and K. V. Shitikova, Fiz. Elem. Chastits At. Yadra **8**, 847 (1977) [Sov. J. Part. Nucl. **8**, 344 (1977)].
[183]G. F. Filippov, Fiz. Elem. Chastits At. Yadra **4**, 992 (1973) [Sov. J. Part. Nucl. **4**, 405 (1973)].
[184]V. V. Vanagas, Fiz. Elem. Chastits At. Yadra **7**, 309 (1976) [Sov. J. Part. Nucl. **7**, 118 (1976)]; Lecture Notes, University of Toronto (1977).
[185]I. N. Mikhailov and E. Nadzhakov, Preprint R4-4293 [in Russian], JINR, Dubna (1969); in: Intern. Conf. on Properties of Nuclear States, Contributions, Montreal (1969), p. 42; C. R. Acad. Bulg. Sci. **22**, 1221 (1969).
[186]I. N. Mikhailov, E. Nadzhakov, and D. Karadzhov, Fiz. Elem. Chastits At. Yadra, **4**, 311 (1973) [Sov. J. Part. Nucl. **4**, 129 (1973)].
[187]A. R. Edmonds, Angular Momentum in Quantum Mechanics, Princeton University Press (1960).
[188]D. A. Varshalovich, A. N. Moskalev, and V. K. Khersonskii, Quantum Theory of Angular Momentum [in Russian], Nauka, Leningrad (1975).
[189]E. Nadjakov, Heavy Ion, High-Spin States and Nuclear Structure, Vol. 1, IAEA, Vienna (1975), p. 493.
[190]D. Karadjov, I. N. Mikhailov, E. Nadjakov, and I. Piperova, Nucl. Phys. **A305**, 78 (1978).
[191]E. Nadjakov, Nuclear Self-Consistent Fields, North-Holland, Amsterdam (1975), p. 69; J. Phys. G: Nucl. Phys. **3**, 1671 (1977).
[192]E. Nadjakov *et al.*, Preprint E4-11831, JINR, Dubna (1978).
[193]D. Karadjov *et al.*, in: Intern. Conf. on Nuclear Physics, Vol. 1, Munich (1973), p. 297.
[194]E. Nadjakov, V. Antonova, and R. Nojarov, Preprint E4-11832, JINR, Dubna (1978).
[195]E. Nadzhakov and I. N. Mikhailov, Izv. Akad. Nauk SSSR, Ser. Fiz. **36**, 876 (1972).
[196]F. Gryummer *et al.*, Preprint R4-11278 [in Russian], JINR, Dubna (1978).
[197]D. Karadjov, I. N. Mikhailov, E. Nadjakov, and I. Piperova, Nucl. Phys. **A305**, 93 (1978).
[198]F. A. Gareev, S. P. Ivanova, V. G. Solov'ev, and S. I. Fedotov, Fiz. Elem. Chastits At. Yadra **4**, 357 (1973) [Sov. J. Part. Nucl. **4**, 148 (1973)].
[199]R. Engfer *et al.*, AD NDT **14**, 509 (1974).
[200]K. E. G. Löbner, M. Vetter, and V. Hönig, NDTA **7**, 495 (1970).
[201]W. Andrejtscheff, K. D. Schilling, and P. Manfrass, AD NDT **16**, 515 (1976).
[202]M. Sakai, AD NDT **15**, 513 (1975); M. Sakai and A. C. Rester, AD NDT **20**, 441 (1977).
[203]E. P. Grigor'ev, Doktorskaya dissertatsiya (Doctoral Dissertation), Leningrad (1973).
[204]J. J. Griffin and M. Rich, Phys. Rev. **118**, 850 (1960).
[205]S. G. Nilsson and O. Prior, K. Dan. Vidensk. Selsk. Mat.-Fys. Medd. **32**, No. 16 (1960).
[206]O. Prior, F. Boehm, and S. G. Nilsson, Nucl. Phys. **A110**, 257 (1968).
[206a]D. Karadzhov *et al.*, Preprint R4-6106 [in Russian], JINR, Dubna (1971).
[206b]A. A. Kuliev and N. I. Pyatov, Yad. Fiz. **20**, 297 (1974) [Sov. J. Nucl. Phys. **20**, 158 (1975)].
[207]T. Kammuri and S. Kusuno, Phys. Lett. **B38**, 5 (1972); Nucl. Phys. **A215**, 178 (1973).
[208]J. Meyer, J. Speth, and J. H. Vogeler, Nucl. Phys. **A193**, 60 (1972).
[209]V. G. Zelevinskii and M. I. Shtokman, Izv. Akad. Nauk SSSR, Ser. Fiz. **36**, 2577 (1972).

[210]S. Frauendorf, D. Janssen, and L. Münchow, Nucl. Phys. **A125**, 369 (1969).
[211]D. Karadzhov, I. N. Mikhailov, and E. Nadzhakov, Preprint R4-6104 [in Russian], JINR, Dubna (1971).
[212]E. Nadjakov, Preprint IC/72/135, Trieste (1972).
[213]M. Sano and M. Wakai, Nucl. Phys. **67**, 481 (1965); **97**, 298 (1967).
[214]K. Y. Chan and J. G. Valatin, Nucl. Phys. **82**, 222 (1966).
[215]K. Y. Chan, Nucl. Phys. **85**, 261 (1966).
[216]T. Udagawa and R. K. Sheline, Phys. Rev. **147**, 671 (1966).
[217]J. Krumlinde, Nucl. Phys. **A121**, 306 (1968); **160**, 471 (1971).
[218]C. W. Ma and C. F. Tsang, Phys. Rev. C **11**, 213 (1975).
[219]I. Hamamoto and T. Udagawa, Nucl. Phys. **A126**, 241 (1969).
[220]C. W. Ma and J. O. Rasmussen, Phys. Rev. C **2**, 798 (1970).
[221]I. M. Pavlichenko, Nucl. Phys. **55**, 225 (1964).
[222]D. R. Bes *et al.*, Nucl. Phys. **65**, 1 (1965).
[223]E. R. Marshalek, Phys. Rev. B **139**, 770 (1965); **158**, 993 (1967); Phys. Rev. Lett. **20**, 214 (1968).
[224]J. Mayer, Nucl. Phys. **137**, 193 (1969).
[225]J. Meyer and J. Speth, Nucl. Phys. **A203**, 17 (1973).
[226]J. Speth *et al.*, in Mössbauer Isomer Shifts, North-Holland, Amsterdam, to be published.
[227]J. Meyer and J. Speth, Yad. Fiz. **17**, 1197 (1973) [Sov. J. Nucl. Phys. **17**, 675 (1973)].
[228]K. Neergård, Preprint, NORDITA, Copenhagen (1974).
[229]H. K. Walter, Nucl. Phys. **A234**, 504 (1974).
[230]D. Ward *et al.*, Nucl. Phys. **A196**, 9 (1972).
[231]D. Karadzhov, I. N. Mikhailov, E. Nadzhakov, and I. Piperova, Yad. Fiz. **24**, 888 (1976) [Sov. J. Nucl. Phys. **24**, 464 (1976)].
[232]I. O. Meredith and R. C. Barber, Can. J. Phys. **50**, 1195 (1972).
[232a]E. Nadzhakov, Doktorskaya dissertatsiya (Doctoral Dissertation), Sofia (1978).
[233]P. Ring, R. Beck, and H. J. Mang, Z. Phys. **231**, 10 (1970).
[234]R. Beck, H. J. Mang, and P. Ring, Z. Phys. **231**, 26 (1970).
[235]B. Banerjee, H. J. Mang, and P. Ring, Nucl. Phys. **A215**, 366 (1973).
[236]P. Ring, H. J. Mang, and B. Banerjee, Nucl. Phys. **A225**, 141 (1974).
[237]H. J. Mang, B. Samadi, and P. Ring, Z. Phys. **A279**, 325 (1976).
[238]F. Grümmer, K. W. Schmid, and A. Faessler, Nucl. Phys. **A239**, 289 (1975).
[239]J. Damgaard, S. Kusuno, and A. Faessler, Nucl. Phys. **243**, 492 (1975).
[240]A. Faessler *et al.*, Nucl. Phys. **A256**, 106 (1976).
[241]K. W. Schmid *et al.*, Phys. Lett. **B63**, 399 (1976).
[242]A. L. Goodman, Nucl. Phys. **A230**, 466 (1974); **A265**, 113 (1976).
[243]A. L. Goodman and J. P. Vary, Phys. Rev. Lett. **35**, 504 (1975).
[244]C. S. Warke and M. R. Gunye, Phys. Rev. C **12**, 1647 (1975); **13**, 859 (1976).
[245]S. Frauendorf, Nucl. Phys. **A263**, 150 (1976).
[246]C. Bloch and A. Messiah, Nucl. Phys. **39**, 95 (1962).
[247]P. O. Löwdin, Rev. Mod. Phys. **36**, 966 (1964).
[248]R. A. Sorensen, Nucl. Phys. **A281**, 475 (1977).
[249]M. Wakai and A. Faessler, Nucl. Phys. **A295**, 86 (1978).
[250]C. W. Ma and J. O. Rasmussen, Phys. Rev. C **16**, 1179 (1977).
[251]M. Ploszajczak and A. Faessler, Z. Phys. **A283**, 349 (1977).
[252]A. Faessler and M. Ploszajczak, Phys. Rev. C **16**, 2032 (1977).
[253]M. Ploszajczak, K. R. S. Devi, and A. Faessler, Z. Phys. **A282**, 267 (1977).
[254]M. Ploszajczak, A. Faessler, G. Leander, and S. G. Nilsson, Nucl. Phys. **A301**, 477 (1978).
[255]M. Ploszajczak, H. Toki, and A. Faessler, Z. Phys. **A287**, 103 (1978).
[256]I. N. Mikhailov and D. Janssen, Phys. Lett. **B72**, 303 (1978); D. Janssen and I. N. Mikhailov Nucl. Phys., to be published.
[257]B. R. Mottelson and J. G. Valatin, Phys. Rev. Lett. **5**, 511 (1960).
[258]M. Sano and M. Wakai, Prog. Theor. Phys. **47**, 880 (1972).
[259]F. S. Stephens and R. S. Simon, Nucl. Phys. **A183**, 257 (1972).
[260]F. S. Stephens *et al.*, Nucl. Phys. **A222**, 235 (1974).
[260a]B. L. Birbrair, Phys. Lett. **B34**, 558 (1971); **B39**, 489 (1972).
[261]A. de-Shalit, Phys. Rev. **122**, 1530 (1961).
[262]P. Vogel, Phys. Lett. **B33**, 400 (1970).
[263]F. S. Stephens, R. M. Diamond, and S. G. Nilsson, Phys. Lett. **B44**, 429 (1973).
[264]P. Thieberger, Phys. Lett. **B45**, 417 (1973).
[265]C. K. Ross and Y. Nogami, Nucl. Phys. **A211**, 145 (1973).
[266]M. Sano, T. Takemasa, and M. Wakai, J. Phys. Soc. Jpn. **34**, 365 (1973).
[267]K. Kumar, Phys. Rev. Lett. **30**, 1227 (1973).
[267a]Yu. T. Grin, Phys. Lett. **B52**, 135 (1974).
[267b]A. Goswami, L. Lin, and G. L. Strubble, Phys. Lett. **B25**, 451 (1967).
[268]M. Reinecke and H. Ruder, Z. Phys. **A282**, 407 (1977).
[269]D. Janssen, F. R. May, I. N. Mikhailov, and R. G. Nazmitdinov, Preprint E4-10959, JINR, Dubna (1977); Phys. Lett. **B73**, 271 (1978).
[270]J. Krumlinde and Z. Szymanski, Phys. Lett. **B36**, 157 (1971); **B40**, 314 (1972); **B53**, 322 (1974); Ann. Phys. (N.Y.) **79**, 201 (1973); Nucl. Phys. **A221**, 93 (1974).
[270a]B. L. Birbrair, Phys. Lett. **B72**, 425 (1978).
[271]A. Faessler and M. Ploszajczak, Ann. Report 1977, IKP KFA Jül-Spez-15, Jülich (1978), p. 97.
[272]A. Faessler, K. R. S. Devi, and A. Barroso, Nucl. Phys. **A286**, 101 (1977).
[273]S. Frauendorf and V. V. Pashkevich, Phys. Lett. **B55**, 365 (1975).
[274]J. H. Hamilton, Selected Topics in Nuclear Structure, Vol. 2, JINR D-9920, Dubna (1976), p. 303.
[275]C. Günther *et al.*, Phys. Rev. C **15**, 1298 (1977).
[276]H. L. Yadav, H. Toki, and A. Faessler, Phys. Rev. Lett. **39**, 1128 (1977).
[277]K. Neergård and P. Vogel, Nucl. Phys. **A145**, 33 (1970); **A149**, 217 (1970).
[278]K. Neergård, P. Vogel, and M. Radomski, Nucl. Phys. **A238**, 199 (1975).
[279]H. Toki, K. Neergård, P. Vogel, and A. Faessler, Nucl. Phys. **A279**, 1 (1977).
[279a]V. M. Martynov and I. M. Pavlichenkov, Yad. Fiz. **24**, 897 (1976) [Sov. J. Nucl. Phys. **24**, 469 (1976)].
[280]K. Neergård and V. V. Pashkevich, Phys. Lett. **B59**, 218 (1975).
[281]K. Neergård, V. V. Pashkevich, and S. Frauendorf, Nucl. Phys. **A262**, 61 (1976).
[282]R. Bengtsson *et al.*, Phys. Lett. **B57**, 301 (1975).
[283]G. Andersson *et al.*, Nucl. Phys. **A268**, 205 (1976).
[284]A. Faessler, R. R. Hilton, and K. R. S. Devi, Phys. Lett. **B61**, 133 (1976).
[285]A. Faessler, M. Ploszajczak, and K. R. S. Devi, Phys. Rev. Lett. **36**, 1028 (1976).
[286]K. Neergård, H. Toki, M. Ploszajczak, and A. Faessler, Nucl. Phys. **A287**, 48 (1977).
[287]M. Ploszajczak, H. Toki, and A. Faessler, J. Phys. G: Nucl. Phys. **4**, 743 (1978).
[288]K. Pomorski and B. Nerlo-Pomorska, Z. Phys. **A283**, 383 (1977).

[289]M. Cerkaski *et al.*, Phys. Lett. **B70**, 9 (1977).
[290]C. G. Andersson and J. Krumlinde, Nucl. Phys. **A291**, 21 (1977).
[291]Th. Døssing, K. Neergård, K. Matsuyanagi, and Chang Hsi-Chen, Phys. Rev. Lett. **39**, 1395 (1977).
[292]D. Janssen *et al.*, Preprint E4-11371, JINR, Dubna (1978); Phys. Lett. B, to be published.
[293]S. Cohen, F. Plasil, and W. J. Swiatecki, Ann. Phys. (N.Y.) **82**, 557 (1974).
[294]V. G. Zelevinskiĭ, Yad. Fiz. **22**, 1085 (1975) [Sov. J. Nucl. Phys. **22**, 565 (1975)].
[295]E. K. Hyde, D. Perlman, and G. T. Seaborg, Sverkhtyazhelye elementy (Superheavy Elements), No. 1; Transuranovye elementy (Transuranium Elements), No. 2 (1967), p. 221; Metody sinteza tyazhelykh yader (Methods of Synthesis of Heavy Nuclei) (1968), p. 36 (Russian translations published by Atomizdat, Moscow).
[296]R. Kaufman and R. Wolfgang, Phys. Rev. **121**, 192, 206 (1961).
[297]A. Fleury and J. M. Alexander, Ann. Rev. Nucl. Sci. **24**, 279 (1974).
[298]I. L. Preiss, H. Bakhru, J. M. D'Auria, and A. C. Li, Ark. Fyz. **36**, 241 (1967).
[299]R. M. Diamond, Preprint UCRL-19961, Lawrence Radiation Laboratory, Berkeley (1970); in: Intern. Conf. on Properties of Nuclei far from the Region of Beta Stability, Vol. 1, CERN 70-30, Geneva (1970), p. 65; Nukleonika **21**, 29 (1976).
[300]K. Alder *et al.*, Rev. Mod. Phys. **28**, 432 (1956).
[301]K. Alder and A. Winther, K. Dan. Vidensk. Selsk. Mat.-Fys. Medd. **32**, No. 8 (1960).
[302]H. Lutken and A. Winther, K. Dan. Vidensk. Selsk. Mat.-Fys. Medd. **2**, No. 6 (1964).
[303]T. D. Thomas, Ann. Rev. Nucl. Sci. **18**, 343 (1968).
[304]V. S. Barashenkov, F. G. Zheregi, A. S. Il'inov, and V. D. Toneev, Fiz. Elem. Chastits At. Yadra **5**, 479 (1974) [Sov. J. Part. Nucl. **5**, 192 (1974)].
[305]D. R. Bes and R. A. Broglia, Nucl. Phys. **80**, 289 (1966); R. A. Broglia and D. R. Bes, Phys. Lett. **B69**, 129 (1977).
[306]R. A. Broglia and P. F. Bortignon, Phys. Lett. **B65**, 221 (1976).
[307]D. R. Bes, R. A. Broglia, O. Hansen, and O. Nathan, Phys. Rep. **C34**, 1 (1977).
[308]R. A. Broglia and A. Winther, Nucl. Phys. **A182**, 112 (1972); Phys. Rep. **C4**, 153 (1972).
[309]J. O. Newton *et al.*, Nucl. Phys. **A141**, 631 (1970).
[310]J. R. Grover, Phys. Rev. **157**, 832 (1967).
[311]J. O. Newton *et al.*, Phys. Rev. Lett. **34**, 99 (1975).
[312]R. S. Simon *et al.*, Phys. Rev. Lett. **36**, 359 (1976).
[313]R. S. Simon *et al.*, Nucl. Phys. **A290**, 253 (1977).
[314]J. O. Newton, S. H. Sie, and G. D. Dracoulis, Phys. Rev. Lett. **40**, 625 (1978).
[315]H. J. Wollersheim *et al.*, Jahresbericht, 1977, GSI-J-1-78, Darmstadt (1978), p. 62.
[316]V. V. Volkov, Fiz. Elem. Chastits At. Yadra **2**, 285 (1971); **6**, 1040 (1975) [Sov. J. Part. Nucl. **2**, Part 2, 1 (1971); **6**, 420 (1975)]; in: Izbrannye voprosy struktury yadra (Selected Questions in Nuclear Structure), Vol. 2, D-9921, JINR, Dubna (1976), p. 45; Phys. Rep. **C44**, 93 (1978).
[317]M. M. Aleonard *et al.*, Phys. Rev. Lett. **40**, 622 (1978).
[318]J. B. Natowitz *et al.*, Phys. Rev. Lett. **40**, 751 (1978).
[319]P. R. Christensen *et al.*, Phys. Rev. Lett. **40**, 1245 (1978).
[320]E. Nadzhakov, Doktorskaya dissertatsiya (Doctoral Dissertation), Sofia (1978).
[321]J. O. Newton, Nuclear Spectroscopy and Reactions, Part C, Academic Press, New York (1974), p. 185.
[322]R. O. Sayer, J. S. Smith, III, and W. T. Milner, AD NDT **15**, 85 (1975).
[323]P. Kleinheinz *et al.*, Nucl. Phys. **A283**, 189 (1977).
[324]D. B. Fossan and E. K. Warburton, Nuclear Spectroscopy and Reactions, Part C, Academic Press, New York (1974), p. 307.
[325]H. Backe *et al.*, Z. Phys. **A285**, 159 (1978).
[326]S. Devons, G. Manning, and D. St. P. Bunbury, Proc. Phys. Soc. London **A68**, 18 (1955).
[327]T. K. Alexander and K. W. Allen, Can. J. Phys. **43**, 1563 (1965).
[328]R. M. Diamond, F. S. Stephens, W. H. Kelly, and D. Ward, Phys. Rev. Lett. **22**, 546 (1969).
[329]J. L. Quebert *et al.*, Nucl. Phys. **A150**, 68 (1970).
[330]E. K. Warburton, J. W. Olness, and A. R. Poletti, Phys. Rev. **160**, 938 (1967).
[331]R. G. Stokstad *et al.*, Nucl. Phys. **A156**, 145 (1970).
[332]D. Ward, Reactions between Complex Nuclei (Nashville), Vol. 2, North-Holland, Amsterdam (1974), p. 417.
[333]R. S. Hager and E. C. Seltzer, NDTA **4**, 1, 397 (1968); **6**, 1 (1969).
[334]O. Dragoun, Z. Plajner, and F. Schmutzler, NDTA **9**, 119 (1971).
[335]K. W. Jones, A. Z. Schwarzschild, E. K. Warburton, and D. B. Fossen, Phys. Rev. **178**, 1773 (1969).
[336]R. Nordhagen *et al.*, Nucl. Phys. **A142**, 577 (1970).
[337]B. Bochev *et al.*, Yad. Fiz. **16**, 633 (1972) [Sov. J. Nucl. Phys. **16**, 355 (1973)].
[338]B. Bochev *et al.*, Nucl. Phys. **A267**, 344 (1976).
[339]L. C. Northcliffe and R. F. Schilling, NDTA **7**, 233 (1970).
[340]B. Bochev *et al.*, Nucl. Phys. **A282**, 159 (1977).
[341]F. Kearns *et al.*, Nucl. Phys. **A278**, 109 (1977).
[342]L. Lindhard, M. Scharff, and H. E. Schiott, K. Dan. Vidensk. Selsk. Mat. Fys. Medd. **36**, No. 14 (1963).
[343]B. C. Robertson, Phys. Lett. **B68**, 424 (1977).
[344]M. M. R. Williams, Nucl. Phys. **A277**, 317 (1977).
[345]S. H. Sie and D. W. Gebbie, Nucl. Phys. **A289**, 217 (1977).
[346]S. H. Sie *et al.*, Nucl. Phys. **A291**, 443 (1977).
[347]J. F. Ziegler and W. K. Chu, AD NDT **13**, 463 (1977).
[348]L. Winsberg, AD NDT **20**, 389 (1977).
[349]H. Bokemeyer *et al.*, in: Intern. Symp. on High-Spin States and Nuclear Structure, ZfK-366, Dresden (1977), p. 78; H. Emling *et al.*, Jahresbericht 1977, GSI-J-1-78, Darmstadt (1978), p. 66.
[350]D. Ward *et al.*, Nucl. Phys. **A266**, 194 (1976).
[351]M. W. Guidri *et al.*, Nucl. Phys. **A266**, 228 (1976).
[352]D. Habs, V. Metag, H. J. Specht, and G. Ulfert, Phys. Rev. Lett. **38**, 387 (1977).
[353]K. Kumar, Phys. Scr. **11**, 179 (1975).
[354]Yu. T. Grin, Phys. Lett. **B59**, 419 (1975).
[355]R. Kalish, Phys. Scr. **11**, 190 (1975).
[356]E. Recknagel, Nuclear Spectroscopy and Reactions, Part C, Academic Press, New York (1974), p. 93.
[357]A. Abragam and R. V. Pound, Phys. Rev. **92**, 943 (1953).
[358]F. Bosch and H. Spehl, Z. Phys. **268**, 145 (1974).
[359]C. Roulet *et al.*, Nucl. Phys. **A285**, 156 (1977).
[360]R. Kalish, B. Herskind, and G. B. Hagemann, Phys. Rev. C **8**, 757 (1973).
[361]B. Skaali *et al.*, Nucl. Phys. **A238**, 159 (1975).
[362]M. B. Goldberg, Phys. Scr. **11**, 184 (1975).
[363]K. H. Speidel *et al.*, Jahresbericht, 1977, GSI-J-1-78, Darmstadt (1978), p. 67.
[364]D. Ward *et al.*, Phys. Rev. Lett. **30**, 493 (1973); Izv. Akad. Nauk SSSR, Ser. Fiz. **37**, 1791 (1973).
[365]D. Ward *et al.*, Izv. Akad. Nauk SSSR, Ser. Fiz. **39**, 37 (1975).
[366]B. Bochev *et al.*, Preprint R7-8531 [in Russian], JINR, Dubna (1975).
[367]B. Bochev *et al.*, in: Intern. Conf. on Nuclear Structure, Contributed Papers, Tokyo (1977), p. 399; Preprint E7-10675, JINR, Dubna (1977).
[368]D. Husar *et al.*, Phys. Rev. Lett. **36**, 1291 (1976); D. Husar *et al.*, Nucl. Phys. **A292**, 267 (1977).
[369]B. Bochev *et al.*, Phys. Scr. **6**, 243 (1972).
[370]B. Bochev, L. Aleksandrov, and T. Kutsarova, Preprint R5-7881 [in Russian], JINR, Dubna (1974); Preprint R5-8321

[in Russian], JINR, Dubna (1974).
[371]K. Alder and A. Winther, Electromagnetic Excitation, North-Holland, Amsterdam (1975).
[372]H. J. Wollersheim and T. W. Elze, Nucl. Phys. **A278**, 87 (1977).
[373]K. Fischer *et al.*, Phys. Rev. **C15**, 921 (1977).
[374]R. M. Ronningen *et al.*, Phys. Rev. **C16**, 2208 (1977).
[375]R. M. Ronningen *et al.*, Phys. Rev. **C15**, 1671 (1977).
[376]F. K. McGowan *et al.*, Nucl. Phys. **A289**, 253 (1977).
[377]F. K. McGowan *et al.*, Nucl. Phys. **A297**, 51 (1978).
[378]W. Gelletly *et al.*, J. Phys. G: Nucl. Phys. **4**, 575 (1978).
[379]I. Y. Lee *et al.*, Phys. Rev. Lett. **37**, 420 (1976).
[380]I. Y. Lee *et al.*, Phys. Rev. Lett. **39**, 684 (1977).
[381]H. Bokemeyer *et al.*, in: Intern. Symp. on High-Spin States and Nuclear Structure, ZfK 336, Dresden (1977), p. 79; P. Fuchs *et al.*, Jahresbericht, 1977, GSI-J-1-78 Darmstadt (1978). p. 65.
[382]P. Fuchs *et al.*, Jahresbericht, 1977, GSI-J-1-78, Darmstadt (1978), p. 195.
[383]T. D. Thomas, Phys. Rev. **116**, 703 (1959).
[384]V. V. Babikov, Zh. Eksp. Teor. Fiz. **38**, 274 (1960) [Sov. Phys. JETP **11**, 198 (1960)]; Preprint R-1351 [in Russian], JINR, Dubna (1963).
[385]M. Lefort, Y. Le Beyec, and J. Péter, in: Reactions between Complex Nuclei (Nashville), Vol. 2, North-Holland, Amsterdam (1974), p. 81.
[386]B. N. Kalinkin and V. P. Permyakov, Preprint R4-7312 [in Russian], JINR, Dubna (1973).
[387]H. Oeschler *et al.*, Nucl. Phys. **A266**, 262 (1976).
[388]J. Wilczynski, Nucl. Phys. **A216**, 386 (1973).
[389]R. Bass, Nucl. Phys. **A231**, 45 (1974).
[390]A. M. Zebelman *et al.*, Phys. Rev. **C10**, 200 (1974).
[391]B. Bochev, S. A. Karamayan, T. Kutsarova, and Yu. Ts. Oganesyan, Yad. Fiz. **23**, 520 (1976) [Sov. J. Nucl. Phys. **23**, 274 (1976)].
[392]H. V. Klapdor *et al.*, Nucl. Phys. **244**, 157 (1975); H. V. Klapdor, H. Reiss, and G. Rosner, Nucl. Phys. **A262**, 157 (1975).
[393]M. Blann, Ann. Rev. Nucl. Sci. **25**, 123 (1975).
[394]H. C. Britt *et al.*, Phys. Rev. Lett. **39**, 1458 (1977).
[395]H. Delagrange, A. Fleury, and J. M. Alexander, Phys. Rev. **C17**, 1706 (1978).
[396]D. G. Sarantities *et al.*, Phys. Rev. **C17**, 601 (1978).
[397]S. A. Karamyan, Yu. V. Melikov, and A. F. Tulinov, Fiz. Elem. Chastits At. Yadra **4**, 456 (1973) [Sov. J. Part. Nucl. **4**, 196 (1973)].
[398]V. N. Bugrov *et al.*, Preprint R7-9690 [in Russian], JINR, Dubna (1976).
[399]D. Ward, F. S. Stephens, and J. O. Newton, Phys. Rev. Lett. **19**, 1247 (1967).
[400]O. Andersen *et al.*, Nucl. Phys. **A295**, 163 (1978).
[401]J. C. Hardy *et al.*, Phys. Rev. Lett. **37**, 133 (1976).
[402]R. Broda *et al.*, Nucl. Phys. **A248**, 356 (1975).
[403]A. Djaloeis *et al.*, Nucl. Phys. **A250**, 149 (1975).
[404]Yu. Ts. Oganessian, Yu. E. Penionzhkevich, and A. O. Shamsutdinov, Acta Phys. Pol. **B6**, 323 (1975).
[405]T. Sikkeland, Phys. Rev. **B135**, 669 (1964).
[406]T. Sikkeland *et al.*, Phys. Rev. **C3**, 329 (1971).
[407]J. D. Jackson, Can. J. Phys. **34**, 767 (1956).
[408]P. A. Seeger, Nucl. Phys. **25**, 1 (1961).
[409]W. D. Myers and W. J. Swiatecki, Preprint UCRL-11980, Lawrence Radiation Laboratory, Berkeley (1965).
[410]W. Newbert and K. Aleksander, Preprint R7-3657 [in Russian], JINR, Dubna (1968).
[411]J. M. Alexander and G. N. Simonoff, Phys. Rev. **B133**, 93 (1964); G. N. Simonoff and J. M. Alexander, Phys. Rev. **B133**, 104 (1964).
[412]W. Neubert, NDT **11**, 531 (1973); Yad. Fiz. **25**, 63 (1977) [Sov. J. Nucl. Phys. **25**, 33 (1977)].
[413]F. Plasil, Phys. Rev. **C17**, 823 (1978).
[414]M. Beckerman and M. Blann, Phys. Rev. **C17**, 1615 (1978).
[415]S. Jägare, Nucl. Phys. **A95**, 481, 491 (1967).
[416]J. R. Grover and J. Gilat, Phys. Rev. **157**, 802, 814, 823 (1967).
[417]G. B. Hagemann *et al.*, Nucl. Phys. **A245**, 166 (1975).
[418]M. L. Halbert *et al.*, Nucl. Phys. **A259**, 469 (1976).
[419]R. J. Liotta and R. A. Sorensen, Nucl. Phys. **A297**, 136 (1978).
[420]A. Zehnder *et al.*, Nucl. Phys. **A254**, 315 (1975).
[421]U. Götz *et al.*, Nucl. Phys. **A192**, 1 (1972).
[422]I. Ragnarsson *et al.*, Nucl. Phys. **A233**, 329 (1974).
[423]C. Ekström, H. Rubensztein, and P. Möller, Phys. Scr. **14**, 199 (1976).
[424]D. Schwalm, E. K. Warburton, and J. W. Olness, Nucl. Phys. **A293**, 425 (1977).
[425]P. M. Walker *et al.*, J. Phys. G: Nucl. Phys. **2**, L197 (1976).
[426]G. D. Dracoulis, P. M. Walker, and A. Johnston, J. Phys. G: Nucl. Phys. **4**, 713 (1978).
[427]F. M. Bernthal *et al.*, Phys. Lett. **B64**, 147 (1976); B. D. Jeltema *et al.*, Nucl. Phys. **A280**, 21 (1977).
[428]P. Auguer *et al.*, Z. Phys. **A285**, 59 (1978).
[429]W. F. Davidson *et al.*, J. Phys. G: Nucl. Phys. **2**, 199 (1976).
[430]Y. Gono *et al.*, in: Intern. Conf. on Nuclear Structure, Contributed Papers, Tokyo (1977), p. 886.
[431]P. M. Walder *et al.*, Nucl. Phys. **A293**, 481 (1977).
[432]L. K. Peker, F. W. N. de Boer, and J. Konijn, Z. Phys. **A285**, 67 (1978).
[433]F. W. N. De Boer *et al.*, Nucl. Phys. **A290**, 173 (1977).
[434]Y. El Masri, J. Vervier, and A. Faessler, Nucl. Phys. **A279**, 223 (1977).
[435]S. W. Yates *et al.*, Nucl. Phys. **A222**, 301 (1974).
[436]J. C. Cunnane *et al.*, Phys. Rev. **C13**, 2197 (1976).
[437]S. A. Hjorth *et al.*, Nucl. Phys. **A262**, 328 (1976).
[438]D. Proetel, R. M. Diamond, and F. S. Stephens, Nucl. Phys. **A231**, 301 (1974).
[439]R. M. Leider *et al.*, Nucl. Phys. **A248**, 317 (1975).
[440]C. Flaum *et al.*, Nucl. Phys. **A264**, 291 (1976).
[441]E. Grosse *et al.*, Phys. Rev. Lett. **35**, 565 (1975).
[442]D. R. Haenni and T. T. Sugihara, Phys. Rev. **C16**, 120 (1977); **16**, 1129 (1977).
[443]E. Grosse, F. S. Stephens, and R. M. Diamond, Phys. Rev. Lett. **31**, 840 (1973).
[444]L. Richter *et al.*, Phys. Lett. **B71**, 74 (1977).
[445]H. Beuscher *et al.*, Nucl. Phys. **A249**, 379 (1975).
[446]E. Grosse, F. S. Stephens, and R. M. Diamond, Phys. Rev. Lett. **32**, 74 (1974).
[447]A. Neskakis *et al.*, Nucl. Phys. **A261**, 189 (1976).
[448]A. C. Kahler *et al.*, Phys. Lett. **B72**, 443 (1977).
[449]D. Ward *et al.*, Phys. Lett. **B56**, 139 (1975).
[450]J. Gizon *et al.*, Nucl. Phys. **A290**, 272 (1977).
[451]S. André *et al.*, Phys. Rev. Lett. **38**, 327 (1977).
[452]F. Bernthal *et al.*, Phys. Lett. **B74**, 211 (1978).
[453]L. L. Riedinger *et al.*, Phys. Rev. Lett. **33**, 1346 (1974).
[454]C. Foin and D. Barnéoud, Phys. Rev. Lett. **33**, 1049 (1974).
[455]C. Foin, S. André, and D. Barnéoud, Phys. Rev. Lett. **35**, 1697 (1975).
[456]A. Faessler, M. Ploscajczak, and K. R. S. Devi, Nucl. Phys. **A301**, 382 (1978).
[457]J. Meyer-ter-Vehn, Nucl. Phys. **A249**, 111, 141 (1975).
[458]G. Alaga and V. Paar, Phys. Lett. **B61**, 129 (1976).
[459]V. Paar, Ch. Vieu, and J. S. Dionisio, Nucl. Phys. **A284**, 199 (1977).
[460]P. Kemnitz *et al.*, Nucl. Phys. **A293**, 314 (1977).
[461]R. M. Diamond *et al.*, Phys. Rev. **C3**, 344 (1971).
[462]N. Rud *et al.*, Nucl. Phys. **A191**, 545 (1972).
[463]D. Ward *et al.*, Izv. Akad. Nauk SSSR, Ser. Fiz. **39**, 44 (1975).
[464]S. W. Yates *et al.*, Phys. Rev. **C17**, 634 (1978).
[465]Ph. Hubert, N. R. Johnson, and E. Eichler, Phys. Rev. **C17**, 622 (1978).

[466]R. O. Sayer *et al.*, Phys. Rev. **C17**, 1026 (1978).
[467]N. R. Johnson *et al.*, Phys. Rev. **C15**, 1325 (1977).
[468]K. Stelzer *et al.*, Phys. Lett. **B70**, 297 (1977).
[469]F. Kearns *et al.*, J. Phys. A: Math. Nucl. Gen. **7**, L11 (1974).
[470]N. R. Johnson *et al.*, Phys. Rev. **C12**, 1927 (1975).
[471]M. W. Guidri *et al.*, Phys. Rev. **C13**, 1164 (1976).
[472]J. O. Newton, F. S. Stephens, and R. M. Diamond, Nucl. Phys. **A210**, 19 (1973).
[473]S. M. Ferguson, H. Ejiri, and I. Halpern, Nucl. Phys. **A188**, 1 (1972).
[474]G. D. Dracoulis *et al.*, Nucl. Phys. **A279**, 251 (1977).
[475]L. R. Greenwood, NDS **13**, 549 (1974); **15**, 559 (1975).
[476]D. J. Horen and B. Harmatz, NDS **19**, 383 (1976).
[477]T. L. Khoo, J. C. Waddington, and M. W. Johns, Can. J. Phys. **51**, 2307 (1973).
[478]T. L. Khoo *et al.*, Phys. Rev. Lett. **35**, 1256 (1975).
[479]S. R. Faber *et al.*, Bull. Am. Phys. Soc. **21**, 975 (1976).
[480]P. Kleinheinz *et al.*, Z. Phys. **A286**, 27 (1978).
[481]M. Ogawa *et al.*, Phys. Rev. Lett. **41**, 289 (1978).
[482]M. V. Banaschik *et al.*, Phys. Rev. Lett. **34**, 892 (1975).
[483]M. Fenzl and O. W. B. Schult, Z. Phys. **A272**, 207 (1975).
[484]J. O. Newton *et al.*, Phys. Rev. Lett. **38**, 810 (1977).
[485]P. O. Tjom *et al.*, Phys. Lett. **B72**, 439 (1978).
[486]D. G. Sarantities *et al.*, Phys. Rev. **C14**, 2138 (1976).
[487]L. Westerberg *et al.*, Phys. Rev. Lett. **41**, 96 (1978).
[488]H. Hübel *et al.*, Phys. Rev. Lett. **41**, 791 (1978).
[489]M. A. Deleplanque *et al.*, Phys. Rev. Lett. **40**, 629 (1978).
[490]F. Folkmann *et al.*, Jahresbericht, 1977, GSI-J-1-78, Darmstadt (1978), p. 68.
[491]J. Pedersen *et al.*, Jahresbericht, 1977, GSI-J-1-78, Darmstadt (1978), p. 70.
[492]M. Piiparinen *et al.*, Phys. Scr. **17**, 103 (1978).
[493]R. Broda *et al.*, Z. Phys. **A285**, 423 (1978).
[494]D. Horn *et al.*, Phys. Rev. Lett. **39**, 389 (1977).
[495]B. Kohlmeyer *et al.*, Jahresbericht, 1977, GSI-J-1-78, Darmstadt (1978), p. 71.
[496]W. Reissdorf *et al.*, Jahresbericht, 1977, GSI-J-1-78, Darmstadt (1978), p. 72.
[497]R. M. Lieder *et al.*, Ann. Report 1977, IKP KFA Jül-Spez-13, Jülich (1978), p. 50.

Translated by Julian B. Barbour